GeoArabia, 2011, v. 16, no. 4, p. 29-82
Gulf PetroLink, Bahrain

Evolution of Cretaceous to Eocene alluvial and carbonate platform sequences in central and south Jordan

John H. Powell and Basem K. Moh'd

ABSTRACT

The Cretaceous to Eocene succession in central and south Jordan is characterised by passive continental margin depositional sequences, which pass upward from alluvial/paralic to carbonate shelf and pelagic ramp settings. Detailed section logging and outcrop mapping have produced robust lithostratigraphic and lithofacies schemes that can be correlated throughout the region and in the subsurface. These schemes are set in a sequence stratigraphic context in relation to the evolution sedimentation on the Arabian and Levant plates. Three major megasequences are described (Kurnub, Ajlun and Belqa), and these are further subdivided into large-scale depositional sequences separated by regional sequence boundaries that represent maximum flooding surfaces. There is close correspondence between maximum flooding surfaces recording major sea-level rise with those derived for the Arabian and Levant plates, although there are some discrepancies with the precise timing of global sea-level fluctuations.

An upward change from braided to meandering stream fluvial environments in central and south Jordan during the Early Cretaceous, reflects a decreasing geomorphological gradient of the alluvial plain, declining siliciclastic sediment flux, and increased floodplain accommodation, associated with a regional Late Albian (second-order) rise in relative sea-level. The Late Albian to Early Cenomanian marine transgression across the coastal alluvial plain marks a major sequence boundary. During Cenomanian to Turonian times a rimmed carbonate-shelf was established, characterised by skeletal carbonates showing small-scale, upward-shallowing cycles (fourth- to fifth-order parasequences) ranging from subtidal to intertidal facies, arranged into parasequence sets. Rimmed carbonate shelf sequences pass laterally to coeval coastal/alluvial plain facies to the south and east. Eustatic (third-order) fluctuations in relative sea level during the Cenomanian and Early Turonian resulted in deposition of ammonite-rich wackestones and organic-rich marls, during high sea-level stands (maximum flooding surfaces). Progradational sabkha/salina facies passing landwards to fluvial siliciclastics were deposited during an Early Turonian sea-level low stand, marks a regional sequence boundary, above which a highstand carbonate platform was established.

A second-order, regional rise in sea level and marine transgression during the Early Coniacian marks a Type 2 sequence boundary, and subsequent drowning of the rimmed carbonate shelf by Late Coniacian times. Sedimentation during the Santonian to Maastrichtian was characterised by a hemi-pelagic chalk-chert-phosphorite lithofacies association, deposited in shallow to moderate water depths on a homoclinal ramp setting, although thicker coeval sequences were deposited in extensional rifts. The marked change in sedimentation from rimmed carbonate shelf to pelagic ramp is attributed to Neo-Tethyan mid-oceanic rifting, tilting, intracratonic deformation and subsidence of the platform; this is reflected in changes in biogenic productivity and ocean currents. Oceanic upwelling and high organic productivity resulted in the deposition of phosphorite together with giant oyster banks, the latter developing within oxygenated wave-base on the inner ramp. Chalk hardgrounds, sub-marine erosion surfaces, and gravitational slump folds indicate depositional hiatus and tectonic instability on the ramp. In the Early Maastrichtian, deeper-water chalk-marl, locally organic-rich, was deposited in density-stratified, anoxic basins, that were partly fault controlled.

Pulsatory marine onlap (highstand sequences) during the Eocene is manifested in pelagic chalk and chert with a paucity of benthic macro-fauna, indicating a highly stressed, possibly hypersaline, and density-stratified water column. Comparison with global and regional relative sea-level curves enable regionally induced tectonic factors (hinterland uplift and ocean spreading) to be deduced, against a background of global sea-level rise, changing oceanic chemistry/productivity and climatic change.

INTRODUCTION

The relatively undeformed Cretaceous – Eocene succession in Jordan and surrounding countries provides an excellent example of the evolution of depositional sequences ranging from alluvial and paralic, through rimmed carbonate-shelf to pelagic ramp settings, on a passive continental margin (Figure 1a-c). This paper summarises the evolution of the Cretaceous – Eocene carbonate platform in a sequence-stratigraphic context during a period of overall marine onlap across the Arabian Craton, and compares the influence of global sea-level fluctuations and regional tectonics on sedimentation and relative sea level in the Levant.

Almost continuous exposure along the Dead Sea Rift (approximately at right angles to the depositional palaeoslope) and along the Ras En Naqb Escarpment (approximately at parallel to the depositional slope; Figure 1a), and borehole data (Andrews, 1992) allow the three-dimensional geometry of the sequences to be determined. Onlap of marine carbonate sediments and progradation of shoreline, coastal plain and fluvial siliciclastics are described, here, in a sequence-stratigraphic context (Posamentier et al., 1988; Sarg, 1988; Galloway, 1989; Schlager, 1992; Hunt and Tucker, 1993).

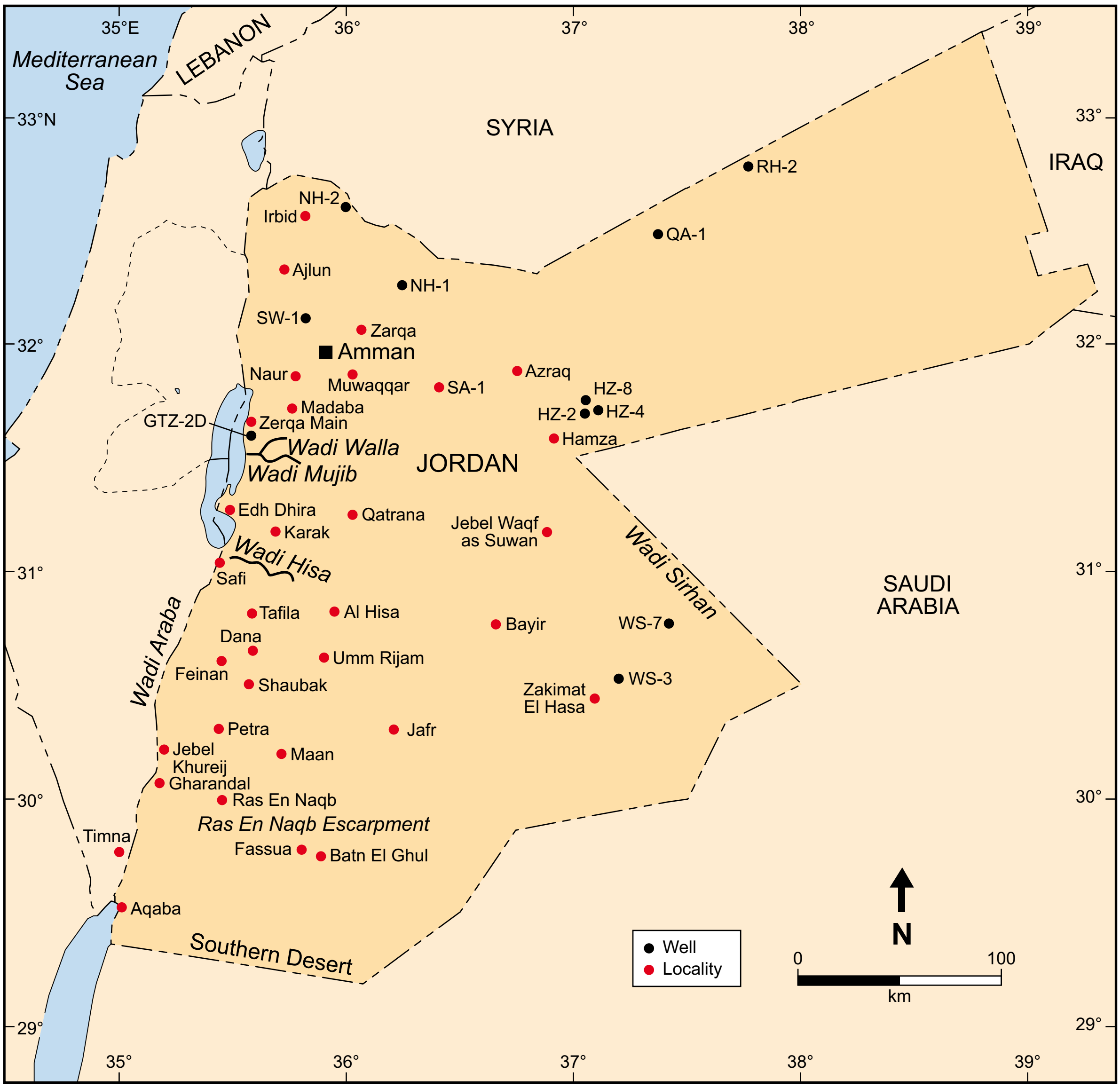

Figure 1a: Location map showing the principal localities and exploration wells (from Andrews, 1992) mentioned in the text (NH: North Highlands; HZ: Hamza; SA: Safra; QA: Qitar Al Abd; RH: Risha; SW: Suweileh; WS: Wadi Sirhan; GTZ: Geothermal).

Reconstruction of Cretaceous – Eocene facies belts and palaeogeography in the region are adjusted for ca. 100 km left-lateral shear of the Levant Plate along the Dead Sea Rift in the Late Neogene (Quennell, 1958; Freund et al., 1970; Powell et al., 1988).

The Cretaceous and Eocene strata are of great importance to the economy of the region since they contain significant resources of phosphorite, oil-shale, and industrial minerals, and also represent the principal aquifer and a hydrocarbon play.

The study is based on a wealth of outcrop and subsurface data, derived from detailed logging of sections, geological mapping, and both petrological and micropalaeontological studies of the Cretaceous to Eocene succession during the Natural Resources Authority (NRA) 1:50,000 scale National Geological Mapping Programme. A number of project-related lithostratigraphic schemes (Masri, 1963; Sir M. MacDonald and partners, 1965; Bender, 1968, 1974; Parker, 1970) have been erected for the succession in Jordan, which has resulted in a confused lithostratigraphic nomenclature. A unified nomenclature, adhering to the North American Stratigraphic Code (NACSN, 1983), has been adopted (NRA), and is

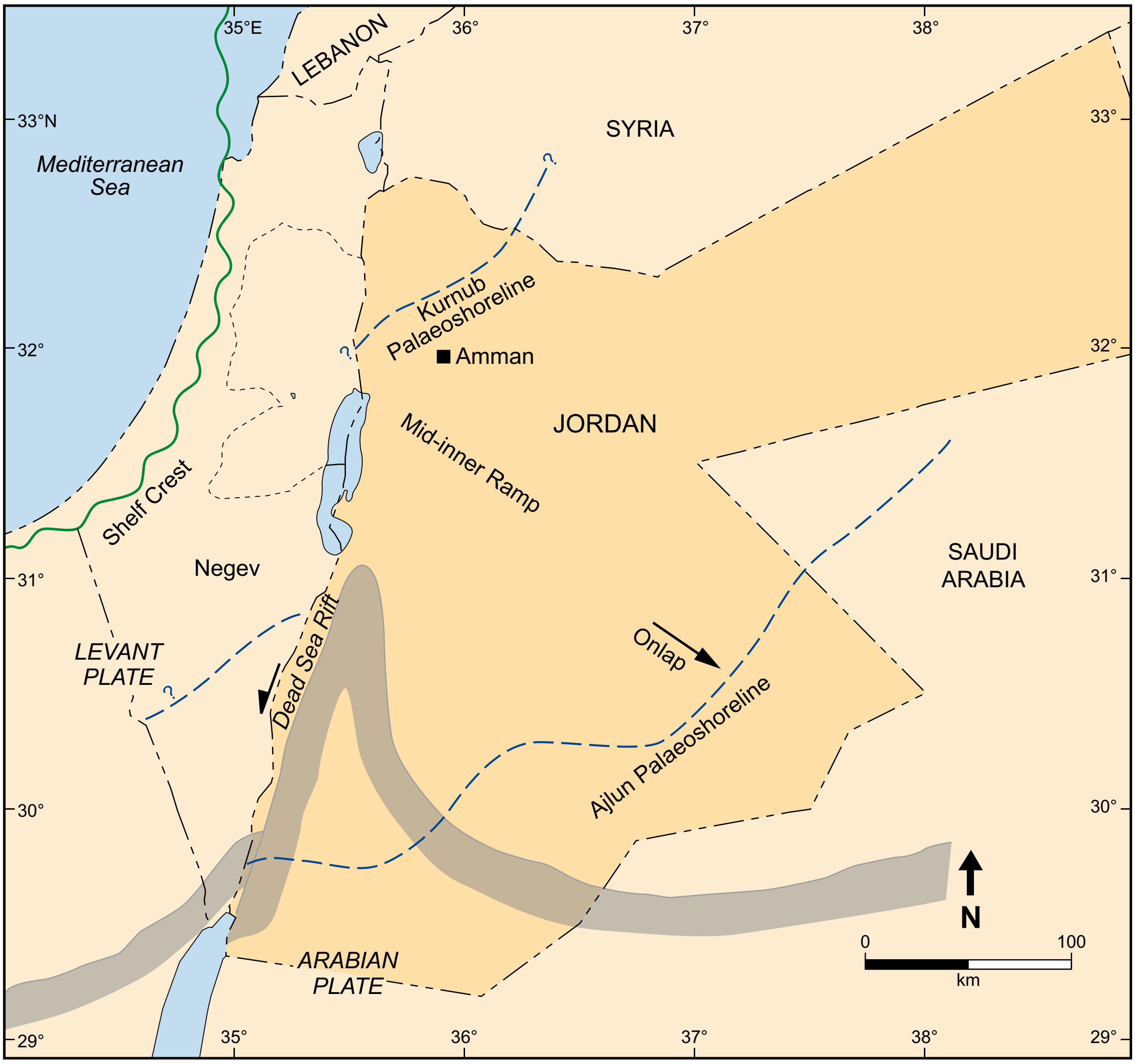

Figure 1b: Generalised palaeogeography showing the position of the palaeoshoreline during the Early Cretaceous (Kurnub Sandstone alluvial plain) and also during deposition of the rimmed carbonate shelf during the Turonian (Ajlun Group); the (green) wavy line shows the position of the shelf crest during the Turonian. Offset of the Levant and Arabian micro-plates, along the Dead Sea Rift in the Neogene is shown by offset of the cratonic basement (grey) (after Flexer et al., 1986).

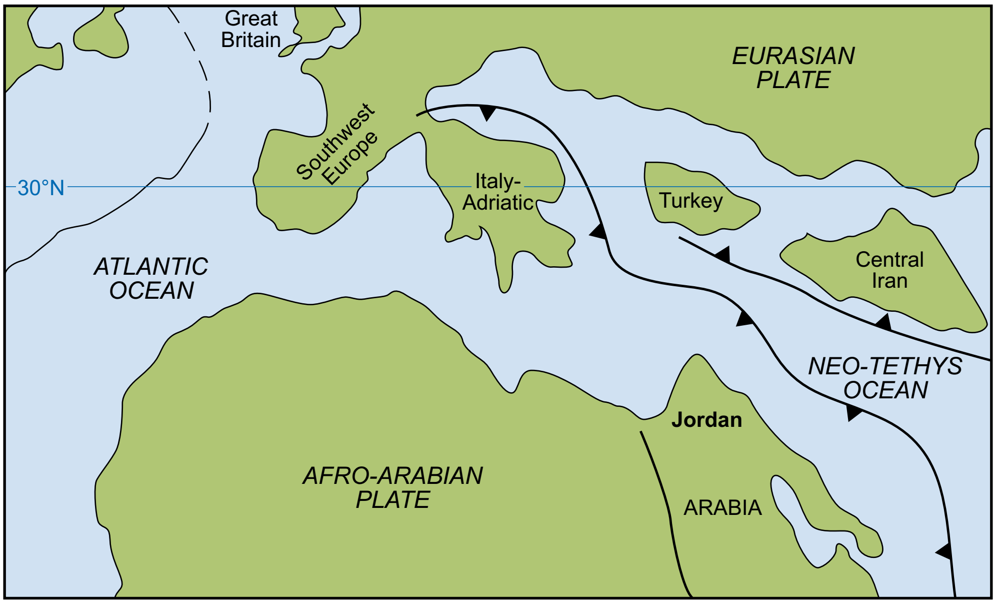

Figure 1c: Late Cretaceous palaeogeographical reconstruction (after Scotese, 1991); line with triangles indicates subduction/obduction.

briefly outlined here in the context of the dynamic evolution of the Cretaceous and Eocene succession in Jordan (Table 1). Further details of the lithostratigraphy and sedimentation of the Cretaceous and Tertiary rocks, at surface, are summarised in El-Hiyari (1985) and Powell (1988, 1989), to which the reader is referred for details (see also Figures 2 and 3; Tables 1 and 2). Sub-surface well data, including geophysical wireline logs, arising from groundwater and hydrocarbon exploration programmes, are summarised in Andrews (1992).

REGIONAL GEOLOGICAL SETTING AND STRATIGRAPHY

During Cretaceous to Eocene time, and for much of the early Mesozoic, Jordan lay at the southern margin of the Neo-Tethys Ocean which, during this period of global sea-level rise, periodically transgressed, south and east, over the margins of the Arabian Craton (Figures 1b and 1c). The present-day Mediterranean coastline corresponds approximately to the Cretaceous (Aptian to Late Turonian) palaeohingeline, which separated the deep-water Tethyan basin from the shallow carbonate shelf/ramp; the ocean-spreading centre was located close to Cyprus (Flexer et al., 1986; Scotese, 1991; Sharland et al., 2001; Stampfli and Borel, 2002). Carbonate platform sequences (Albian to Eocene in age) can be traced southwestwards, approximately parallel to the palaeoslope, to the Sinai Peninsula and the Eastern Desert of Egypt (Lewy, 1975; Kuss, 1992; Kuss and Bachmann, 1996; Bachmann and Kuss, 1998; Buchbinder et al., 2000; Schulze et al., 2003, 2005; Bauer et al., 2001, 2003; Kuss et al., 2003 and Bachmann et al., 2010).

Sedimentation and sequence architecture on the southern passive continental margin of Tethys (present-day North Africa and Arabia) was largely controlled by three extrinsic factors. First, longer-term fluctuations in climatically driven eustatic sea level (Haq et al., 1988; Sharland et al., 2001); second, the configuration of the Neo-Tethys Ocean and its spreading centre near Cyprus; and third, the isostatic and intra-plate tectonic deformation of the Arabian Neoproterozoic Shield and its Palaeozoic sedimentary cover rocks, to the south and east, which influenced terrigenous siliciclastic sediment flux. Subsequent to Late Jurassic – Early Cretaceous extensional rifting (Bandel, 1981; Powell and Moh'd, 1993) and associated intra-plate continental volcanic activity (Lang and Mimran, 1985), the Early Cretaceous marks a period of post-rift flexural subsidence of the 'passive' continental margin. However, superimposed on this general trend were phases of local extensional tectonics (Barremian to Albian) in the Sinai (Bachmann et al., 2010), compressional/transpressional (Levant Plate/Syrian Arc) and extensional deformation (Arabian Plate), isostatic uplift, karstic erosion and gravitational slump-folding, in Late Cretaceous (Coniacian to Maastrichtian) times (Flexer et al., 1986; Cohen et al., 1990; Powell, 1989).

Table 1: Summary of the lithology, fossils and depositional environments for the Ajlun Group and Belqa Group in central and south Jordan.

Lithostratigraphy	Lithology	Main Fauna (microfauna in brackets)	Depositional Environment
BELQA GROUP (Coniacian to Eocene)			
Wadi Shallala Fm (WS)	Marl, chalky limestone, quartz-rich calcarenite	Echinoids, Nummulites (calcareous nanoplankton)	Pelagic chalk; shoaling upward
Umm Rijam Chert-Limestone Fm (URC)	Chalky limestone, thin-bedded chert, nummulitic packstone-grainstone; sparse phosphate	Fish fragments, Nummulites, gastropods (calcareous nanoplankton; silicoflagellates)	Deep-water pelagic; locally hypersaline; locally shallow lagoons
Muwaqqar Chalk-Marl Fm (MCM)	Chalk, chalky marl, locally bituminous; limestone and chert concretions	Bivalves, ammonites, gastropods, fish fragments (calcareous nanoplankton)	Deep-water pelagic, epeiric sea
Al Hisa Phosphorite Fm (AHP) (*see below)	Phosphate, chert, chalk, chalky marl, oyster-rich coquina and bioherms	Oysters (large), gastropods, bivalves, fish and reptile fragments, ammonites (silicoflagellates, radiolaria, calcareous nanoplankton, foraminifera)	Shallow-water pelagic ramp; oyster bioherms on inner ramp
Amman Silicified Limestone Fm (ASL) (*locally not differentiated from overlying unit, e.g., Amman area)	Chert, microcrystalline limestone, chalky marl, sparse phosphorite; oyster-rich coquina	Gastropods, bivalves, including oysters, sparse ammonites, fish and reptile fragments (silicoflagellates, radiolaria)	Shallow-water, pelagic ramp (inner)
Wadi Umm Ghudran Fm (WG) (locally absent)	Chalk (locally thick), thin-bedded chert, sparse phosphate, dolomitic grainstone; passes SE to sandstone (Alia Mbr)	Bivalves, gastropods, fish fragments (mostly calcareous nanoplankton)	Pelagic ramp (mid-to inner); shallow shoreline siliciclastics in SE
AJLUN GROUP (Cenomanian to Coniacian)			
Jibal Khureij Fm (K) (locally present along rift margins)	Micrite, wackestone, grainstone, packstone, sparse ooidal grainstone	Bivalves, gastropods, echinoids (ostracods, foraminifera)	Rimmed carbonate shelf with locally subsiding basins
Wadi As Sir Limestone Fm (WS)	Micrite, wackestone, packstone, sparse ooidal grainstone, chert nodules	Bivalves, gastropods, echinoids, rudists (foraminifera)	Rimmed carbonate shelf; rudist patch reefs; shoaling, inner shelf (central Jordan)
Shueib Fm (S)	Marl, locally bituminous, thin wackestone/packstone, evaporites, siliciclastics in SE	Bivalves, gastropods, ammonites (locally large and common in Wala Mbr)	Mid-carbonate shelf, periodically deep water; regressive supratidal and locally fluvial
Hummar Limestone Fm (H)	Micrite, wackestone, packstone	Bivalves, gastropods, sparse rudistids, stromatoporoids (foraminifera)	Shoaling mid-carbonate shelf (North and Central Jordan)
Fuheis Fm (F)	Marl, clay, thin nodular wackestone/packstone	Bivalves, gastropods	Deep-water, mid-carbonate shelf
Naur Limestone Fm (N)	Wackestone, packstone, and grainstone, interbedded with marls and nodular limestone; rudistid biostromes; calcareous sandstone and siltstone with glauconite at base (Wadi Juheira Mbr (WJ))	Rudistids, bivalves, gastropods, corals, stromatoporoids, corals (foraminifera)	Shoaling, subtidal to intertidal; inner carbonate platform; rudist reefs and biostromes

Table 2: Summary characteristics of the alluvial plain/paralic, rimmed carbonate shelf and pelagic ramp facies associations found in the Cretaceous – Eocene sequences in central and south Jordan.

Facies Association	Dominant lithologies	Lithostratigraphical Unit(s)
Alluvial plain/paralic facies associations (AP)		
AP1: Braided to low-sinuosity alluvial plain	Medium- to coarse-grained quartz arenite; lag conglomerate including mudstone rip-up clasts; ferralitic crusts	Kurnub Sandstone (lower)
AP2: Meandering to high-sinuosity alluvial plain	Medium- to coarse-grained quart arenite; lensoid mudstone/siltstone; plant fragments	Kurnub Sandstone (upper)
AP3: Coastal plain, paralic	Medium- to fine-grained sandstone; glauconite; laterally accreted channels; lensoid mudstone/siltstone; thin coal; gleysols	Naur Formation (basal Wadi Juhra Member)
AP4: Marine, intertidal to subtidal, heterolithic	Fine- to medium-grained sandstone; glauconite; sandy dolomite; bioturbation common; marine fauna	Locally in Kurnub Sandstone - north Jordan
Rimmed carbonate shelf facies associations (RCS)		
RCS1: Subtidal carbonate platform	Micrite, shelly wackestone, calcareous mudstone, bituminous marl; bivalves and sparse ammonites	Ajlun Group - typically Fuheis and Shueib formations
RCS2: Intertidal carbonate platform	Ooid/shelly wackestone/packstone, locally grainstone; dolomite; fenestral, algal micrite; *Thalassinoides*	Ajlun Group - typically Naur, Hummar and Wadi As Sir Limestone formations
RCS3: Rudistid biostrome/bioherm	Grainstone; rudistid boundstone; calcrete; quartz sand	Naur and Wadi As Sir Limestone formations
RCS4: Peritidal sabkha/salina	Gypsum; anhydrite; algal micrite; dolomite	Uppermost Shueib Formation
Pelagic ramp facies associations (PR)		
PR1: Pelagic outer ramp	Chalk, detrital chalk, bedded chert, porcellanite, marl bituminous marl	Belqa Group - Wadi Ghudran, Muwaqqar Chalk-Marl, Umm Rijam and lower Wadi Shallala formations
PR2: Hemi-pelagic mid-inner ramp	Chalk, bedded chert, marl, limestone, dolomite, phosphorite	Amman and Al Hisa Phosphorite formations
PR3: Oyster biostrome/bioherm	Bivalve grainstone and oyster banks	Al Hisa Phosphorite and Amman formations
PR4: Shallow-marine siliciclastic	Quartz arenite locally bioturbated, dolomite, porcellanite, chert and marl	Alia Member; Batn El Ghul facies of Belqa Group (SE Jordan)
PR5: Siliciclastic/carbonate shoal	Nummulitic packstones, quartz arenite	Wadi Shallala Formation (upper); Umm Rijam Formation

Final regression and closure of the Neo-Tethys Ocean in the Late Palaeogene is attributed to Alpine earth movements in the Syrian Arc, including incipient Dead Sea rifting, as the African–Arabian Plate moved northwards against the Euro–Asian Plate (Scotese, 1991; Stampfli and Borel, 2002). Fossil evidence indicates that the Cretaceous was a period of global high temperatures and high atmospheric carbon dioxide levels with no substantial polar ice caps (i.e. 'Greenhouse' conditions). A global cooling trend throughout the Late Cretaceous has been correlated with declining atmospheric carbon dioxide (Spicer and Corfield, 1992; Jarvis et al., 2006). Furthermore, plate tectonic reconstruction indicates that the Arabian Craton drifted northwards from an equatorial position in the Early Cretaceous to ca. 20 degrees north palaeolatitude by Maastrichtian time (Scotese, 1991; Stampfli and Borel, 2002), inferring a probable low to mid-latitude, warm climate during deposition of the succession in Jordan.

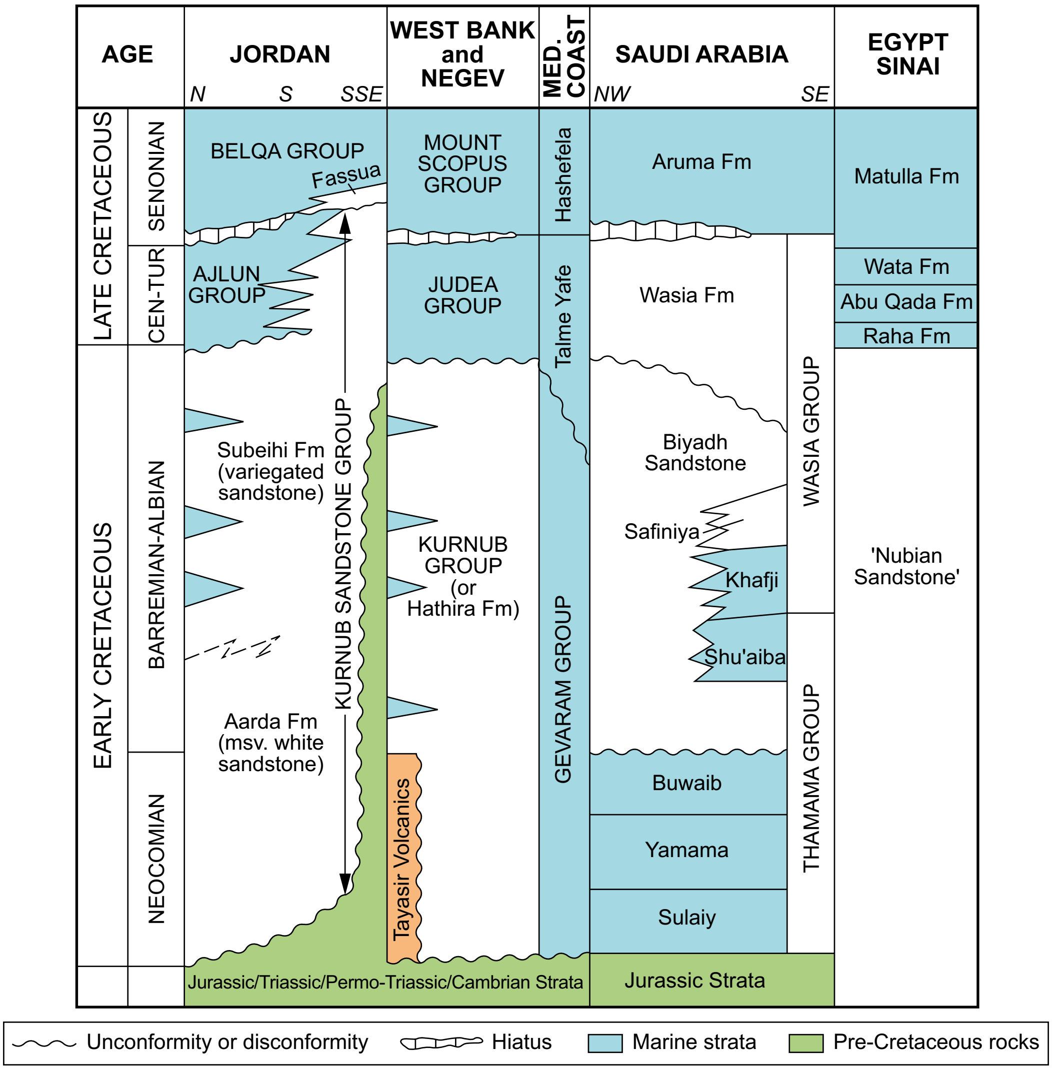

Figure 2: Early Cretaceous lithostratigraphy and sequences in Jordan and adjacent areas. Based on Powell (1989), Bartov et al. (1972), Flexer et al. (1986) and Powers (1968).

Superimposed on the longer-term variables, noted above, are regional factors that influenced sedimentation during each of the depositional sequences. These include accommodation potential and rates of sediment supply to the depositional system, isostatic uplift of the hinterland (the Arabian-Nubian Shield) due to erosion of sedimentary cover sequences and basement rocks which, in turn, influenced siliciclastic sediment flux, bioproductivity (e.g. vertical carbonate accretion) on the carbonate platform, ocean nutrient supply and sea-water chemistry (Schlager, 1992). Many of these factors are, of course, inter-related, and one of the aims of this paper is to unravel the significance of these variables during evolution of the Cretaceous to Eocene sequences in the region, against a back-drop of global sea-level fluctuations (Haq et al., 1988; Miall, 1991; Sharland et al., 2001; Haq and Al-Qahtani, 2005).

Lithostratigraphy

The principal lithostratigraphic units at outcrop in Jordan (Figures 2 and 3) are briefly reviewed so as to provide a framework for the discussion of lithofacies associations and sequence-stratigraphic concepts; further details can be found in Powell (1989), Kuss (1992), Schulze et al. (2003, 2005) and Wendler et al. (2010). Most of these units are recognised in the subsurface on geophysical wireline logs (Andrews, 1992). Lithological, petrological and sedimentological characteristics of the units at

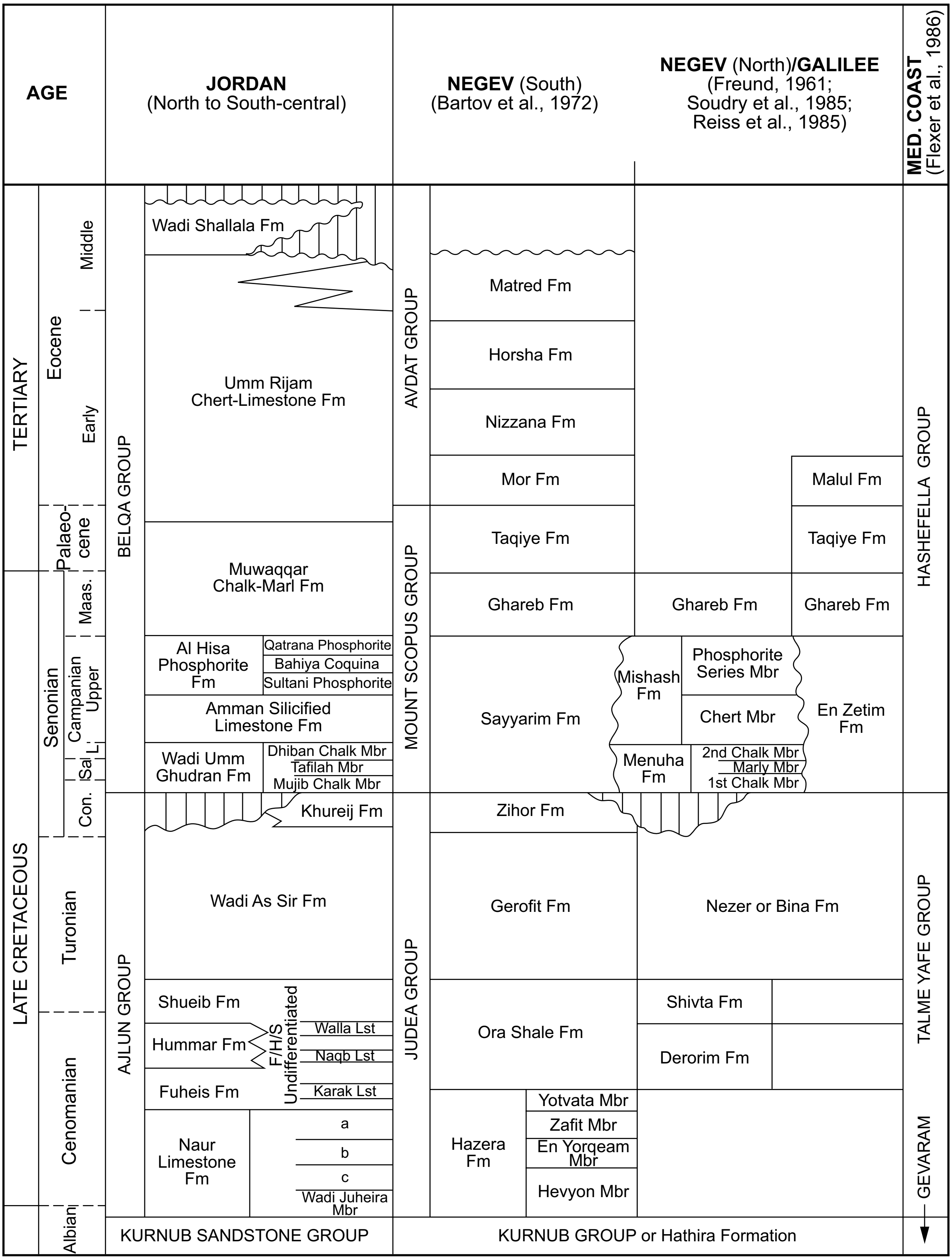

Figure 3: Late Cretaceous and Palaeogene lithostratigraphic nomenclature and correlation in the region (after Powell, 1989).

formation level are summarised in Table 1. The Cretaceous succession of Jordan (Figures 2 and 3) is conveniently divided into three lithostratigraphic groups, bounded by regional unconformities, here interpreted as megasequence boundaries (Mitchum, *in* Vail et al., 1977). These are described, below, in upward sequence.

Kurnub Sandstone Group

The Kurnub Sandstone Group (Berriasian to Albian), ca. 200–450 m thick, unconformably overlies strata ranging in age from Neoproterozoic/early Palaeozoic in south Jordan, to Jurassic in north Jordan (Figure 2). It consists predominantly of fluvial quartz-arenite in south and central Jordan, with subordinate thin beds of alluvial mudstone, and marine limestone and siltstone in north Jordan (Figure 4). In north Jordan the group was divided into the Aarda Formation and overlying Subeihi Formation (Parker, 1970), but these subdivisions, largely based on subtle colour differences, cannot be traced with any certainty throughout the country.

Isopach data (Powell, 1989; Andrews, 1992) show a general trend of thickening northwestwards, from about 50 m in the east of the country, to 350 m in the area west of Amman (Figure 5a). The westward thickening trend (up to ca. 604 m west of the Dead Sea Rift; Figure 4) is attributed to higher sedimentation rates in fluvial and shallow-marine settings on the margin of the rapidly subsiding Neo-Tethys basin, the palaeohingeline of which was located along the present-day Mediterranean coast (Aharoni, 1964; van Houten et al., 1984; Flexer et al., 1986). Coeval, transgressive shallow-marine sequences are present to the north and west in Sinai (Bachmann et al., 2010) and the Mediterranean coast (Rosenfeld et al., 1998).

Ajlun Group

The overlying Ajlun Group (Late Albian/Cenomanian to Mid-Coniacian) consists largely of shallow-marine carbonates (Table 1) deposited on a rimmed-shelf (Read, 1985). The group interfingers with marine and fluvial siliciclastics to the south and east, and passes abruptly into basinal facies to the northwest (Flexer et al., 1986). Marine siliciclastics are present, at the base, marking the major, Early Cenomanian transgression, and thin tongues of fluvial siliciclastics and peritidal evaporites are present in central and south Jordan (Abed and ElHiyari, 1986; Powell, 1988; Andrews, 1992, and Figures 6 and 7). Along the escarpment from Ras En Naqb to Batn El Ghul, the group passes south-eastward into a coeval fluvial sandstone facies of Cenomanian to Senonian (Coniacian to Maastrichtian) age (Figures 4 and 6).

The group, at outcrop, is subdivided into six formations, in upward sequence: Naur Limestone, Fuheis, Hummar Limestone, Shueib, Wadi As Sir Limestone and Jibal Khureij (Table 1; Figure 3). The latter is present locally along the Dead Sea Rift margins in central Jordan (Figure 1a; Jibal Khureij; Mukawir). The remaining fivefold division is traceable throughout Jordan and is broadly equivalent to the subdivisions recognised by previous workers (Wolfart, 1959; Sir M. MacDonald and partners, 1965; Parker, 1970). South of Wadi Mujib, the Fuheis, Hummar and Shueib formations cannot be distinguished easily due to southward lithofacies change of the Hummar Limestone to a marly lithofacies facies (Figure 6). In the subsurface, in east Jordan, only the Wadi As Sir Limestone can be distinguished, and consequently the lower formations are informally termed the 'lower Ajlun Group' (Andrews, 1992).

The Ajlun Group ranges in thickness from zero in the southeast (Batn El Ghul) to about 800 m in the north (Irbid) (Figure 5b; Powell, 1989; Andrews, 1992). The overall trend of thickening basinwards towards the northwest is substantiated by borehole records west of the Dead Sea Rift, with up to ca. 1,000 m of coeval carbonates proved near the Mediterranean coast (Flexer et al., 1986). In the latter area, the carbonate platform sequence passes abruptly to over 3,000 m of basinal chalks, marls and shales (Talme Yafe Group; Bein and Weiler, 1976; Figure 3). Despite the overall trend of thinning south-eastward, towards the Arabian Craton, local rift-related subsidence during Cenomanian – Turonian times resulted in deposition of a thick succession (ca. 600 m thick) in the Azraq-Hamza Basin (Andrews, 1992).

Regionally, the Ajlun Group (Figure 3) is equivalent to the carbonate Judea Group (Shaw, 1948; Arkin and Hamaoui, 1967; Freund and Raab, 1969; Bartov et al., 1972; Lewy, 1975; Bartov and Steinitz, 1977; Garfunkel, 1978) in the West Bank and the Negev. To the east, in Saudi Arabia, the coeval Wasia Formation was deposited in fluvial to shallow-marine environments close to the margins of the

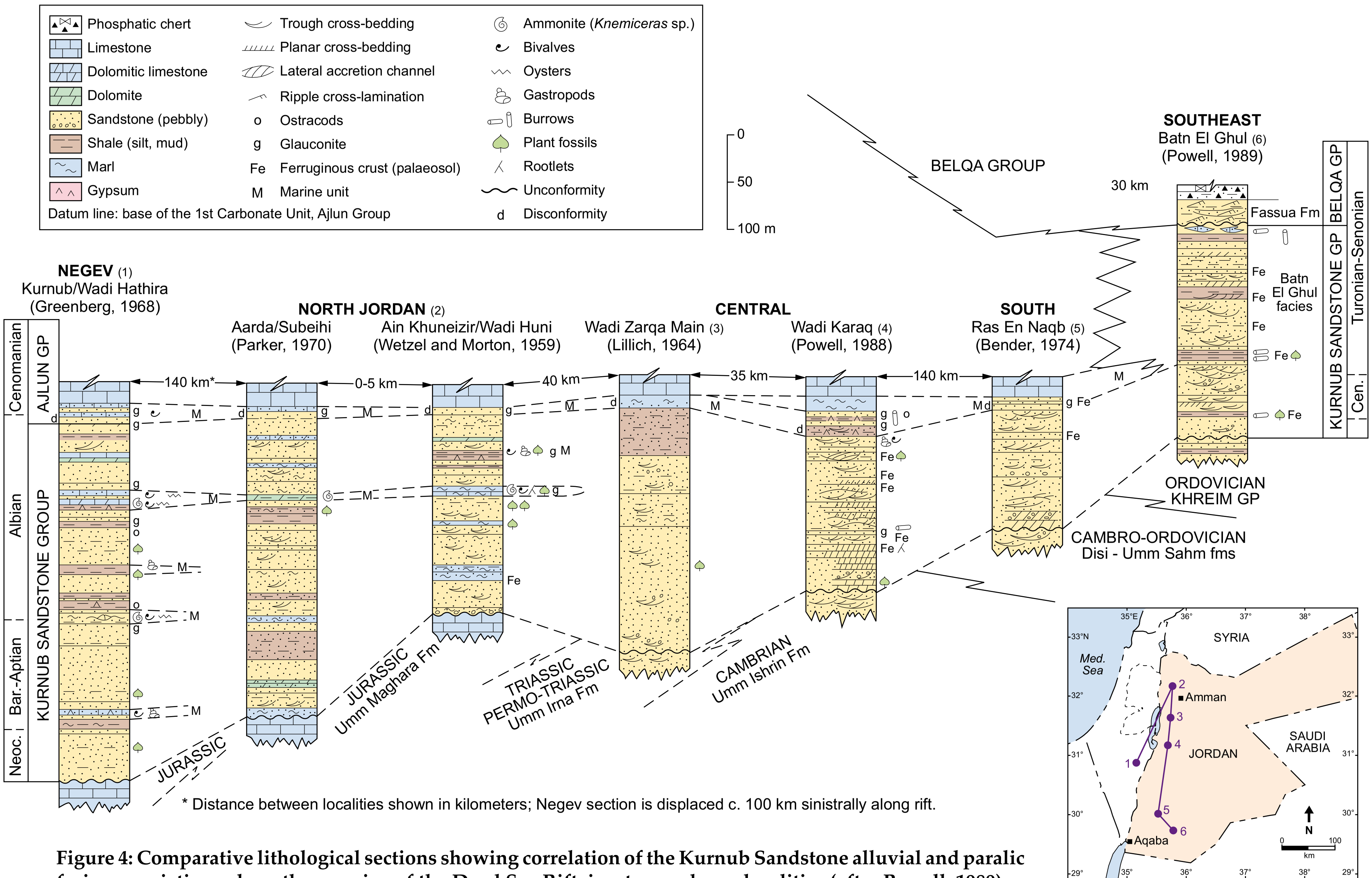

Figure 4: Comparative lithological sections showing correlation of the Kurnub Sandstone alluvial and paralic facies associations along the margins of the Dead Sea Rift; inset map shows localities (after Powell, 1989).

Sakaka-Ha'il Arch of the Arabian Shield (Sharief et al., 1989; Le Nindre et al., 2008). These siliciclastics are probably equivalent to the sandy, paralic facies of the Batn El Ghul area in southwest Jordan (Figure 4).

Belqa Group

The Late Cretaceous – Eocene Belqa Group (Table 1) consists mainly of chalk, chert and phosphorite deposited in a pelagic or hemi-pelagic ramp setting (Read, 1985; Burchette and Wright, 1992). A regional unconformity (disconformity) at the base of the group marks a sudden change of depositional environment. Succeeding sediments were deposited during pulsatory phases of marine onlap southward and eastward across the Arabian Craton.

The Belqa Group is subdivided into five formations (Parker, 1970), in sequential order: Wadi Umm Ghudran, Amman, Muwaqqar, Umm Rijam and Wadi Shallala formations (Table 1). In central Jordan the Amman Formation of Parker (1970) was divided into two units, the Amman Silicified Limestone, and the overlying Al Hisa Phosphorite (El-Hiyari, 1984; Powell, 1989) (Figure 3). The lower part of the group crops out along the Yarmouk River in North Jordan, and along the eastern margins of the Dead Sea Rift (Figure 6). Except where it is obscured by Neogene/Quaternary sediments and volcanic rocks, the group forms the greater part of the Jordan plateau from the Yarmouk River, in the north, to the Ras En Naqb–Batn El Ghul escarpment, in the south.

Along the Dead Sea Rift margins, where the group is overlain with erosional, angular unconformity by the continental, syn-tectonic Dana Conglomerate (Oligocene – Neogene), it is 450–520 m thick (Powell, 1988; Barjous, 1992). A thicker succession has been proved in boreholes in the east of the country (Andrews, 1992) with thicknesses of 550–600 m in the Jafr area and 600–800 m in the Azraq-Wadi Sirhan area. Rapid thickening to 2,400–3,000 m in the Azraq-Hamza Basin has been attributed to synsedimentary extensional rifting of this basin during Coniacian to Maastrichtian time (Bender, 1974; Andrews, 1992). Outside of this basin there is a trend of gradual thickening, accompanied by lateral facies changes, to the northwest, that is, towards the deeper-water of the Neo-Tethys Ocean (Flexer et al., 1986). Intra-formational diagenetic/gravitational slump folds are present in the lower part of the group (Powell et al., 1990) which may be associated with more pronounced transpressional deformation which influenced sedimentation in the Negev-Sinai area during the Senonian (Cohen et al., 1990).

The lower four formations (Figure 3) are equivalent to the Mount Scopus Group of the West Bank and Negev areas (Shaw, 1948; Bentor et al., 1960; Bartov et al., 1972; Bartov and Steinitz, 1977; Lewy, 1975; Soudry et al., 1985; Reiss et al., 1985). The equivalent of the Umm Rijam Formation and overlying units are included, there, in the Avdat Group. Basinwards, the Belqa Group is equivalent to the lower part of Hashefella Group (Flexer et al., 1986). Shorewards, it is correlated with the Aruma Group in Saudi Arabia (Powers, 1968).

Biostratigraphic Framework

Kurnub Sandstone Group

The age of the Kurnub Sandstone, based on sparse shelly marine faunas, including ammonites, from north Jordan, ranges from Berriasian (Neocomian) to Albian (Edwards, 1929; Wetzel and Morton, 1959; Bender, 1974). Marine microfloras from boreholes in northwest and east Jordan indicate a Berriasian to Cenomanian age (Andrews, 1992). Between Ras En Naqb and Batn El Ghul (Figures 4 and 6) the sandstone lithofacies (Kurnub) youngs diachronously south-eastward at the expense of carbonate lithofacies of the Ajlun Group; fluvial sandstones in the Batn El Ghul area yielded a Cenomanian flora (Bender and Mädler, 1968). It is predicted that the major Sequence Boundary (SB1) marked by the change from fluvial/paralic to carbonate platform environments (see Depositional Sequences section) is present in the Batn El Ghul sequence at the change from fluvial- to coastal plain-lithofacies. A good case can be made for the Batn El Ghul lithofacies to be distinguished as a separate unit (Fassua Formation) from the Kurnub and Ajlun groups. West of the Dead Sea Rift in the Kurnub

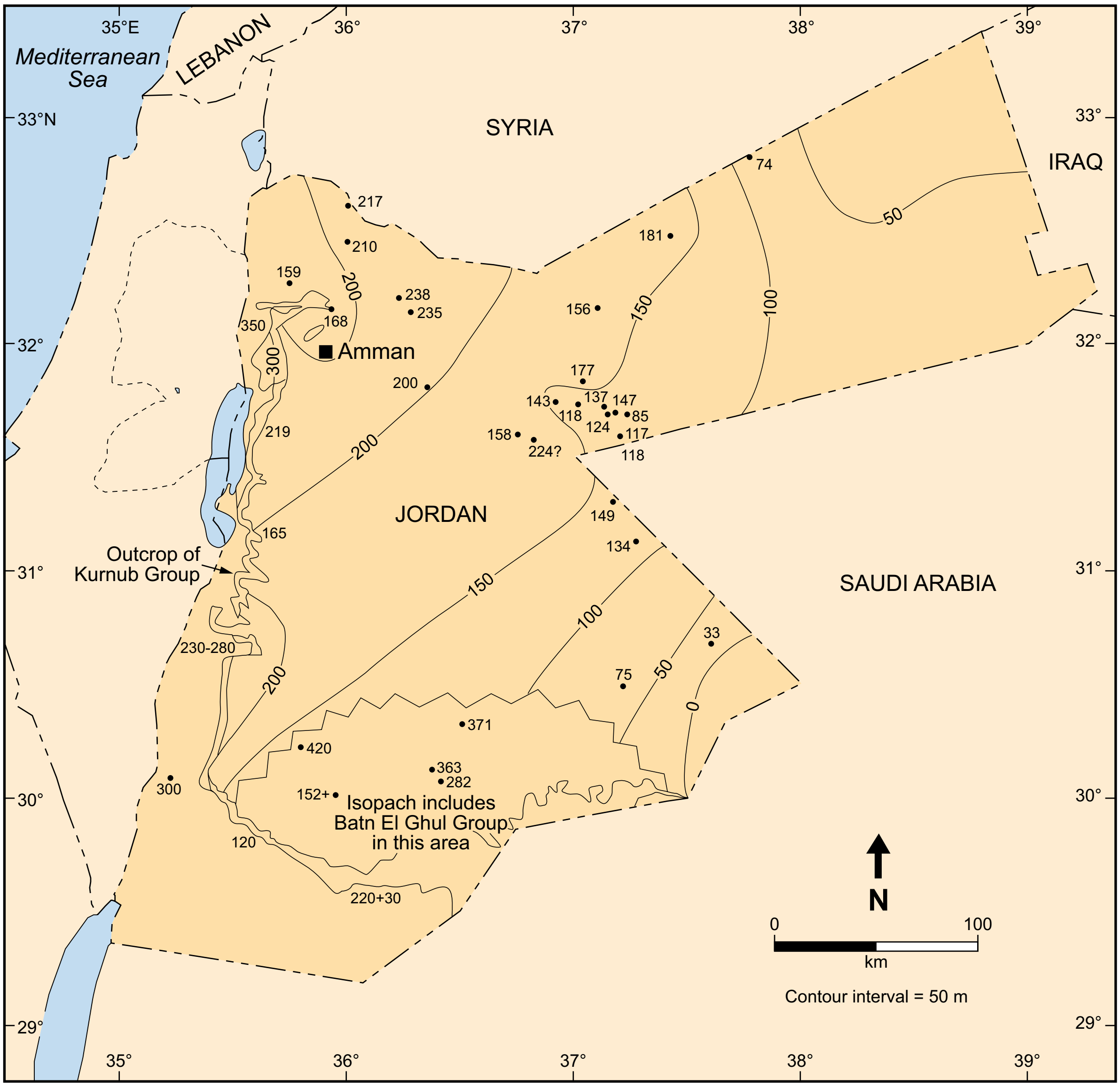

Figure 5a: Isopach map of the alluvial plain sequence (Kurnub Sandstone Group) in Jordan (after Andrews, 1992).

(Hathira) area (Figure 4), the unit ranges from Berriasian to Hauterivian at the base (Rosenfeld and Raab, 1984) and Barremian to Albian for the middle and upper part (Greenberg, 1968). Volcanic rocks intercalated in the basal Kurnub Sandstone, west of the Dead Sea Rift indicate a Berriasian to Valanginian age (Lang and Mimran, 1985).

Ajlun Group

A biostratigraphic framework has been established for the Ajlun Group and coeval strata in neighbouring areas (Freund, 1961; Freund and Raab, 1969; Bender, 1974; Basha, 1978; Dilley, 1985; Andrews, 1992; Schulze et al., 2003, 2004; Morsi and Wendler, 2010). The age of the major marine onlap in the region is Late Albian to Early Cenomanian (Wetzel and Morton, 1959; Arkin and Hamaoui, 1967; Bartov et al., 1972; Bender, 1974; Basha, 1978). The Cenomanian/Turonian boundary (Freund and Raab, 1969; Lewy, 1990; Schulze et al., 2004; Morsi and Wendler, 2010) has been recognised on the basis of ammonites in the lower part of the Shueib Formation, especially the macroconch ammonite fauna in the Wala Limestone Member (Powell, l989; Schulze et al., 2004) in north and central Jordan. This chronostratigraphic boundary was also recognised in foraminifera in the Shueib Formation in

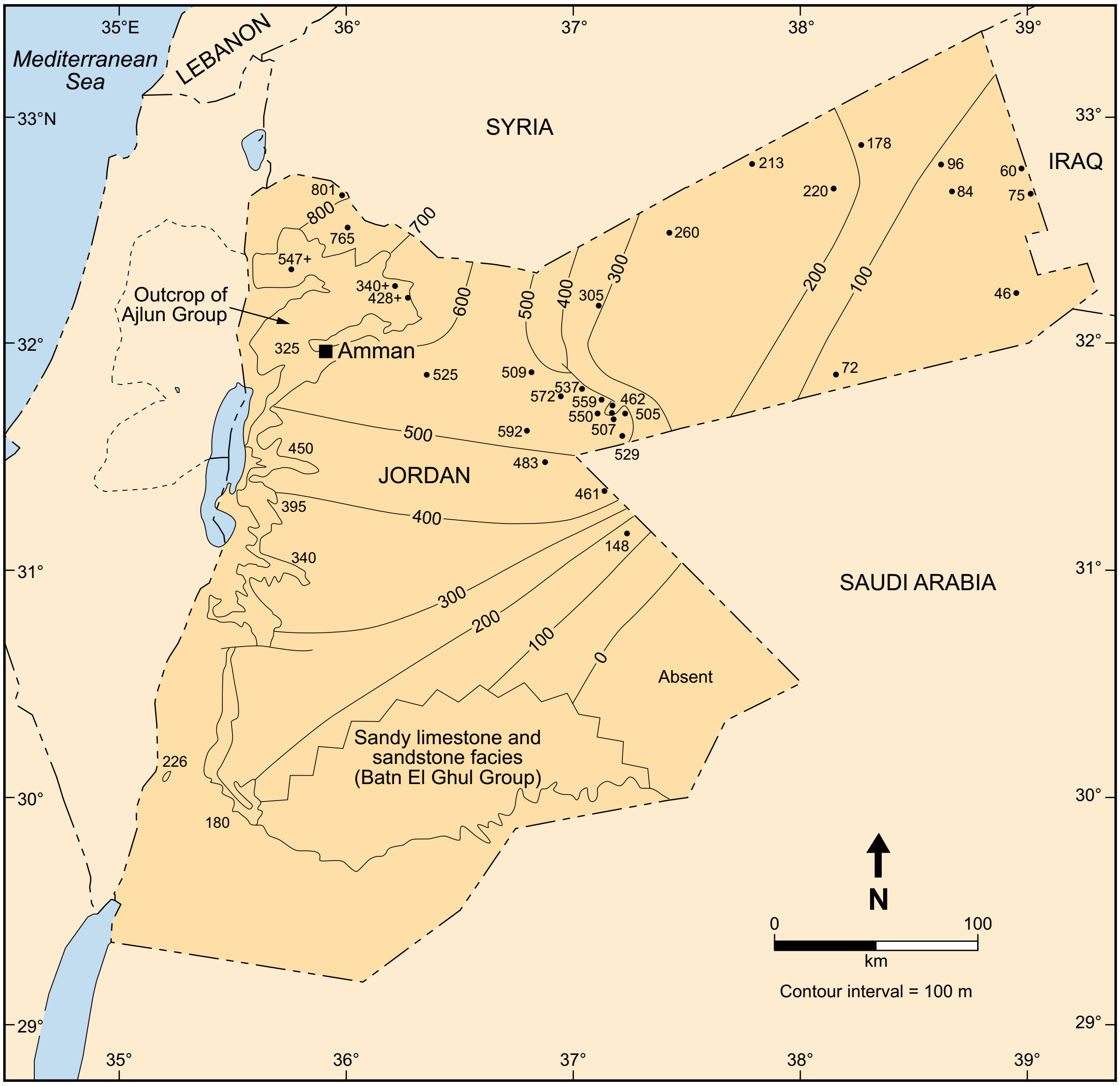

Figure 5b: Isopach map of the rimmed carbonate shelf sequence (Ajlun Group) in Jordan (after Andrews, 1992).

the Azraq-Hamza Basin (Dilley, 1985). The upper part of the group is generally considered to be of Late Turonian age (Wetzel and Morton, 1959; Basha, 1978; Lewy, 1990) and the unit is disconformably overlain by basal Coniacian chalk of the Belqa Group. However, evidence from Sinai and Negev (Lewy, 1975) and Jabal Khureij (Powell et al., 1988), suggests that younger Coniacian platform carbonates are locally preserved in small basins below the disconformable Upper Coniacian to Santonian chalk. Consequently, the topmost beds of the Ajlun Group may, locally, be of Late Turonian to Coniacian age, depending on the level of erosion and/or duration of the depositional hiatus.

Belqa Group

The Belqa Group ranges in age from Late Coniacian to Late Eocene and spans the Cretaceous/Tertiary boundary, which is marked by a depositional hiatus in the upper part of the Muwaqqar Chalk-Marl (Yassini, 1979). The age of the lowermost chalk was formerly considered to be Santonian (Burdon, 1959; Wetzel and Morton, 1959; Parker, 1970; Bender, 1974), although more recent studies in the Negev indicate a Late Coniacian age for the basal chalk unit (Lewy, 1975; Garfunkel, 1978; Reiss et al., 1985). The uppermost beds of the Belqa Group, which comprise nummulitic limestone

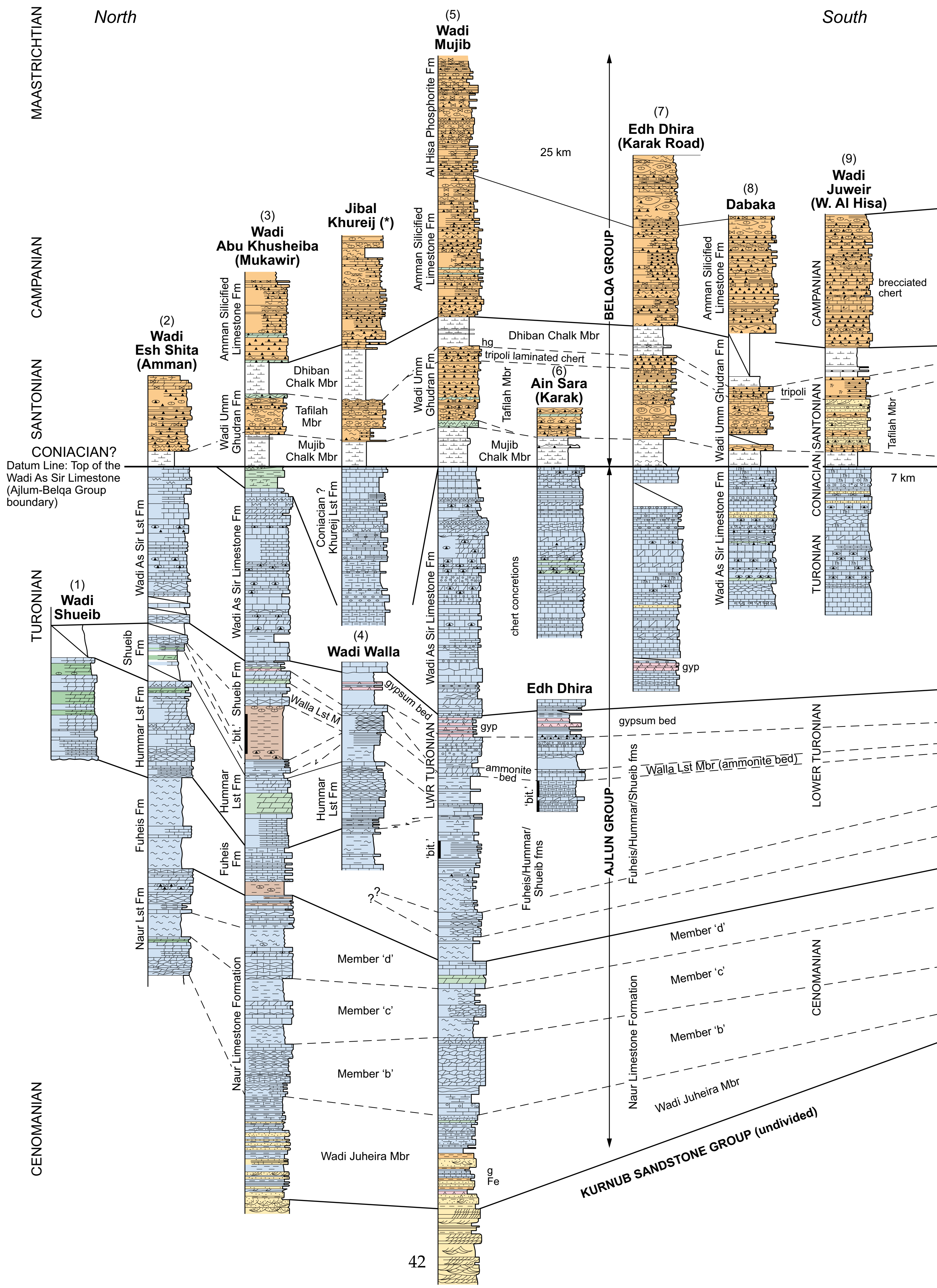
North
South
MAASTRICHTIAN
CAMPANIAN
SANTONIAN
CONIACIAN?
TURONIAN
CENOMANIAN
Datum Line: Top of the Wadi As Sir Limestone (Ajlum-Belqa Group boundary)
(1) Wadi Shueib
(2) Wadi Esh Shita (Amman)
(3) Wadi Abu Khusheiba (Mukawir)
Jibal Khureij (*)
(4) Wadi Walla
(5) Wadi Mujib
(6) Ain Sara (Karak)
Edh Dhira
(7) Edh Dhira (Karak Road)
(8) Dabaka
(9) Wadi Juweir (W. Al Hisa)
Al Hisa Phosphorite Fm
Amman Silicified Limestone Fm
Wadi Umm Ghudran Fm
Dhiban Chalk Mbr
Tafilah Mbr
Mujib Chalk Mbr
hg
tripoli laminated chert
tripoli
brecciated chert
25 km
7 km
BELQA GROUP
AJLUN GROUP
Wadi As Sir Lst Fm
Wadi As Sir Limestone Fm
Coniacian ? Khureij Lst Fm
chert concretions
Shueib Fm
Hummar Lst Fm
Fuheis Fm
Naur Lst Fm
Naur Limestone Formation
Walla Lst M
gypsum bed
gyp
'bit.'
ammonite bed
LWR TURONIAN
LOWER TURONIAN
Fuheis/Hummar/Shueib fms
Walla Lst Mbr (ammonite bed)
?
Member 'd'
Member 'c'
Member 'b'
Wadi Juheira Mbr
g
Fe
KURNUB SANDSTONE GROUP (undivided)

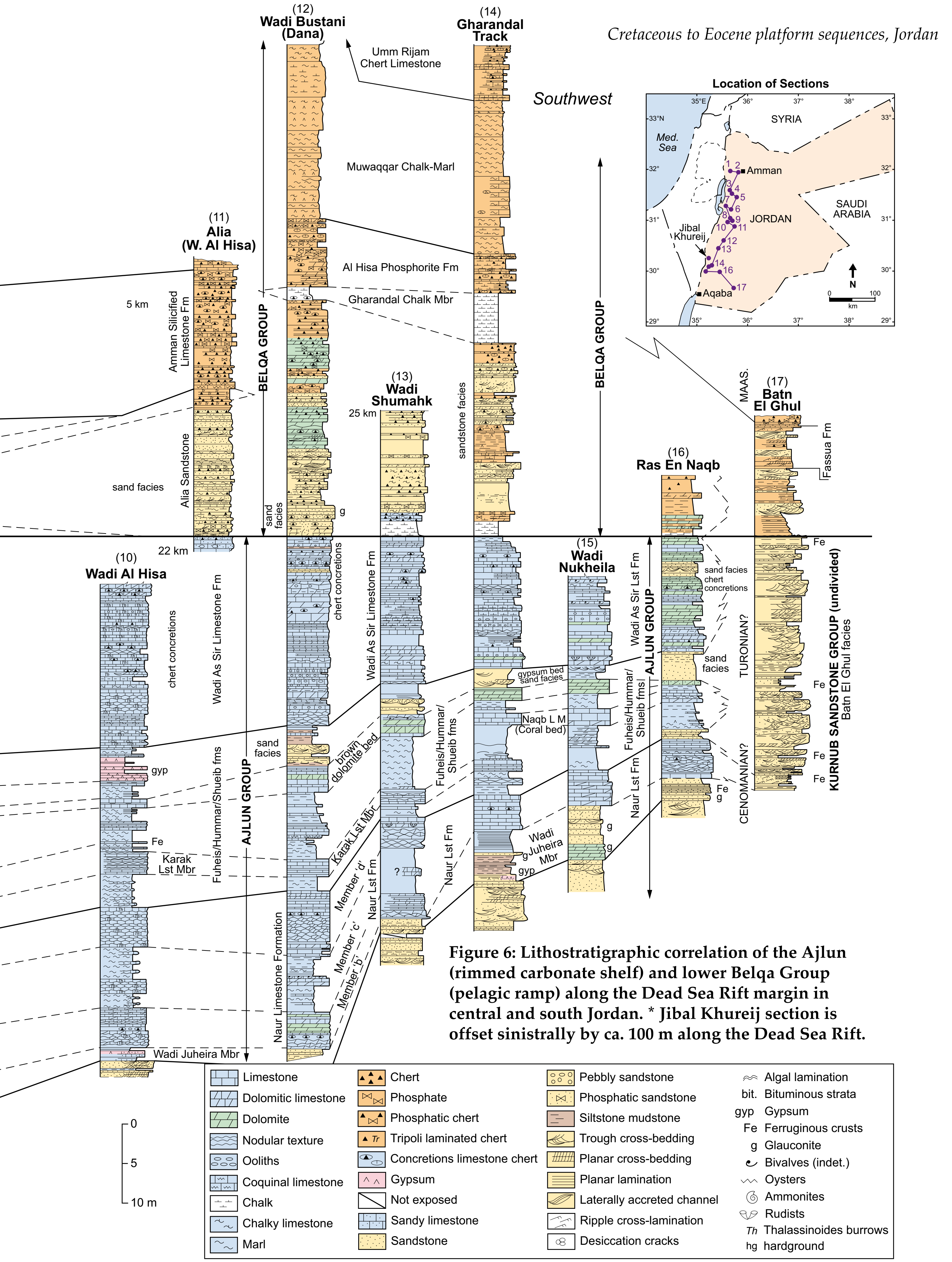

Figure 6: Lithostratigraphic correlation of the Ajlun (rimmed carbonate shelf) and lower Belqa Group (pelagic ramp) along the Dead Sea Rift margin in central and south Jordan. * Jibal Khureij section is offset sinistrally by ca. 100 m along the Dead Sea Rift.

Should Mujib, Dhiban and Gharandal chalk members be left in white (now in green)?

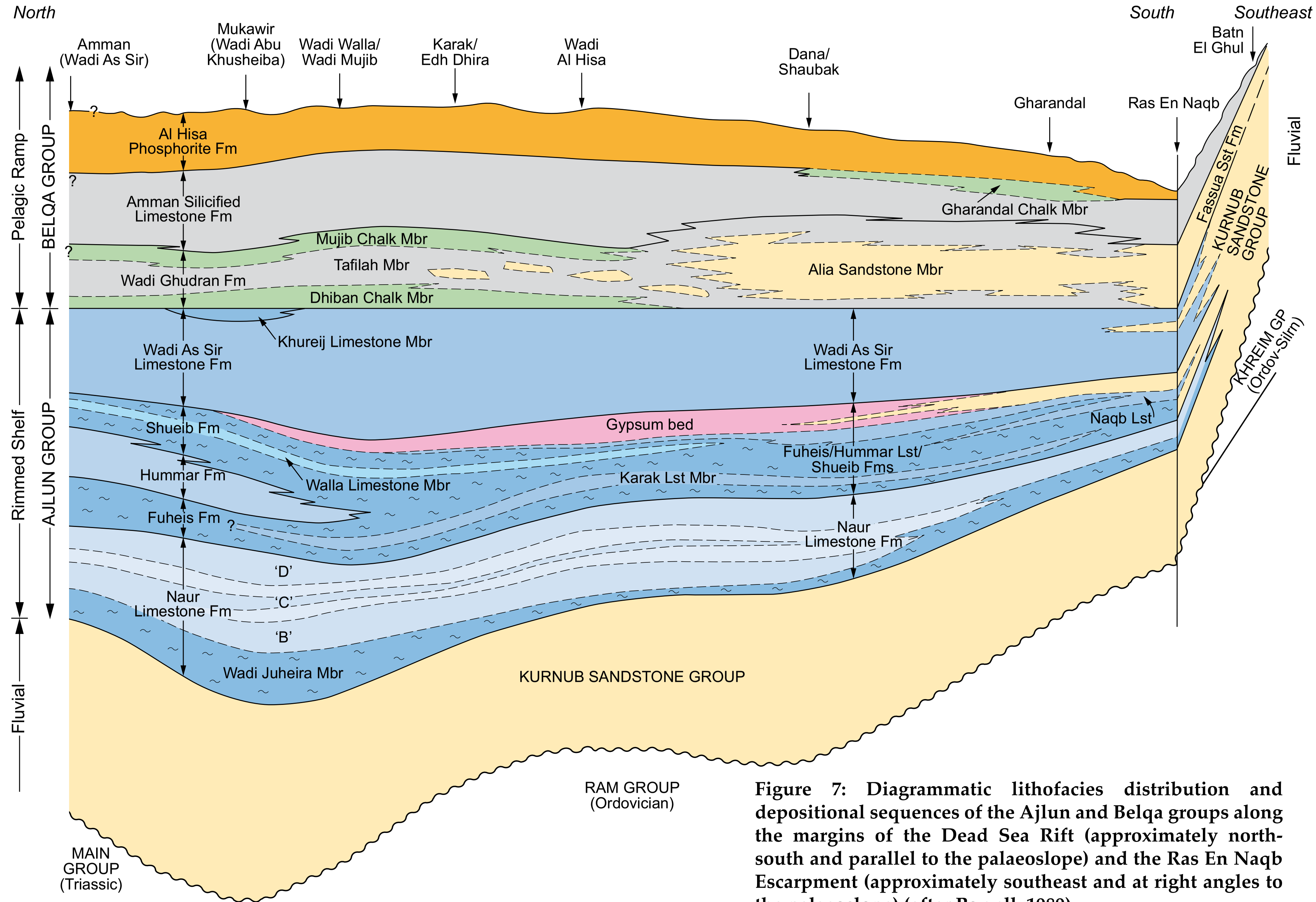

Figure 7: Diagrammatic lithofacies distribution and depositional sequences of the Ajlun and Belqa groups along the margins of the Dead Sea Rift (approximately north-south and parallel to the palaeoslope) and the Ras En Naqb Escarpment (approximately southeast and at right angles to the palaeoslope) (after Powell, 1989).

in Gharandal and Maan (Bender, 1974), and marl, chalky limestones with chert concretions overlain by nummulitic wackestones and sandy carbonates at Dahikiyah has been assigned a Late Eocene age (Koch, in Bender, 1974).

SEDIMENTOLOGY AND FACIES ASSOCIATIONS

Three main lithofacies associations (Table 2) have been recognised, namely: Alluvial Plain/Paralic (AP), Rimmed Carbonate Shelf (RCS) and Pelagic Ramp (PR); the principal associations and their subdivisions are described below.

Alluvial Plain Facies Associations (AP) – mostly Kurnub Sandstone

The Early Cretaceous strata (Kurnub Sandstone) comprises predominantly fluvial lithofacies in south and central Jordan (Powell, 1988, 1989; Amireh, 1992, 1997), passing basinward, in north-central and north Jordan, to low-gradient alluvial plain lithofacies with paralic and marine intercalations (Bender, 1974; Abed, 1982a; Andrews, 1992). Palaeocurrent measurements in central Jordan indicate a north to northeast palaeoflow (Powell, 1989; Amireh, 1997).

In south and central Jordan (Figure 4) the sandstones comprise rounded to sub-rounded, medium- to coarse-grained quartz arenite. Rare corroded feldspars are present in the basal sandstones but the rock is both texturally and mineralogically mature. The cement, where present, is generally ferruginous (goethite or iron carbonate) with rim (homoaxial) quartz overgrowth; carbonate cement is present locally. High porosity is due to dissolution of clay minerals (kaolinite) and/or carbonate cements. Heavy-mineral studies (Greenberg, 1968; Schneider et al., 1984; Weissbrod and Nachmias, 1986; Amireh, 1992; Kolodner et al., 2009) reveal a mature assemblage of stable grains, consisting predominantly of zircon, tourmaline and rutile (ZTR), with small proportions of barite, hornblende and epidote over narrow stratigraphic intervals. The high proportion of ZTR suggests recycling of older sediments, probably Palaeozoic sandstones, rather than a first cycle cratonic 'granitoid basement' provenance.

Four lithofacies associations (Table 2), described below, have been recognised in the Kurnub Sandstone in Jordan (Abed, 1982a; Powell, 1988; Amireh, 1992). Recognition of these associations in geographically widespread areas from Batn El Ghul (south) to Karak (central) and north Jordan (Figures 8 and 9) (Parker, 1970; Bender, 1974; Abed, 1982a) and the type Kurnub area (Shaw, 1948; Greenberg, 1968), have enabled a spatial and temporal reconstruction of the depositional environments (Table 1).

AP1: Braided to Low-Sinuosity Alluvial Plain Association

AP1 is characterised by white, grey-yellow, buff, red, medium- to coarse-grained quartz arenite. Quartz pebbles and intraformational mudstone rip-up clasts are locally present at the base of channels or erosional scours. Bedforms comprise large-scale lenticular sets with scoured erosive bases, internally structured by large-scale trough and planar cross-bedding; tabular sets with planar to slightly tangential cross-bedding are also present (Figure 10). Upward-fining cycles (parasequences) characterised by an upward change from trough cross-bedding to ripple cross-lamination, and locally capped by mottled, clayey, fine-grained sandstone are common. Pedogenic ferruginous horizons, penetrated by root traces (rhizoliths), are locally preserved at the top of cycles.

Channel sandstones with pebble-lined erosional scours and large-scale trough cross-bedding, and the absence of inter-channel fines indicate deposition in braided to low-sinuosity rivers as large transverse and longitudinal dunes; planar tabular sets are interpreted as deposition as sand-wave and/or transverse bars. Fine-grained, rippled sandstones represent floodplain deposition as sheet-floods under upper flow-regime and waning flow. Rhizoliths and ferruginous (brunified) palaeosols (Duchafour, 1982) indicate intermittent oxidation of the floodplain and local colonisation by plants in a humid climatic regime (Bachmann et al., 2010).

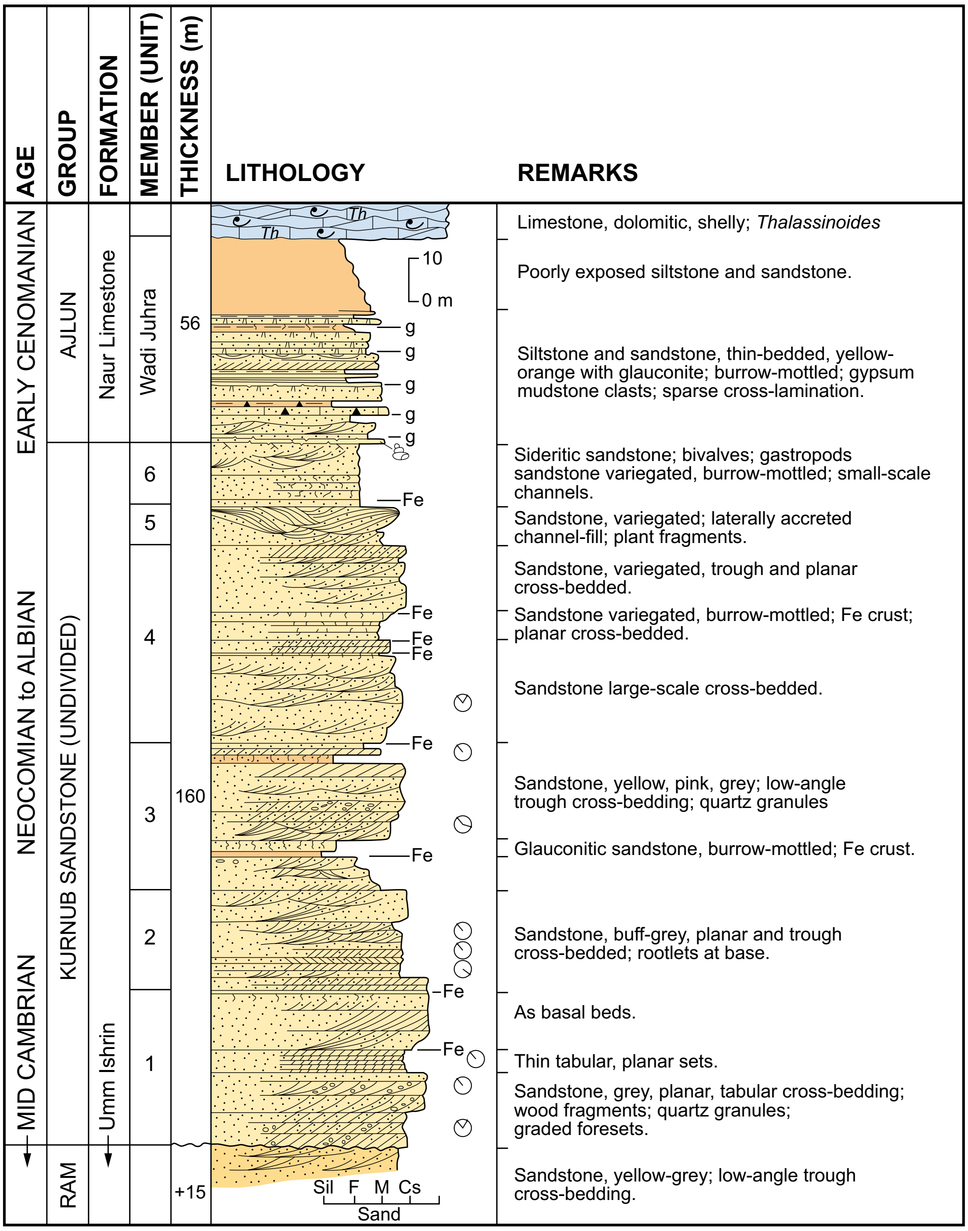

Figure 8: Graphic log of the alluvial plain lithofacies (Kurnub Sandstone), mostly AP1 facies association with AP2 facies association at the top, Wadi Karak; circles represent palaeocurrent orientations (after Powell, 1988). See also Figure 12.

AP2: Meandering to High-Sinuosity Alluvial Plain Association

Varicoloured, fine- to medium-grained sandstone and siltstone comprise the greater part of this association, but mudstone and leached claystones are also common at some horizons, particularly in north Jordan (Abed, 1982a). Channel or lensoid sand-bodies with low-angle (epsilon) laterally accreted sets, and small-scale internal cross-stratification are common in the upper part of the Kurnub Sandstone (Powell, 1989). Plant fragments, rootlets and sparse coal partings are common in both claystones and ripple cross-laminated siltstones and sandstones (floodplain deposits).

Bedforms in the channelised sand bodies (Figure 11) of this association indicate deposition in meandering rivers largely on point-bars (Allen, 1965). Overbank floodplain deposits are represented by small-scale, cross-bedded sandstone, passing up to ripple cross-laminated sandstone and siltstone (probably of crevasse-splay origin) and leached claystone (representing small lakes or abandoned clay-filled channels). The low-gradient alluvial plain was periodically colonised by plants, which are preserved as thin coals (histosols), and humic palaeosols rich in organic material (Figure 11). The latter suggest a relatively high water table on the floodplain compared to the braided, low-sinuosity

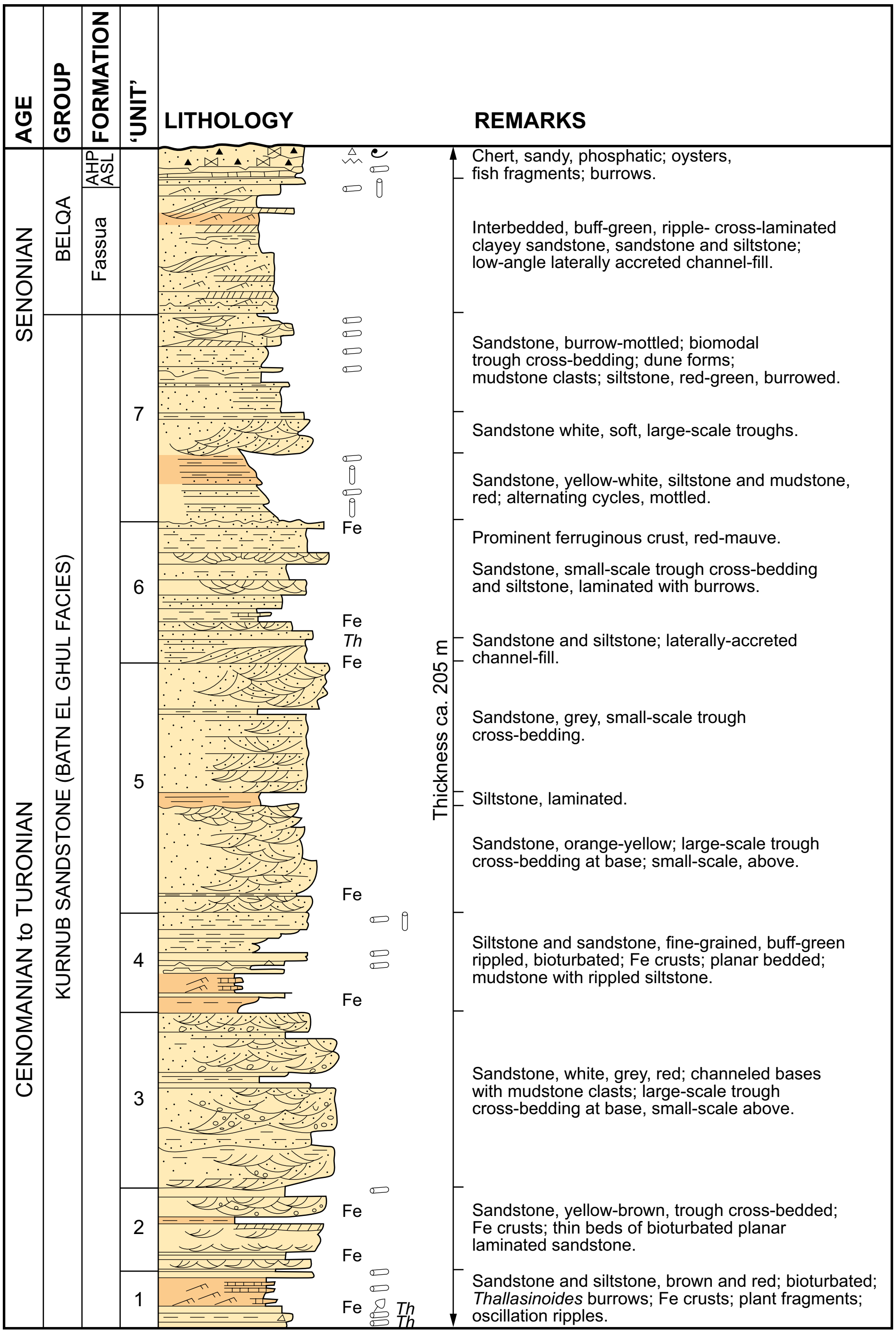

Figure 9: Graphic log of the shallow marine and coastal plain alluvial plain Batn Al Ghul lithofacies (AP3 facies association) (Cenomanian to Turonian) and the overlying Fassua Formation - mostly AP2 facies association. Batn Al Ghul, south Jordan (after Powell, 1989). See also Figure 25.

association (Figure 12). Leached claystones, locally preserved in abandoned channels indicate gleying processes under hydromorphic conditions (Duchafour, 1982; Besly and Fielding, 1989).

AP3: Coastal Plain (Paralic) Association

This association comprises varicoloured (red, buff, yellow, green, grey and mauve) fine- to medium-grained sandstone; sparse glauconite peloids are present in some beds. The sandstone beds are generally planar-bedded, internally rippled cross-laminated and are commonly bioturbated. Bivalves, *Thalassinoides* burrows, indeterminate surface traces, and sparse plant fragments are sometimes present.

Figure 10: Bitumen-stained foresets in unidirectional trough cross-bedded Kurnub Sandstone Group, Wadi Zerqa Main; hammer length 0.33 m (photo by J. Powell).

Figure 11: Dark grey, plant-rich mudstone infilling meander channel, Jerash road, north Jordan; height of channel-fill 2.6 m; base of channel marked by arrow (photo by J. Powell).

The characteristics of this association suggest deposition in a low-gradient, coastal alluvial plain environment, locally with paralic swamp conditions on the interfluves. *Thalassinoides* burrows, sparse bivalves and the presence of glauconite peloids demonstrate periodic marine incursions across the coastal plain which resulted in reworking of siliciclastics in the littoral zone during marine transgressions.

AP4: Marine, Intertidal to Subtidal Heterolithic Association

This association consists of yellow, brown, and green, fine- to medium-grained, sandstone, locally glauconitic, and thin beds of sandy dolomite and sandy limestone (Figure 12). Planar-bedding is common, but multi-directional cross-stratification is also present. Bioturbation is common and a sparse shelly fauna, comprised of bivalves, gastropods, ostracods, and rare ammonites, is locally present; some beds have monotypic bivalve or gastropod faunas.

A marine, intertidal to subtidal depositional environment is inferred. This association is more common in basinward locations west of the Dead Sea Rift (Greenberg, 1968; Bachmann et al., 2010), and is considered to be a marine end-member of Lithofacies Association 3, which it often overlies.

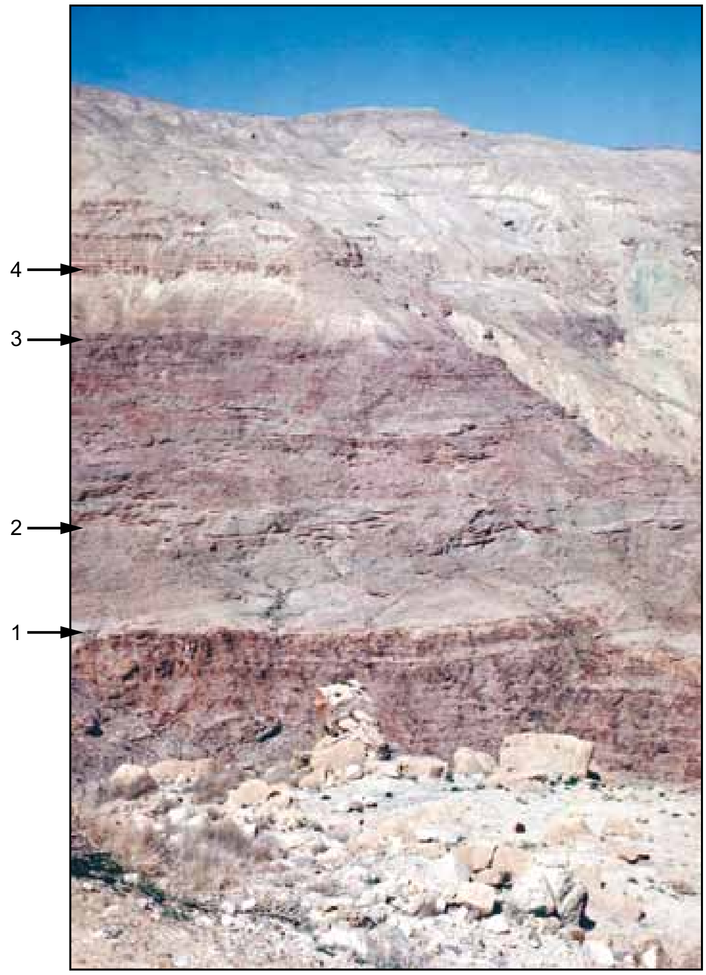

Figure 12: Lower Cretaceous Kurnub Sandstone (braided alluvial plain) (1 to 3), unconformable on Cambrian sandstone (Ram Group) (1) and overlain by the transitional Wadi Juheira Member (coastal plain) (3-4), passing up to the Naur Formation (4), Ajlun Group (rimmed carbonate shelf); (2) marks the top of unit 2 in Figure 8. Wadi Karak, north flank; Kurnub Sandstone is ca. 200 m thick (photo by J. Powell).

Rimmed Carbonate Shelf Facies Associations (RCS) – mostly Ajlun Group

Deposition of the Late Albian to Early Coniacian rimmed carbonate-shelf facies associations (Ajlun Group) reflect a balance between marine onlap and accretion of the carbonate platform, and hinterland progradation of fluvial and coastal plain facies. Overall, the sedimentation rate for the carbonate shelf is relatively high, between 3–5 cm/Ky, based on geochronology (Kent and Gradstein, 1985; Gradstein et al., 2004); carbonate accretion on the shelf generally kept pace with relatively steady subsidence. However, regional fluctuations (third order) in relative sea level, are reflected in deeper-water facies (bituminous marls and ammonite-rich limestone), and peritidal/fluvial facies on the inner shelf.

The rimmed carbonate-shelf sequence (Figure 13) can be subdivided into four lithofacies associations (Table 2), based on logged sections (Figures 6 and 7) in central and south Jordan (Powell, 1988, 1989; Schulze et al., 2003, 2004) and north Jordan (Abed, 1982b; Moh'd, 1985).

RCS1: Subtidal Carbonate Platform Association

This association is dominated by clayey micrite (locally dolomitic), calcareous mudstone and thin bedded shelly wackestone. Laterally discontinuous bituminous marl beds are present, reflecting deeper-water sedimentation and locally anoxic bottom conditions. Bivalves are common in the shelly wackestone beds, and sparse ammonites are locally present. Abundant large foraminifera are locally present; these thrived in shallow, protected lagoons on the inner shelf. Deeper-water calcareous

Figure 13: Rimmed carbonate platform mega-sequence (Ajlun Group) overlying alluvial plain siliciclastics (Kurnub Group) and overlain by the chalk-chert-phosphorite association Belqa Group (above the Coniacian drowning unconformity mega sequence boundary), Wadi Mujib, south flank; (1) Base of carbonate platform, Naur Formation; (2) and (3) upward-shoaling parasequences; (4) level of regressive lowstand sabkha unit in Shueib Formation; (5) Wadi As Sir Formation, top of platform carbonates; (6) level of drowning unconformity Ajlun-Belqa group boundary; (7) base of Dhiban Chalk (upper pelagic chalk); (8) base of Amman Silicified Limestone (chert); (9) base of Al Hisa Phosphorite; and (10) base of Pleistocene basalt. Height of section is about 1 km (photo by J. Powell).

mudstone (marl) was deposited on the inner platform during transgressions and highstands; anoxia on the inner shelf is reflected in bituminous marl, including the ocean-global OAE 2 event during the Late Cenomanian to Early Turonian (Schulze et al., 2004; Wendler et al., 2010). Marine red beds reported from the Early Turonian marly carbonate suggest syn-sedimentary reddening following the OAE 2 event (Wendler et al., 2009).

RCS2: Intertidal Carbonate Platform Association

The intertidal carbonate platform association comprises ooid and bivalve-rich wackestone/packstone and occasionally grainstone, and micrite (locally rich in globigerinids or ostracods). Early diagenetic dolomite is locally present, particularly at the top of beds and in coarse-grained burrow-fill of *Thalassinoides*. Bioclasts commonly include fragments of rudistids, oysters and other bivalves, echinoids and bryozoa. Macroconch ammonites are present in some beds (Figure 14). Micrite is locally devoid of macrofossils and commonly has abundant *Thalassinoides* burrow networks in the upper part of individual, ca. 1 m thick beds; algal lamination, locally preserved as polygonal mats, is sometimes present in the upper part of the beds (Figure 15). Early diagenetic chert nodules, probably derived from biogenic silica (sponge spicules) are sometimes present. This association commonly forms the upper part of upward-shallowing parasequences (Hunt and Tucker, 1993), overlying lithofacies RCS1. Supratidal, desiccated algal micrites (Powell, 1988) and subaerial erosion features (Abed and Schneider, 1982; Abed, 1984) in the upper part of these parasequences indicate temporary emergence of the shelf (Figure 15).

RCS3: Rudistid Biostrome/Bioherm Association

Rudistid-coral bioherms developed at the shelf crest (Bein, 1976; Bartov and Steinitz, 1982; Ross, 1992; Figure 1b). Rudistid banks and biostromes, associated with coarse grainstones and pedogenic calcretes

Figure 14: Walla Limestone Member (TST) with large ammonites (*Choffaticeras* spp. and *Thomasites* sp.) indicating an Early Turonian age; hammer length 0.33 m (photo by J. Powell).

Figure 15: Desiccated algal mats at top of shallowing-upwards parasequence set (Naur Formation), Wadi Mujib; lens cap 0.05 m diameter (photo by J. Powell).

also developed on the inner-shelf lagoon (Moh'd, 1985). These lithofacies are locally intercalated with quartz sand lenses in central Jordan (Powell, 1989).

RCS4: Peritidal Sabkha/Salina Association

This association is characterised by dolomite with sparse ostracods, faint burrow traces and, locally, glauconitic peloids, commonly overlain by alternating beds of unfossiliferous claystone and gypsum

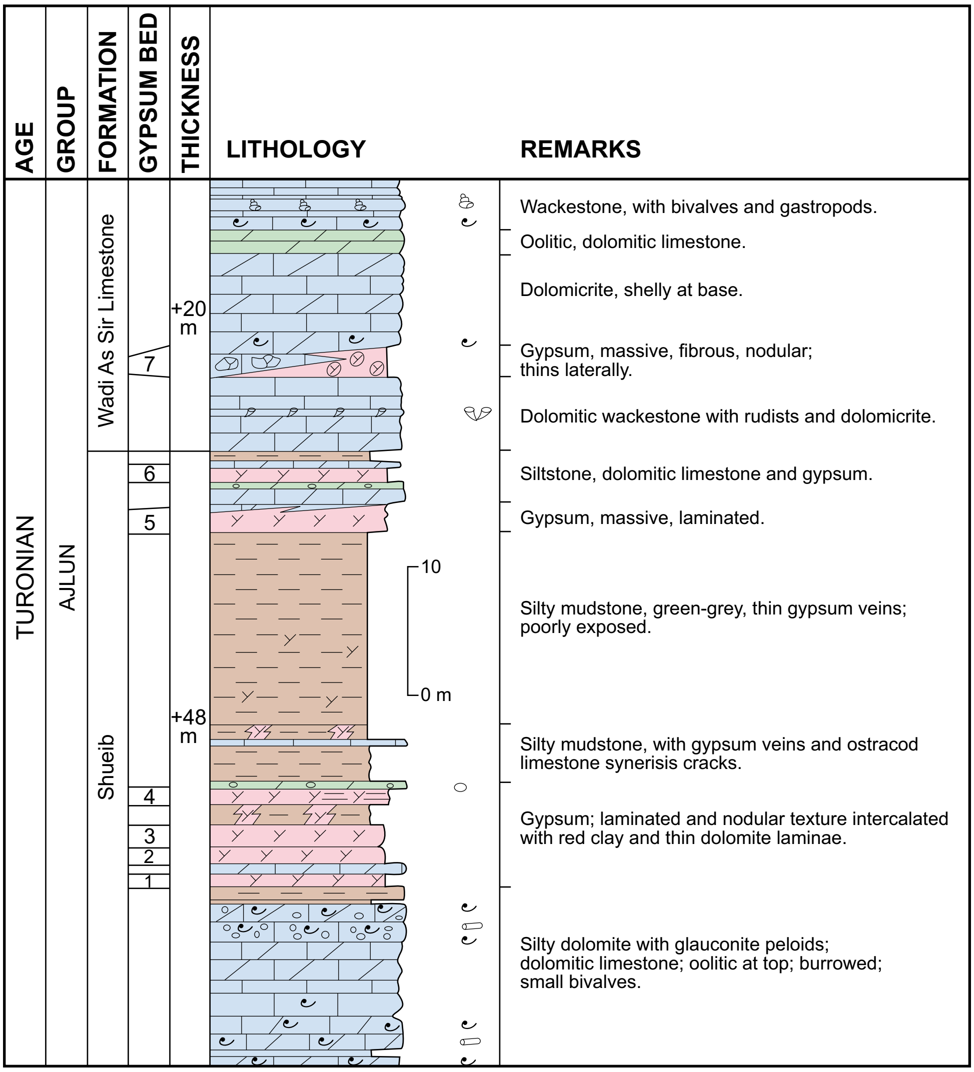

Figure 16: Graphic log of the peritidal-evaporite succession (regressive lowstand sequence) in the upper part of the Shueib Formtion, Wadi Mujib (after Powell, 1989).

Figure 17: Nodular (chicken-wire) gypsum and thin bedded limestone/marl marking the major Early Turonian low-stand (sabkha-salina facies) in the Shueib Formation, Wadi Mujib, north flank; hammer length 0.35 m (photo by J. Powell).

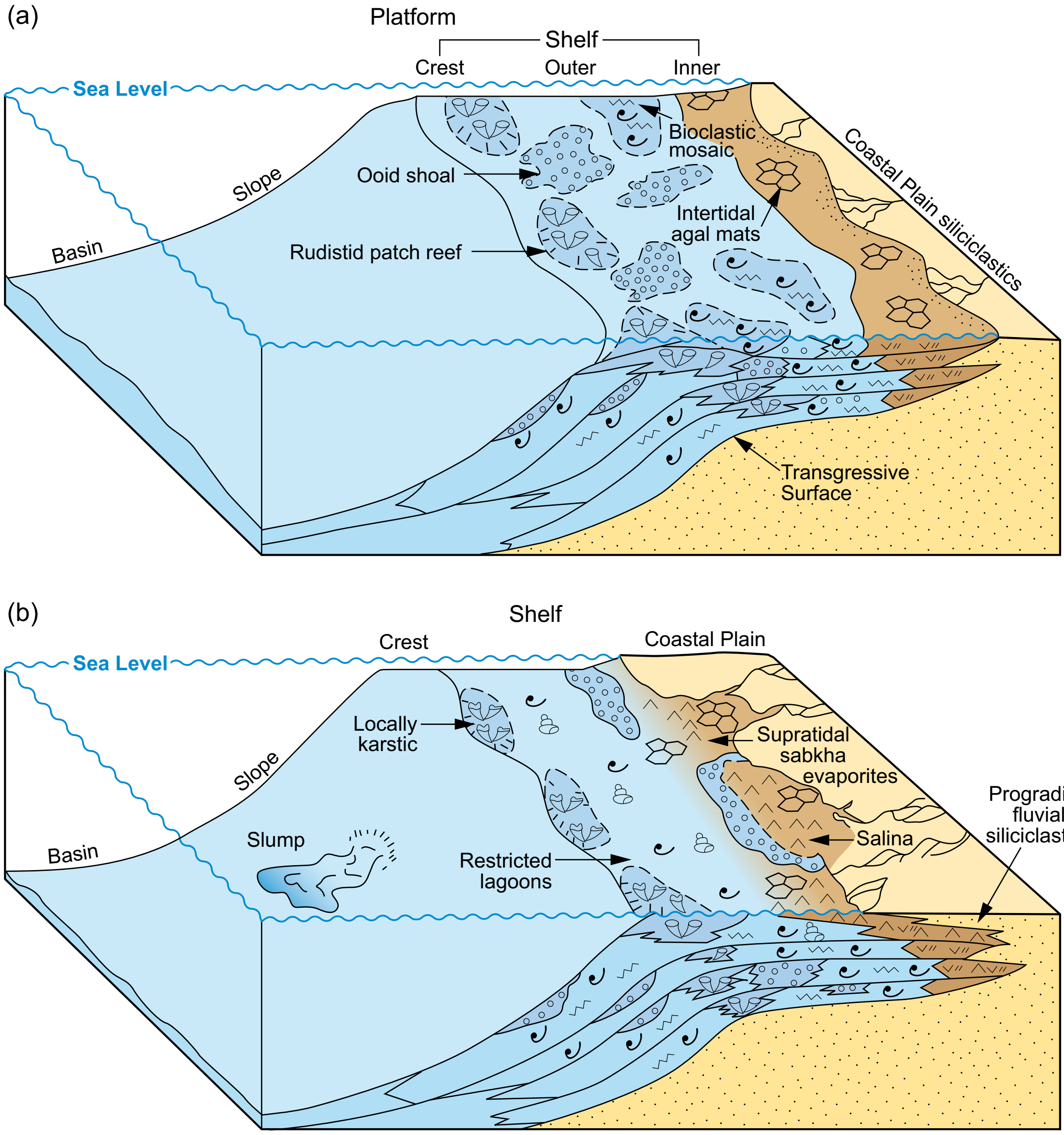

Figure 18: Diagrammatic facies models for the rimmed carbonate shelf: (a) transgressive and highstand sequences during Early Cenomanian (Naur Formation) and Mid- to Late Turonian (Wadi As Sir Formation) times; and (b) regressive lowstand (progradational wedge) during the Early Turonian (upper Shueib Formation).

with thin dolomite laminations (Figure 16). Thin laminae (ca. 4 mm) of fine-grained bioclasts (ostracods, bryozoa, shell fragments) and sparse ooids are present in the upper part of the association. Wavy-laminated gypsum with porphyroblastic texture is dominant, intercalated with millimetric-scale, clay-rich dolomite laminae (Figure 17). These textures suggest vertical evaporitic accretion in shallow, saline ponds (salinas) (Warren and Kendall, 1985). In addition, nodular (chicken-wire) texture and 'teepee' structures suggest deposition in sabkha environments (Abed and El-Hiyari, 1986; Schulze et al., 2004).

The depositional environment is interpreted as a series of small, possibly barred, depressions on a lowgradient, upper tidal flat (Figure 18), which were periodically breached by saline stormwaters driven onto the inner shelf. Evaporation of these brines in saline lagoons resulted in the deposition of finely laminated gypsum and clay (or clayey dolomite). Sabkha flats (nodular gypsum) may have developed seaward of the salina ponds. Bioclasts and ooids were probably deposited during storms, which transported this material from an offshore site to the upper tidal flat.

Figure 19: Upward-shoaling parasequences at the top of the Wadi As Sir Limestone Formation passing up to alternating chalk-chert-chalk pelagic ramp lithofacies (Wadi Umm Ghudran Formation, Belqa Group) – the basal Coniacian Mujib Chalk Member (1); Tafilah Member (2); and upper Dhiban Chalk Member (3) are clearly shown. Wavy bedded (penecontemporaneous) chert (4) of the overlying Amman Silicified Limestone (Campanian) forms the upper part of the section.

Pelagic Ramp Facies Associations (PR) – mostly Belqa Group

The lower part (Coniacian to Maastrichtian) of the Belqa Group (Table 2) mainly consists of chalk, marl, chert and phosphorite in central and north Jordan (Figures 6, 7 and 19); to the south and east (outside of the Azraq-Hamza Basin), quartz sandstone and fine-textured dolomite are common. Microcrystalline limestone concretions, coquinal grainstones and oyster bioherms are locally present. In the more rapidly subsiding, extensional Azraq-Hamza Basin a thick succession of claystone, sandstone, dolomite, chert and chalky limestone was deposited during Coniacian to Maastrichtian time (Andrews, 1992). The upper part of the group (Maastrichtian-Eocene) is more uniform in lithology and comprises a monotonous sequence of marl, chalky marl, and chalky limestone with chert beds and subsidiary microcrystalline limestone. However, nummulitic limestone is locally present in the Gharandal and Maan areas. Bitumen content is locally high in the marls and chalks (Speers, 1969; Abu Ajamieh, 1980; Abed et al., 2005). On the more stable ramp areas, the average sedimentation rate for the group was about 1.2 cm/Ky, but in the rifted Araq-Hamza Basin it was about 6.5 cm/Ky.

PR1: Pelagic Outer Ramp Association

This association consists of chalk composed of calcareous nanoplankton and planktonic foraminifera, locally with up to 50% detrital phosphatic skeletal fragments (francolite-dahlite), including fish teeth, and bivalve fragments at the base (Schneidermann, 1970; Magaritz, 1974; Powell et al., 1990). Magaritz (1974) concluded that the lower chalk, west of the Dead Sea Rift, showed evidence of meteoric lithification during a period of emergence; this may have been associated with intraformational folding and hardground development prior to deposition of the upper chalk (Powell et al., 1990).

Thin chert, locally interbedded with the chalk, consists of microquartz and cryptoquartz with chalcedonic quartz infilling fractures. SEM studies (Powell et al., 1990) reveal that it is composed of euhedral, bipyramidal microquartz with sparse silicified foraminiferal and coccolith ghosts, suggesting silicification of a mixed carbonate/siliceous sediment originally composed of siliceous microfossils such as diatoms, silicoflagellates, sponge spicules and radiolaria (Kolodny, 1969; Moshkovitz et al., 1983).

Figure 20: Penecontemporaneous, auto-brecciated chert fabric (Amman Silicified Limestone), Wadi Karak; lens cap 0.05 m diameter (photo by J. Powell).

PR2: Hemi-Pelagic Mid- to Inner Ramp Association

This association is characterised by laterally impersistent intercalations of chalk, porcellanite, chalky marl, chert and phosphorite. Chalks are petrographically similar to lithofacies PR1, but are generally less than a metre thick, and have a higher proportion of phosphate grains and siliceous microfossils. Porcellanite is usually pink, white or buff in colour, and is composed of siliceous microfossils including silicoflagellates (Moshkovitz et al., 1983). The presence of large displacive carbonate concretions, dolomitization, and silicification of the tripoli-laminated chert indicate early diagenesis.

Senonian chert in the region (Moshkovitz et al., 1983; Kolodny, 1969; 1980) is biogenic in origin (diatoms, silicoflagellates, sponge spicules, radiolaria), although much of the original sediment was either calcitic, or calciticphosphoritic. Silicification occurred during early diagenesis and proceeded through various stages to produce the distinctive chert textures (Figure 20), including early diagenetic breccias (Kolodny, 1969; Steinitz, 1981; Fink and Reches, 1983). It is not certain, however, whether fine lamination in the chert was due to primary variation in the concentration of siliceous microfossils in the sediment or to very early silicification of carbonate sediment at the seawater interface. The occasional presence of gypsum and anhydrite in the chert (Steinitz, 1977) may indicate periods of high marine salinity (stratified ocean), but not necessarily peritidal depositional environment.

A large proportion of the coarse-grained phosphorite (Figures 21 and 22) is recognisable as skeletal remains (fish and reptiles), which together with phosphomicritised oyster fragments and peloids indicate that the water column supported a rich, prolific nektonic fauna that was preserved in low Eh/Ph bottom conditions. Phosphomicritisation of the carbonate took place through a process of endolithic boring and cyanobacterial alteration in an anoxic (reducing) environment at, or above, the sediment-water interface (Soudry and Champetier, 1983; Powell et al., 1990) . The low diversity of foraminifera, diatoms and ostracods (Moshkovitz et al., 1983; Lifshitz et al., 1985) indicates a restricted environment, at least west of the Dead Sea Rift. Concentration of phosphate (francolite) in this unit, which reaches economic proportions along a NW-trending belt on the Jordan Plateau (Bender, 1974; Sunn'a, 1974; El-Hiyari, 1985; Abed and Kraishan 1991; Abed et al., 2007), resulted from high organic productivity in the Neo-Tethys Ocean (Flexer and Starinsky, 1970; Flexer and Honigstein,

Figure 21: Exhumed oyster bank showing mega cross-beds (large arrow indicates foresets) of oyster coquina, and onlap of phosphate-rich marls and chert (3); off-bank, the coquinal limestone between (1) and (2) is laterally equivalent to the oyster bank; Al Hisa Phosphorite Formation (Upper Campanian), Al Hisa; inset shows geopetal fabric in *in-situ* oysters; lens cap 0.05 m (photo by J. Powell).

1984; Soudry et al., 1985; Almogi-Labin et al., 1993). Initial concentration of phytoplankton may have been due to oceanic upwelling of nutrient-rich water from deeper parts of the ocean, with further concentration, by winnowing, on the inner ramp (Figure 23).

PR3: Oyster Biostrome/Bioherm Association

Cross-bedded, oyster grainstone (coquina), and low-diversity oyster banks (bioherms) cover large areas in central Jordan (El-Hiyari, 1985; Powell, 1989; Abed and Sadaqah, 1998). The oyster banks (Figures 21 and 24) developed and maintained relief above the sea-floor in a more turbulent zone, up to 20 m, above a critical level of anoxic, reducing, nutrient-rich water (Bartov and Steinitz, 1982; Powell, 1989). Oxygenation of the sea-bed resulted initially as a result of lower sea-level stands which developed along the shallow inner-shelf zone aligned north-northeast, that forms the present-day 'phosphate belt' in central Jordan (Figure 23).

Overturn of the water column by wave and storm effects on these highs enabled oysters to thrive, initially encrusting hardgrounds. Once initiated, vertical accretion of the oyster bioherms maintained

Figure 22: Thick dark grey, organic-rich marls overlying pale brown phosphorite ore body and overlain by chalk-chert-marl beds Al Hisa Phosphorite Formation (Upper Campanian), Abyad Phosphate mine (photo by J. Powell).

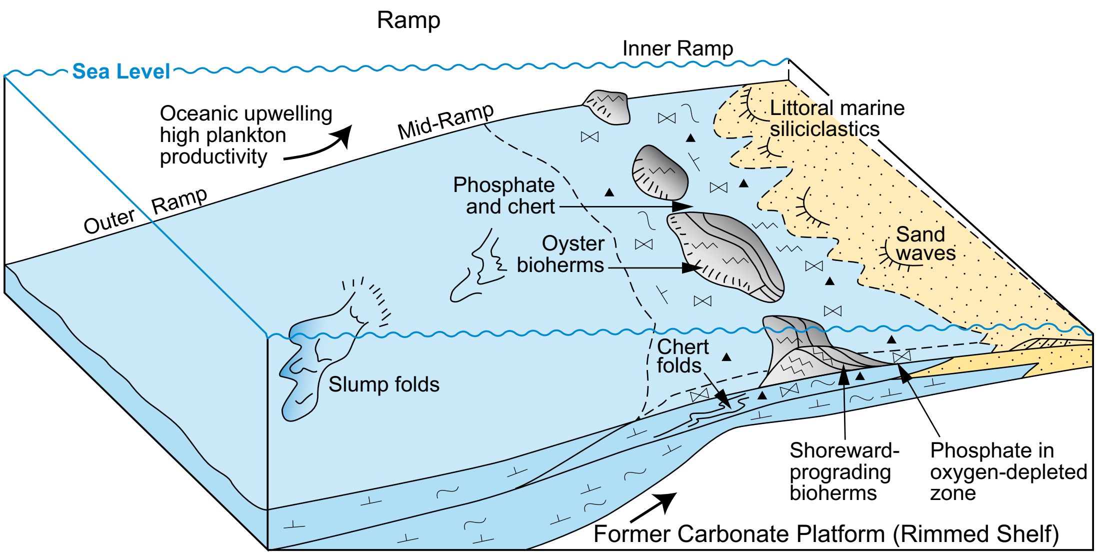

Figure 23: Diagrammatic facies model for the pelagic ramp facies associations (lower Belqa Group) during Santonian to Campanian time during deposition of transgressive pelagic and regressive shallower water sequences.

their relief above the basal, more anoxic, nutrient-rich water mass during rising sea level. Wave resistance resulted in increased turbulence and oxygenation on the tops of the bioherms (Figure 23). Shells were abraded and fragmented during storms, which swept grainstone shell debris off the banks as large-scale, shoreward prograding, foresets (Khdeir, 1974; Abed and Sadaqah, 1998). Off-bank, the grainstones were admixed with nektonic skeletal fragments and phytoplanton as level-bedded phosphatic grainstones. The large size (up to 25 cm length) and abundance of the oysters suggests that nutrient supply was high in the upper water column, and the contrast between both coeval faunas and sediment on- and off-bank, further implies that the water column was density-stratified.

Figure 24: Cross-section through an oyster bank showing core and lateral off-bank progradation (to left, east) of mega cross-beds; height of oyster bank ca. 30 m; (1) base of mega-cross bedded storm deposits overlying core facies; and (2) reactivation surface and new cycle of oyster coquina storm deposits. Sediments below the oyster bank comprise interbedded phosphorite, marl and chert (photo by J. Powell).

PR4: Shallow-Marine Siliciclastic Association

This predominantly consists of fine- to medium-grained quartz arenite, commonly with low-angle planar or hummocky cross-stratification, and locally intercalated with dolomite, porcellanite, chert and marl (Figure 25). Phosphatic fragments (fish bones and teeth) are locally common, and in some areas the sandstone is extensively bioturbated with long, subvertical burrows preserved. Low-angle planar and trough cross-bedding suggest deposition as sub-marine dunes and sand waves, respectively, in the shallow littoral zone.

PR5: Siliciclastic/Carbonate Shoal Association

This association consists of thick nummulitic packstones and grainstones, locally cross-bedded with a high proportion of quartz sand. Echinoids and bivalves are locally abundant. This association was deposited in agitated lagoon and shoreface environments.

DEPOSITIONAL SEQUENCES

Sequences recognised in the Cretaceous to Eocene succession in Jordan reflect various orders of genetically related strata (*sensu* Galloway, 1989; Sharland et al., 2001) bounded by maximum flooding surfaces (mfs) and/or sub-aerial or sub-marine unconformities or their correlative conformities (Mitchum, *in* Vail et al., 1977). Higher fourth- or fifth-order cycles are defined as parasequences or parasequence sets (Van Wagoner et al., 1988).

Careful observation of bounding surfaces and the lithofacies developed above and below, allow the relative basinward-landward shift of lithofacies belts to be determined and thus relative sea-level fluctuations on the platform. Critical boundaries observed in this study are major stratigraphic hiatus including subaerial erosion surfaces, hardground surfaces (important marine flooding and deepening events associated with sediment starvation), bioturbated horizons at the top of parasequences, and maximum marine flooding surfaces (MFS). These surfaces are more readily traceable at outcrop and at field mapping scale than correlative unconformities – hence the genetically related scheme adopted

Figure 25: Cenomanian – Turonian coastal plain facies (red marls, sandstones and thin limestones) overlain by green sandstone and chert of the Fassua Formation (Coniacian to Santonian) at Batn El Ghul, southeast Jordan; arrow marks the base of the Fassua Formation; Hijaz Railway in foreground; height of section ca. 230 m (photo by J. Powell).

here. Systems tracts (*sensu* Van Wagoner et al., 1988) cannot be defined categorically because of the difficulty of tracing time lines and critical boundaries from basinal sites, located west of the Dead Sea Rift, to platform and landward settings, east of the Dead Sea Rift. Consequently, in Jordan we see mostly evidence for inner- to mid-platform sequences from Cenomanian to Eocene times. However, we predict that second-order sequences and their bounding surfaces are present in the basinward areas (cf. Flexer et al., 1986). During 1:50,000-scale geological mapping that formed the basis of this study, third-order and fourth-order sequences, in the carbonate platform succession were traced approximately perpendicular to the palaeoslope along the Dead Sea Rift margins in Jordan (Figures 6 and 7). We predict that these signatures, boundaries and stacking patterns, reflecting third- to fourth-order cycles can be recognised in the succession to the west of the Dead Sea Rift.

Four orders of sequence can be determined, corresponding to cycles, primarily based on time, as recognised by Galloway (1989) and Vail et al. (1991), and recognised in part for the Arabian Plate (Sharland et al., 2001, 2004; Haq and Al-Qahtani, 2005). These correspond to: (a) mega-depositional sequences (second-order; 3 to 50 My); (b) large-scale depositional sequences (third-order; 0.5–3 My); (c) high-frequency sequences (fourth-order; 0.08–0.5 My); and (d) very high frequency (fifth-order; 0.03–0.08 My). The fourth- and fifth-order cycles correspond to carbonate parasequences as defined by Sarg (1988). Similar third- to fifth-order depositional sequences were identified in the Cenomanian to Turonian carbonate platform of Oman (van Buchem et al., 1996).

Megasequence 1: Berriasian to Albian Alluvial Plain Sequence (Kurnub Sandstone)

In central and southern Jordan (Karak to Ras En Naqb; Figure 4) deposition of the Kurnub Sandstone commenced, in Early Cretaceous time, with high-energy/high bed-load (high flux), braided rivers eroding and depositing mature siliciclastics (AP1) derived from the lower Palaeozoic sandstones at the margins of the Arabian Shield (Weissbrod and Nachmias, 1986; Amireh, 1992, 1997; Kolodner et al., 2009). During periods of relatively low water table, subaerial oxidation of floodplain deposits resulted in pedogenesis in the form of brunified ferruginous crusts (ferralitic palaeosols of Duchafour, 1982). Palaeocurrent flow was unimodal, predominantly towards the north-northwest or north-

northeast (Figures 5a and 10). The shoreline lay to the northwest, in southern Lebanon, and to the west in Sinai but third-order fluctuations in relative sea level resulted in southward, transgressive marine onlap (north Jordan: Abed, 1982a; Negev: Greenberg, 1968; Bartov et al., 1972; Bachmann et al., 2010) (Figure 4) across the geomorpholgically mature, low-gradient alluvial plain in north Jordan (AP3 and AP4, in basinward sequence). These oscillations of relative sea level were probably related to the effects of local flexural subsidence and extensional faulting (Bachmann et al., 2010) at the basin margin, since they cannot be traced in the hinterland fluvial succession of central and south Jordan. Increased accommodation space during relative sea-level rise is reflected in basinward progradation of paralic lithofacies. Uplift of the hinterland supplied abundant siliciclastic sediments during periods of high sediment flux.

During Aptian – Albian time, there was a gradual upward transition from braided stream lithofacies to deposition by predominantly high-sinuosity/meandering rivers on an alluvial plain of low to moderate geomorphological gradient (AP2) (Figures 10 to 12). Third-order fluctuations in relative sea level resulted in southward onlap of marine units in north Jordan and west of the Dead Sea Rift, where the alluvial/coastal plain was periodically invaded by the sea. A thin bed of oolitic, bioclastic limestone in north Jordan and the Negev (Figure 4) is probably equivalent to the Early Aptian MFS K70 (ca. 122.5 Ma) of Sharland et al. (2001) and Haq and Al-Qahtani (2005) representing marine transgression across the alluvial plain. Coastal onlap did not reach central and south Jordan until the Late Aptian – Early Cenomanian (AP3 and AP4, and the overlying Wadi Juhra Member; Figures 5, 7 and 12).

Towards the top of the sequence, throughout Jordan, the hinterland was eroded to produce a low-gradient alluvial plain of wide geographical extent, occupied by meandering rivers and coastal plain deposits (AP2 and AP3). The upward passage from braided stream facies to high-sinuosity, meandering channel facies in the upper part of the sequence (Figures 8 and 11) fits the alluvial model of Wright and Marriott (1993) which predicts that during periods of marine transgression, high-sinuosity/meandering channels and increased alluviation occur on the floodplain, due to increased floodplain accommodation. High water tables and poorly drained soil conditions are also reflected in the gleysol pedogenesis, plant colonisation and the formation of thin beds of coal in north Jordan (Figures 4 and 11). The upward change in fluvial depositional system is probably a result of progressive marine onlap during the Late Aptian through Albian times (Haq and Al-Qahtani, 2005). A Late Aptian (so-called 'Austrian') unconformity has been observed in many platform sequences in the Middle East and North Africa (van Buchem et al., 2002; Haq and Al-Qahtani, 2005) but has not been observed in the fluvial siliciclastic succession in central Jordan and, furthermore, has not been identified in the basinward carbonate settings to the west where continuous marine sedimentation took place (Bachmann et al., 2010). This suggests that regional intra-plate tectonics local to the Levant area was a controlling factor on sedimentation.

Megasequence 2: Late Albian to Turonian Rimmed Carbonate Shelf Sequence (Ajlun Group)

The upward change in Kurnub alluvial architecture, noted above, corresponds with the transgressive marine sequence observed in basinward areas such as north Sinai (Kuss, 1992; Bachmann et al., 2010). This is probably related to the long-term sea-level rise (second-order oscillation of Haq et al., 1988), which extended through the Cenomanian during the establishment of the rimmed carbonate platform (Figure 26). The development of a low-gradient coastal/alluvial plain in Late Albian times facilitated rapid marine onlap onto the hinterland in Late Albian – Early Cenomanian times (Figures 5b and 6). An approximately NE-trending, fluctuating shoreline was established in central-south Jordan.

In Jordan and surrounding areas the marked rise in sea level was accompanied by progressive, step-wise, marine onlap at around the Albian/Cenomanian boundary. This event is thought to be equivalent to Late Albian MFS K110 (ca. 101 Ma) of Sharland et al. (2001). The Ajlun Group megasequence internally comprises three large-scale depositional sequences (transgressive to highstand), recording successive south-eastward onlap from Cenomanian to Early Turonian times (Figure 26). The three large-scale sequences (third-order), described below, are separated by sequence boundaries (Type 2 unconformities), where only part of the platform was sub-aerially exposed.

Large-Scale Depositional Sequence (Ajlun 1)

This depositional sequence corresponds to the Naur Formation, and comprises transgressive to highstand parasequence sets (Figures 13 and 15).

Transgressive Parasequence Set: The initial shoreline advance across the hinterland is manifested in marine reworking of siliciclastics (AP4) (Wadi Juhra Member, Figure 4), deposited locally in paralic environments; quartz sand, locally rich in glauconite peloids, was reworked along an oscillating shoreline that reached as far south as the Dana area (Figures 6 and 7). Thin interbeds of dolomitic and clayey limestone with stunted, low-diversity faunal assemblages (monotypic cerithid gastropods, bivalves, and ostracods), drifted plant fragments and thin gypsum laminae indicate fluctuating salinities with environments ranging from brackish marine to high salinities in shallow evaporating lagoons (salinas). Taken together with intensive bioturbation, these features suggest deposition in the intertidal to subtidal zone of the coastal plain (Figure 18a) as the shoreline migrated south-eastward.

Late Transgressive to Highstand Carbonate Shelf Parasequence Set: Carbonate sedimentation was quickly established over a wide area on the shelf (ca. 250 km width) following a rapid relative sea-level rise in the Early Cenomanian. Sedimentation on the rimmed carbonate shelf was characterised by upward-shoaling cycles (parasequences), ca. 5–10 m thick (Figures 6 and 13), which are stacked as parasequence sets (broadly equivalent to the Naur Limestone and the Hummar Limestone).

Subtidal to intertidal carbonate sedimentation (RCS1 and RCS2) was uniformly established on the carbonate shelf over hundreds of square kilometres (Figure 18a). Three upward-shallowing cycles (parasequences) in the carbonate members (RCS1 to RCS2) are typified by passage from shelly wackestones, at the base, through intensely burrowed (*Thalassinoides)* skeletal wackestones, locally overlain by burrowed dolomite and micrite with a variety of large macrofauna (rudists, oysters). Supratidal, desiccated algal micrites (Powell, 1988) and subaerial erosion features (Abed and Schneider, 1982) indicate temporary emergence at the top of the cyles (Figure 15), the most marked of which is at the top of Naur Formation, and represents a sequence boundary of probable mid-Cenomanian age (Figure 26). The intervening marl and calcareous siltstone beds (RCS1) with a subtidal benthic fauna were deposited during subsequent phases of increased water depth on the inner shelf. Increased subsidence caused temporary deepening and low rates of carbonate accretion on the inner shelf.

Repeated upward shallowing, subtidal to intertidal parasequence cycles (Sarg, 1988) can be traced over wide areas of the platform and are interpreted as autocyclic response (fourth-/fifth-order minor relative sea-level fluctuations) to gradual platform subsidence (Ginsberg, 1971; Sarg, 1988; Hunt and Tucker, 1993; Shulze et al., 2004). Thus, biogenic carbonate accretion resulted in shoaling cycles from subtidal to intertidal zones with a concomitant decrease in accommodation space. Intervening marl-rich units were deposited during phases of rapid deepening of the water-column, probably caused by increased rates of subsidence (Ginsburg, 1971; Hardie and Shinn, 1986; Sarg, 1988). An alternative causal mechanism for these upward shoaling parasequences is precession (ca. 21 Ky) or obliquity (ca. 41 Ky) driven Milankovitch cycles (Gale, 1989).

During deposition of these mid- to inner-shelf lithofacies, coeval, rudistid-coral bioherms (RCS3) developed at the shelf crest (Bein, 1976; Ross, 1992) which separated the inner shelf from the deeper-water slope and basin, the latter characterised by the marly, calcareous siltstones (Talme Yafe Group; Bein and Weiler, 1976). Coeval, shallower-water *Thalassinoides* burrowed carbonates (RCS2), locally with rudistid biostromes (RCS), were established on the mid-shelf in north-central Jordan (Mukawir). During the initial transgression sea-level rise was not sufficiently high to submerge the coastal plain south of the Dana area, and it was not until 'late Naur' times that the shoreline transgressed south of Ras En Naqb (Figure 6).

Large-Scale Depositional Sequence (Ajlun 2)

This sequence comprises deeper-water, subtidal carbonate platform lithofacies, and corresponds, in upward order, to the Fuheis, Hummar and lower Shueib formations.

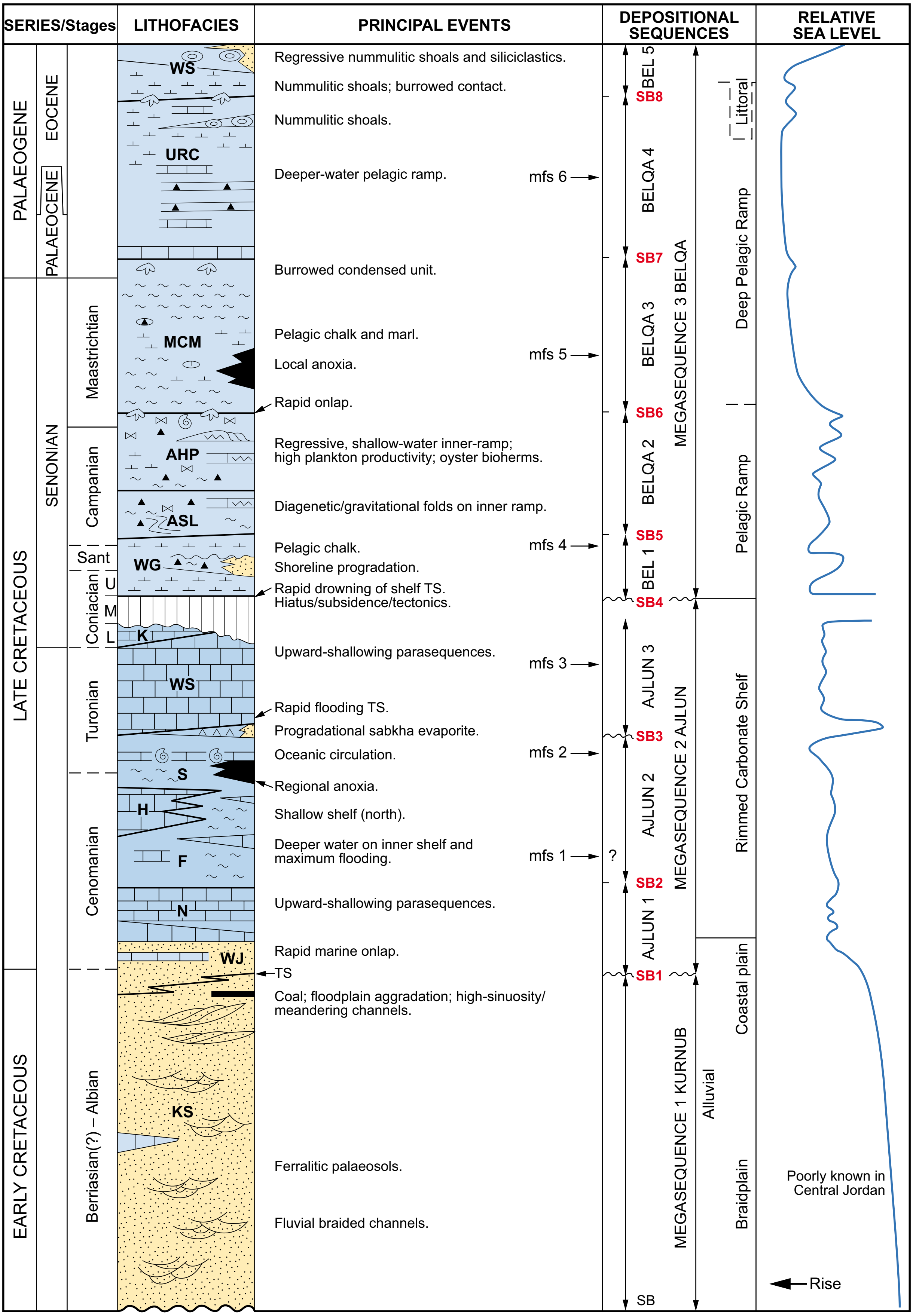

Figure 26: Schematic comparison of lithofacies, principal events, depositional sequences and relative sea-level curve for the Cretaceous and Palaeogene succession in central Jordan. Lithostratigraphic abbreviations as in Table 1. SB: Sequence Boundary; TS: Transgressive Surface; mfs: maximum flooding surface.

The base is taken at the intertidal/supratidal surface (Sequence boundary, SB 2) at the top of Sequence Ajlun 1, which corresponds with the top of the Naur Formation. This is overlain by deeper-water marls and thin-bedded calcareous mudstone/limestone beds. The maximum flooding surfaces are identified by marl (locally bituminous and gypsiferous), thin-bedded limestone and calcareous mudstone, with an abundant, diverse shelly macrofauna and abundant planktonic foraminifera (Fuheis Formation; Figures 6 and 7) thought to be equivalent to Early Cenomanian MFS K120 (98 Ma) of Sharland et al. (2001) and Late Cenomanian to Early Turonian OAE 2 event (Schulze et al., 2004; Wendler et al., 2010) which is probably equivalent to MFS K130 (ca. 95 Ma) of Sharland et al. (2001). These lithofacies (RCS1) were deposited in marine subtidal to restricted-lagoonal depositional environments resulting from continued subsidence and marine onlap, following subsidence and blanketing of the intertidal, inner carbonate platform. In north Jordan (Figure 7), however, local shoaling conditions, probably resulting from reduced subsidence, are represented by the bioclastic carbonates (RCS1, 2 and 3) of the Late Cenomanian Hummar Limestone (ca. 20 m thick) which contains subtidal oyster-rudist biostromes, and which may have become temporarily emergent, resulting in early dolomitisation. Carbonate shoals prograded basinward, and are capped by a local sequence boundary in central-north Jordan.

The overlying bituminous marl lithofacies (mfs 2; Figure 26) was probably the result of localised deepening of the water column and restricted water circulation, resulting in sea-bed anoxia on the inner shelf. Coeval bituminous facies have been described from boreholes in the Azraq-Hamza Basin (Andrews, 1992). Increased water depth on the shelf during this Late Cenomanian to Early Turonian highstand sequence reflects the Late Cenomanian to Early Turonian oceanic anoxic event (OAE 2), which is attributed to a eustatic sea-level rise that can be traced throughout the Neo-Tethyan realm (Jenkyns, 1980; Gale, 2000; Wendler et al., 2010) (see later discussion). It is probably equivalent to the regional MFS K130 (ca. 95 Ma) of Sharland et al. (2001) and clay-rich mudstones in Oman (van Buchem et al., 1996, 2002); in Jordan this flooding surface marks the maximum Late Cenomanian transgression along the Ras En Naqb escarpment (Figure 6). Further south (i.e. shorewards, Figure 6) the shallow subtidal-intertidal platform was colonised by corals, stromatoporoids and algae (Naqb Limestone; RCS1 and RCS2).

This deeper-water sequence is overlain by a thin, shelly wacke-packstone bed (Walla Limestone Member; Figure 14), which contains large benthic bivalves, gastropods and abundant macroconch ammonites (*Choffaticeras pavillieri*, *Ch. luciae Thomasites rollandi*, and *Fagesia lenticularis*), representing re-establishment of the carbonate platform and deposition in shallower, more oxygenated bottom conditions. The macroconch ammonite fauna (Early Turonian age) can be correlated throughout the region (Freund, 1961; Freund and Raab, 1969; Powell, 1989; Shulze, 2004; Aly et al., 2008; Wendler et al., 2010) and suggests maximum onlap (mfs 2, Figures 6 and 26) and full connection with the open-marine Neo-Tethys Ocean. The ammonite bed (Walla Limestone) represents a short-lived transgressive sequence overlain by deeper-water globigerina marls, which are probably equivalent to the MFS K140 (93 Ma) of Sharland et al. (2001) at the base of the LA4 Ajlun cycle of Andrews (1992). Shorewards (Figure 6) the carbonate is increasingly dolomitised, a precursor to the overlying Regressive Lowstand Parasequence set described below.

Large-Scale Depositional Sequence (Ajlun 3)

This sequence (Figure 26) comprises a regressive lowstand parasequence set, transgressive and highstand sequences, and corresponds to the uppermost part of the Shueib Formation, Wadi As Sir Limestone and, locally, the Khureij Limestone.

Regressive, Lowstand Parasequence Set (Salina/Sabkha): The regressive fluvial siliciclastic/sabkha/salina unit (uppermost Shueib Formation; Figure 16) marks a regional lowstand sequence with a sequence boundary (SB3) at its base (Figures 17 and 18b). A peritidal facies association (RCS4) was deposited on the inner part of the shelf; this passed south-southeast to rippled and trough cross-bedded, fluvial sand (AP3) locally inter-bedded with mud, and deposited by rivers prograding northwards across the coastal plain (Figure 18b). This regressive phase was terminated, regionally, by submergence of the shelf and adjacent, low-gradient alluvial plain by transgressive-highstand carbonate parasequence set (Wadi As Sir Limestone).

This lowstand event is apparent in the Early Turonian sea-level curves for both Levant (Figure 26) and NE Egypt (Kuss, 1992). It may have resulted from geomorphic uplift (cf. Schumm, 1993) of the North African/Arabian craton and concomitant fluvial progradation, since it has not been observed on global sea-level curves (Haq et al., 1988), although it may be equated to the Early Turonian lowstand below K140 (93 Ma) recognised by Haq and Al-Qahtani (2005). In central and south Jordan, the sequence boundary (SB3) between the lowstand peritidal/fluvial sequence and the underlying carbonate platform sequence (Ajlun 2) represents a Type 2 unconformity (Sarg, 1988) where only the inner part of the platform is subaerially exposed (Figure 18b).

Highstand Carbonate Shelf Parasequence Set: The overlying platform carbonate sequence (Wadi As Sir Formation) represents renewed transgression and rapid marine onlap, which extended eastward from near the present Mediterranean coastline to a palaeoshoreline (Figure 18) located close to the Saudi Arabia border (Jabal Waqf as Suwan, Zakimat Al Hasa, Azraq-Hamza Basin; Figures 1a and 5b). It represents a transgressive, highstand and maximum marine flooding sequence on the rimmed carbonate shelf during the Turonian (mfs 3, Figure 26), although the palaeoshoreline did not migrate more than a few tens of kilometres further east than during the earlier (Cenomanian) phase of the rimmed carbonate platform. At outcrop, the parasequence set is about 200 m thick, but it thickens in differentially subsiding sub-basins such as the Azraq-Hamza (ca. 250 m) and north Irbid (ca. 340 m) areas (Andrews, 1992). Rudistid biostromes, bryozoan banks, laterally wedging gypsum beds and algal micrites with monotypic ostracod and cerithid gastropod faunas, at the base of the sequence (Figures 16 and 28), indicate that shallow subtidal to intertidal conditions prevailed over central and southern Jordan during the initial transgression over the peritidal coastal/alluvial plain. To the north, in the Irbid area (Figure 1) the sequence is thicker, and the basal lithology is again poorly fossiliferous micrite and dolomicrite, interpreted as quiet-water lagoonal sedimentation, overlain by shallow-water molluscan packstone banks (Moh'd, 1985).

During Turonian to Early Coniacian times, upward-shoaling parasequence sets, about 3–5 m thick, comprising beds of shelly wackestone, grainstone and algal micrite, with burrowed tops, aggraded vertically on the platform. There was a balance between carbonate accretion, and both subsidence and compaction (cf. 'keep-up' carbonate system of Schlager, 1981), so that shallow water depths (ca. 5–20 m) were maintained (Figure 18a). Intertidal facies and emergent features were developed, locally, at the top of upward-shallowing parasequences sets in north Jordan (Moh'd, 1985). Ooids and rudist bioclasts (Figures 6 and 18a) found in inner-shelf locations in central Jordan were probably redistributed shorewards by storms from their original platform-margin sites of formation (tidal shoals and/or rudist reefs, respectively).

Rudistid banks associated with coarse grainstones and pedogenic calcretes in the middle of the section in north Jordan (Moh'd, 1985), interpreted as seaward of the inner-shelf lagoon, indicate periodic emergence (Figure 29a). Quartz sand lenses intercalated with these carbonates in the Wadi Mujib and Karak areas were probably dispersed onto the platform from the coastal plain by storm surge-ebb events. In central Jordan, coeval ooid shoals (Wadi Mujib), chalky micrites (Wadi Karak) and shelly wackestones (Wadi Hisa) were variably developed (Figures 6 and 7), suggesting that local currents, and micro-relief on the platform produced a mosaic of carbonate lithofacies, dependent on local biogenic activity and hydrodynamical regime (Figure 18a). Thick, monotonous beds of unfossiliferous micrite with *Thalassinoides* burrowed tops (Wadi Abu Khusheiba) indicate vertical accretion of lime-mud in shallow-water lagoons, with periodic shallowing leading to bioturbation of substrates at the top of individual (1 to 3 m thick parasequences). The upper burrowed surfaces of these cycles probably represent 'firmgrounds' formed during brief phases of low accommodation on the platform.

In north Jordan the upper part of the sequence consists of foraminiferal-peloidal micrites and subsidiary molluscan wacke-packstone (Moh'd, 1985) indicating a return to shallow-water lagoonal sedimentation with local shell banks. Further south (Amman, Madaba, Karak; Figure 6) shell and ooid-rich wackestone/packstones are present at the top, suggesting that slightly shallower, shoal conditions prevailed here.

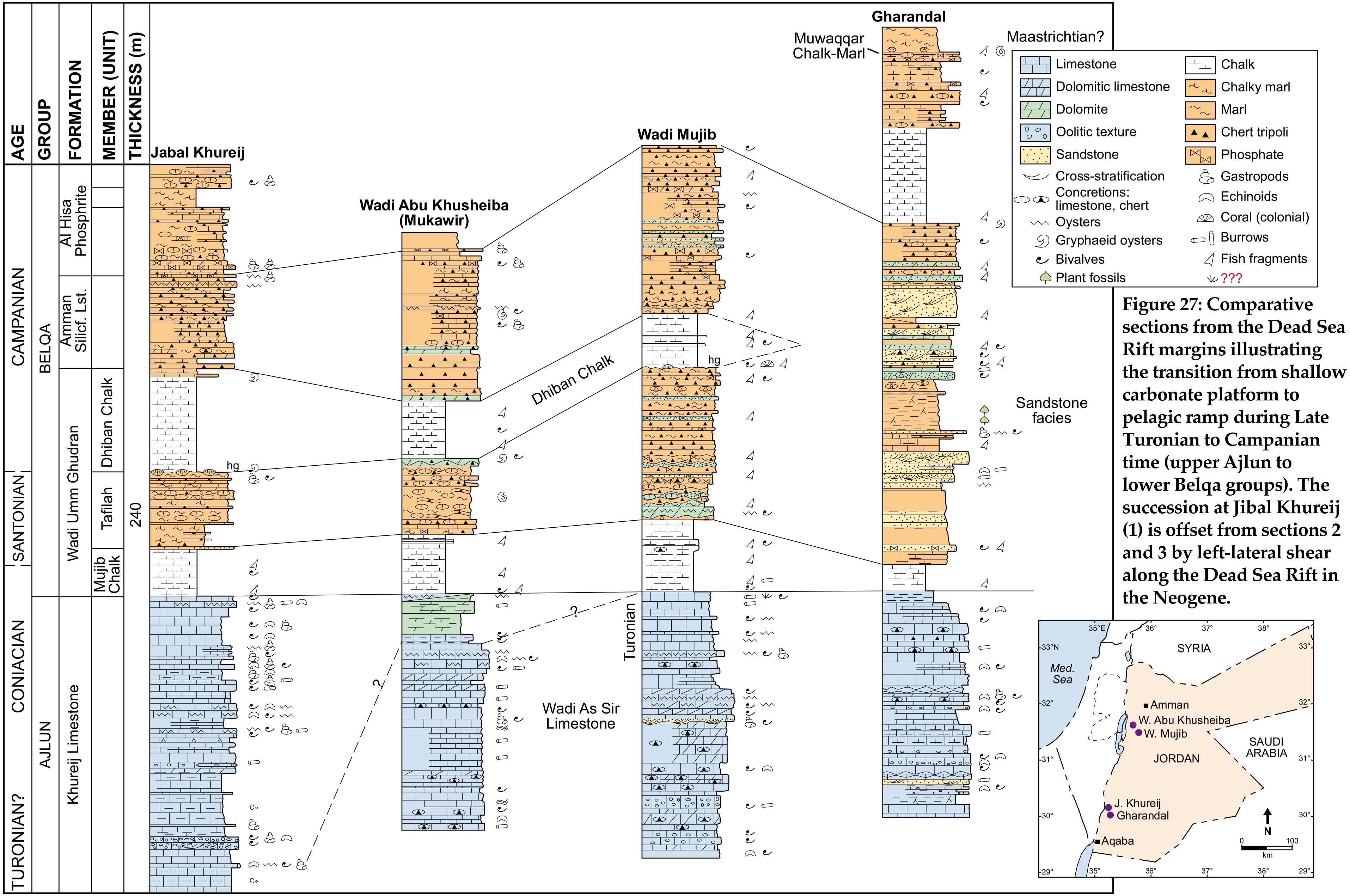

Figure 27: Comparative sections from the Dead Sea Rift margins illustrating the transition from shallow carbonate platform to pelagic ramp during Late Turonian to Campanian time (upper Ajlun to lower Belqa groups). The succession at Jibal Khureij (1) is offset from sections 2 and 3 by left-lateral shear along the Dead Sea Rift in the Neogene.

Farther south in the Gharandal-Ras En Naqb area, variably dolomitised, shelly wackestones and oyster packstones were deposited in shallow subtidal environments on the inner part of the platform. Here, the presence of locally dolomitised oyster packstones may indicate brief emergence. A fluctuating shoreline in the Ras En Naqb area is indicated by the presence of a wedge of cross-bedded siliciclastics, deposited in a fluvial or coastal plain environment (Figures 6, 18 and 29). In the Gharandal area (Figures 6 and 7) sandy (quartz) dolomites with calcite and quartz-filled druses (possibly of evaporite origin) are present at the top of the unit, and together with glauconite and drifted plant fragments, indicate shallow-water deposition near the shoreline. Similar peritidal/evaporite facies have been described in the upper part of the unit in cores from the Azraq area (Andrews, 1992) suggesting a northwest-trending belt of shoreline facies.

In the Batn El Ghul area (southeast) Cenomanian to Turonian siliciclastics (Figures 6 and 25), coeval with platform carbonates (Ajlun Group), comprise meandering or low-sinuosity fluvial facies associations (AP 2), which are locally intercalated with marginal marine facies (AP3). The major Sequence Boundary (SB1) that marks the change from fluvial/paralic to carbonate platform environments along the Dead Sea Rift in central Jordan is present in the Batn El Ghul sequence at the change from fluvial- to coastal plain-lithofacies in the Batn El Ghul area.

The upper part of the rimmed carbonate platform sequence (Ajlun Group) in central Jordan and the West Bank, is generally considered to be of Late Turonian age (Wetzel and Morton, 1959; Basha, 1978; Dilley, 1985; Andrews, 1992; Shulze et al., 2004). It is overlain unconformably (disconformably) by the Coniacian pelagic chalk (Belqa Group) in the west, but passes both laterally and vertically to siliciclastic facies to the southeast, and in the Azraq-Hamza Basin (Figures 6 and 7). The depositional hiatus probably spans Late Turonian to Mid-Coniacian time, and the major change in lithofacies (see below) marks a major regional sequence boundary (SB4) at this level (Figure 26). However, evidence from the Sinai and Negev (Lewy, 1975) and from the Jordan Dead Sea Rift margin (Powell et al., 1988) shows that early-Mid Coniacian shelf carbonates (RCS1 to RCS3) (Figure 27) are locally preserved in small sub-basins, also overlain by Upper Coniacian to Campanian pelagic chalks (basal Belqa Group). Equivalents of Late Coniacian shelf carbonates were removed by subaerial karstic erosion over parts of the locally emergent platform such as the West Bank (Arkin and Hamaoui, 1967; Weiler and Sass, 1972). In central Jordan, where well-developed karstic surfaces are absent, the interval may represent a submarine depositional hiatus prior to a drowning unconformity (cf. Schlager, 1992). This interval is referred to as the 'Middle Turonian Unconformity' by Haq and Al-Qahtani (2005) and is attributed to onset of ophiolite obduction on northeast Arabia (see below).

Sequence Boundary SB4: Drowning of the Rimmed Carbonate Shelf

A rapid fall in sea level in Late Turonian to Early Coniacian time resulted in a depositional hiatus (possibly from Early to Mid-Coniacian) and local karstification on the platform (West Bank). This event is attributed to tectonic (intra-plate) foundering, subsidence and tilting of the platform margin possibly linked to ophiolite obduction on northeast Arabia (Haq and Al-Qahtani, 2005), and is also associated with extensional rifting in the Azraq Basin. The event marks a change from predominantly shallow-water carbonate sedimentation on a broad, rimmed shelf (Sass and Bein, 1982) to a low-gradient pelagic ramp association of chalk, chert, and phosphorite, which passed shorewards to marine and fluvial siliciclastics during Coniacian to Maastrichtian time (Figure 6). The rapid Late Coniacian rise in sea level resulted in drowning of the carbonate-shelf, extensive marine onlap and the establishment of a wide homoclinal ramp, with its point of tilt close to the present-day Saudi Arabia border (Figure 29). The rapid fall and subsequent rapid rise can be traced as a major sequence boundary throughout the region (Harris et al., 1984; Flexer et al., 1986; Camoin, 1991; Kuss, 1992; Sharland et al., 2001; Schulze et al., 2005; Haq and Al-Qahtani, 2005). However, the boundary is not precisely synchronous with the Late Turonian lowstand recognised on the global curve (Haq et al., 1988), during which this region was a period of stable rimmed carbonate shelf development (e.g. Wadi As Sir Limestone). The basal (Mujib) pelagic chalk represents the Early Coniacian MFS K150 (88 Ma) of Sharland et al., (2001).

The transition represents a drowning unconformity (cf. Schlager, 1981), which geometrically resembles a lowstand unconformity, but in reality the transition occurs during a major rise or highstand of sea level (Schlager, 1992). The disconformity-unconformity resembles a Type 2 unconformity (Van Wagoner et al., 1988). Although subaerial palaeokarstic erosion at the top of the rimmed carbonate-shelf has been reported west of the Dead Sea Rift (Weiler and Sass, 1972), the boundary in central Jordan is remarkably planar at local outcrop scale (Figures 13 and 19). Small fissures, ca. 0.05 m deep, at the top of the Wadi As Sir Limestone, locally infilled with detrital chalk, are occasionally present, but extensive hardgrounds with endolithic burrow surfaces have not been observed. The preservation of Late Coniacian platform carbonates in isolated, locally subsiding sub-basins in Sinai and south Jordan (Lewy, 1975; Powell et al., 1988) suggests that the disconformity surface represents a submarine depositional hiatus during Late Coniacian times over much of central Jordan.

The abrupt change from rimmed carbonate shelf to pelagic ramp was associated with a change in ocean productivity, nutrient supply, biogenic sediment production and sea-water chemistry, which resulted in a profound change in sedimentation. Causal factors may have been changes in ocean configuration (Scotese, 1991) and concomitant marine circulation patterns, resulting from mid-oceanic rifting (Flexer et al., 1986) or subduction/obduction of the Semail Ophiolite in Oman (Sharland et al., 2001; Haq and Al-Qahtani, 2005). Associated crustal extension and rifting on the Arabian Craton during Coniacian to Maastrichtian times is indicated by rapidly subsiding Araq-Hamza Basin (Figure 5b; Andrews, 1992).

Megasequence 3: Coniacian to Eocene Pelagic Ramp Sequence (Belqa Group)

Belqa Group sedimentation is conveniently described in terms of genetic depositional sequences (*sensu* Galloway, 1989), which reflect marine onlap/offlap, and the development of lithofacies belts of related to varying water depth, on a predominantly hemi-pelagic/pelagic carbonate ramp (Figure 29c). Subtle variations in slope geometry on the ramp are reflected in gradational depositional environments (Burchette and Wright, 1992). These pass, shorewards, from deeper-water chalk and marl associations (PR1) in the northwest, through hemi-pelagic mid- to inner-ramp associations (PR2) and oyster bioherm associations in central Jordan, to shallow-marine dolomite or marine-siliciclastic associations (PR4 and PR5) in south and east Jordan. Incipient folding during the Coniacian to Maastrichtian, associated with the development of the Syrian Arc (Chaimov et al., 1992; Shahar, 1994), is well developed west of the rift within the Levant Plate (Cohen et al., 1990), but the area to the east (Arabian Plate) was not subjected to such intense, intra-plate compressional folding. Consequently, growth folds, which affected sedimentation in the Negev area during Coniacian to Maastrichtian times (Cohen et al., 1990), are not apparent on the mid- to inner-platform (central Jordan), with the result that Belqa Group facies belts and sequences can be traced over a wide area on the relatively stable part of the platform. However, in the Amman area (north Jordan) compressive folds are thought to have been initiated in Coniacian to Campanian times (Mikbel and Zacher, 1986), resulting in deposition of shallow-water chert compared to deeper water chalks typical of the stable ramp located to the south.

Large-scale Depositional Sequence (Belqa 1)

Transgressive Pelagic Parasequence Set: The Coniacian transgressive parasequence (Wadi Ghudran Formation) is represented by the lower Belqa chalks (PR1) and coeval marine siliciclastics (PR4) in shoreline locations (south and east).

Pelagic chalk associated with the Late Coniacian transgression was deposited over a wide area of the Arabian Craton during Late Coniacian to Santonian time (Lewy, 1975; Powell, 1989; Kuss, 1992). Deposition of the basal chalk in Jordan (Figures 13 and 19) was affected by local tectonics, so that the sequence in the Amman area is attenuated compared to more rapidly subsiding areas to the north (Irbid) and south (Karak). The presence of detrital, phosphatic chalk with laminated 'flamey' texture (Figures 27 and 28) overlying the slightly irregular, upper surface (SB 4) of the Ajlun Group, suggests submarine erosion or corrosion, followed by the deposition of allochthonous chalk, possibly resulting from turbulent fluid-flow on the seafloor (Bromley and Ekdale, 1987). The overlying pelagic chalk contains benthic foraminifera, scattered bivalves including oysters and *Thalassinoides* burrows suggesting deposition in a shallow realm, probably ca. 20–50 m water depth.

In south Jordan (Tafilah to Ras En Naqb), coeval siliciclastics (Alia Formation) sourced from lower Palaeozoic sandstones in the hinterland were deposited along the coastal margins (Batn El Ghul; Figures 6, 23 and 25). The shoreline eventually transgressed south-eastward over this area during the Maastrichtian; siliciclastics were deposited in small-scale, tidal channels and inshore bars in the coastal plain. Sand was dispersed north-westwards where it was intercalated in the littoral zone, with shallow-water carbonates (dolomite) and pelagic chert (Dana-Shaubak area; Figure 7). Trough cross-bedding in some sandstone beds in the Dana-Ras En Naqb area indicates shallow-water deposition as submarine dunes. Local subsidence in the Gharandal area (Figure 27) resulted in deposition of pelagic chalk similar to the areas in the north.

North-westward progradation of the Alia Sandstone and Tafilah Member lentils (Figures 7 and 27) in south Jordan, during the Santonian, probably resulted from a combination of renewed geomorphic uplift of the hinterland source area, and increased accommodation space on the inner ramp resulting from marine onlap. Fluvial siliciclastic facies were deposited on the coastal plain; gypsiferous siltstone with plant fragments indicates paralic coastal swamps in the Gharandal area. Quartz sand was dispersed and reworked offshore by storm and wave energy into a bioturbated sand 'blanket' (Alia area) and large-scale cross-stratified sand bars (Figure 23), which developed further offshore (Tafilah-Wadi Hisa area). Pelagic sediments (chalky marl and chert) intercalated with the quartz sandstone suggest periods of quiet-water sedimentation interspersed with periods storm or ebb-surge deposition within storm wave-base, represented by cross-stratified, bioturbated sandstones. This sandy unit passes basinwards to dolomite, chalk, dolomitic chalk, laminated chert and marl in the Karak-Madaba area (Tafilah Member) as shallow-water pelagic sediments become more dominant offshore (Powell, 1988, 1989).

In Wadi Mujib (Figure 28) a locally developed oyster-coquina at the base of the Tafilah Member is completely altered to coarse-crystalline dolomite with shell voids, suggesting early dolomitization due to temporary emergence or, perhaps, penecontemporaneous hydrothermal alteration. Chalk sedimentation appears to have been continuous in north Jordan during this phase (Santonian). South of Amman (Figure 27) intraformational folding and hardgrounds developed (erosion and bioerosion, and encrustation by oysters and corals) prior to deposition of the Dhiban Chalk (Powell et al., 1990). This depositional hiatus and subsequent flooding surface (SB 5) can be traced over tens of kilometres (Figure 7) and the overlying chalk may be represent the Santonian MFS K160 (85 Ma) of Sharland et al. (2001). The lowermost part of this overlying Dhiban Chalk is rich in detrital fragments (cf. Mujib Chalk) and marks the base of a second upward-shallowing cycle (parasequence) from chalk to chert/marl/sandstone (Figure 28). Subsequent to the initial turbulent flow of allochthonous detrital chalk, more uniform deeper-water conditions prevailed during deposition of pelagic chalk during the Early Campanian in central Jordan. During this time, the area south of Tafilah and in the east of the country was the site of shallow-water siliciclastic or dolomite-chert sedimentation (Andrews, 1992).

Large-scale Depositional Sequence (Belqa 2)

Regressive, Shallow-Water, Inner-Ramp Parasequence Set: Upward passage to shallower-water, chalky marl-chert-phosphorite association (PR2) with bio-eroded hardgrounds on the inner ramp, reflects oscillating sea level and depositional hiatuses (fourth-/fifth-order cycles) during Santonian and Campanian times (Figures 23 and 28). This was associated with penecontemporaneous, gravitational, down-palaeoslope slump-folding in some units. Lowstands on the inner ramp are represented by shoreward progradation of oyster banks (PR3) in the oxygenated zone, and coeval concentration and winnowing of phosphorite in anoxic (low Eh/Ph), level-bottom conditions. A condensed phosphorite unit with extensive *Thalassiniodes* burrows marks the top of this sequence (SB 6).

A fall of relative sea level during the Mid-Campanian times resulted in shallower water depths on the inner-platform (central Jordan), and deposition of PR2 facies association, comprising thick-bedded,

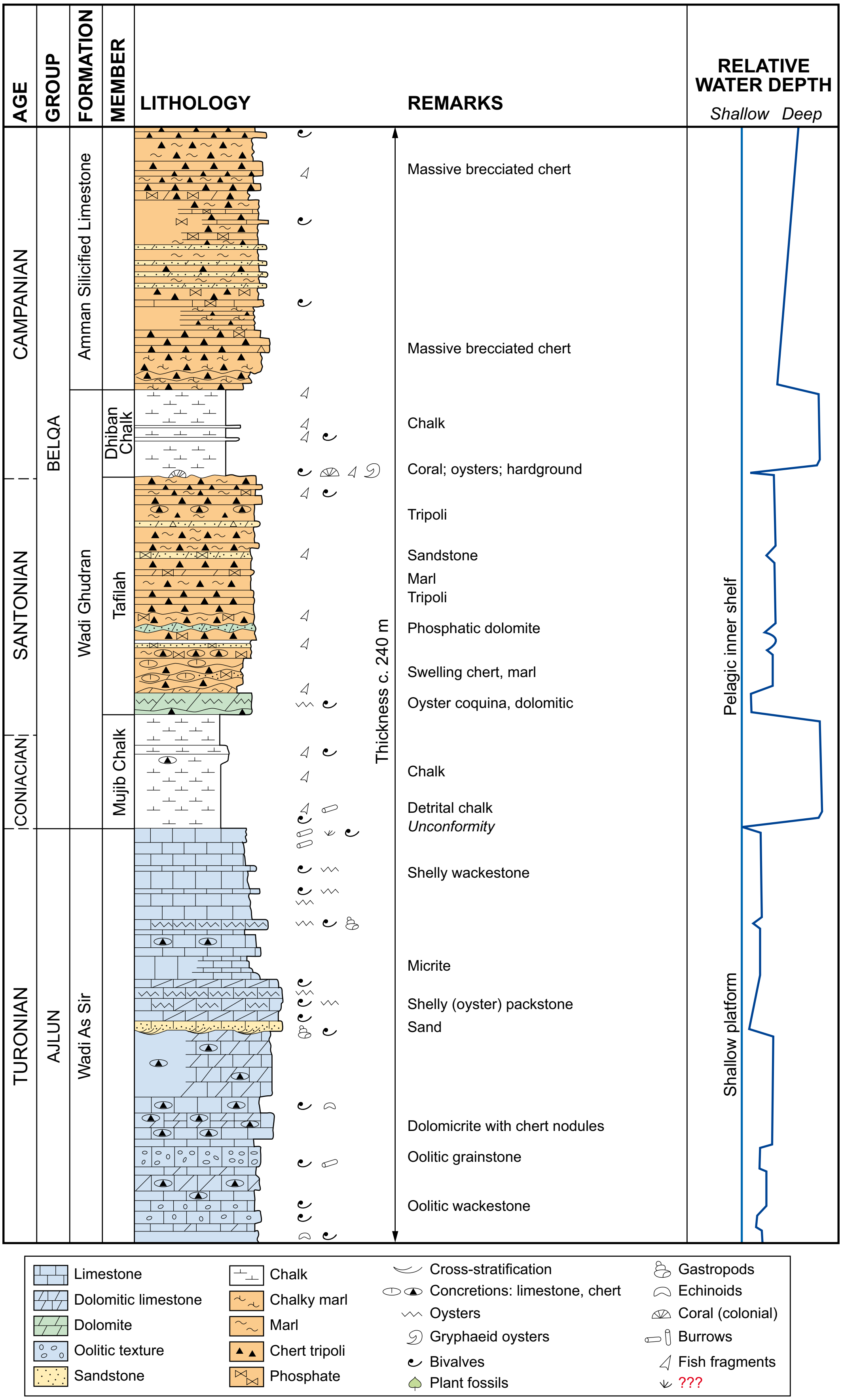

Figure 28: Graphic log of the Turonian to Campanian succession in Wadi Mujib. Symbols as in Figure 4.

auto-brecciated and laminated chert, chalky marl, porcellanite and subsidiary phosphorite (Amman Silicified Limestone). Further oscillations in relative sea level are manifested in the overlying strata (Al Hisa Phosphorite) which, in addition to the lithofacies of PR2, includes thick beds of economic phosphorite, locally rich in organic matter (Sunn'a, 1974; El-Hiyari, 1985; Powell, 1989; Abed and Kraishan, 1991; Kolodny and Garrison, 1994; Pufahl et al., 2003; Abed et al., 2007) and cross-bedded oyster banks (PR3) (Figure 23). Concentration of phosphate in the NS-trending 'phosphorite belt' is attributed to a number of factors. These include: (1) high organic productivity on the oyster banks that produced abundant carbonate clasts for phosphatization; (2) winnowing and concentration of nektonic skeletal fragments and phosphatized grains, particularly in the topographically low areas between oyster banks; and (3) relatively low subsidence rate and low pelagic sedimentation rate (chalk-chert) resulting in a series of condensed sequences in this facies belt, compared to deeper-water, basinal areas to the west (Mujib, Karak). A similar relationship was noted between anticlinal and synclinal facies in the Negev, where phosphate is concentrated in condensed successions on the highs (Soudry et al., 1985).

Regional studies (Flexer, 1968; Flexer and Honigstein, 1984; Powell, 1989; Glenn and Arthur, 1990; Abed and Kraishan, 1991) have shown that sediment type was controlled predominantly by water depth and plankton productivity across the ramp. Thus, chert-carbonate facies, rich in ostracods and siliceous microfossils, were deposited in the midramp (north and central Jordan) whilst chalk, rich in calcareous nanoplankton and pelagic foraminifera, typifies deeper water settings on the outer-ramp. Shallow-water conditions on the midramp are further substantiated by the crossbedded coquinal grainstones in central Jordan (Khdeir, 1974; El-Hiyari, 1985; Powell, 1988; Abed and Sadaqah, 1998), which indicate shoaling conditions within storm wave-base, probably about 5–20 m water depth.

Coeval siliciclastics are present to the south and southeast (Figures 6 and 7). At Batn El Ghul there is an upward gradational passage from crosslaminated, bioturbated quartz sandstone with phosphatic fragments to chert-chalk-dominated sediments, indicating deposition in a littoral marine environment. Local subsidence in the Gharandal area during the Campanian (Figure 27) resulted in deeper-water pelagic chalk facies in a small basin, which probably extended westwards to the southern Negev/Sinai (Lewy, 1975).

Large-scale Depositional Sequence (Belqa 3)

Transgressive Pelagic Parasequence Set: A rapid eustatic sea-level rise in Early Maastrichtian time resulted in widespread marine onlap over an extensive area of the Arabian Craton (Figures 7 and 29a), with the shoreline migrating to southern Egypt (Issawi, 1972) and central Saudi Arabia (Powers, 1968; Sharief et al., 1989). The base of the sequence (PR1; Muwaqqar Chalk Marl) is marked by a flooding surface, overlying a phosphate-rich burrowed horizon (SB 6). This may be equivalent to the Mid-Maastrichtian MFS K180 (68 Ma) of Sharland et al. (2001) but the transgressive event seems to be earlier (Early Maastrichtian age) in Jordan. Sedimentation was characterised by deposition of monotonous, deep-water pelagic chalk locally with chert, marl and porcellanite; early diagenetic microcrystalline limestone concretions are locally abundant.

Bitumen accumulated, locally, in anoxic basins (Figures 29c and 30) at the base of a density-stratified watermass where reducing, hypersaline bottom conditions were characterised by intense algal activity (Speers, 1969; Spiro and Aizenshtat, 1977; Spiro et al., 1983). It seems likely that differentially subsiding basins, such as the Lajun oil-shale deposits in central Jordan (Abu Ajamieh, 1980; Abed et al., 2005), were bounded by extensional normal faults, similar to the Azraq-Hamza Basin (Andrews, 1992). However, they could also be attributed to gentle, synformal folding ('basin and swell') associated with intraplate compressional deformation of the Arabian Craton (Figure 29c).

A depositional hiatus and condensed sequence (SB 7) is marked by a thin bed of glauconitic marl with phosphate nodules, and *Thalassinoides*-burrowed marly chalk with abundant benthic foraminifera, near the top of the formation, at the level of the Cretaceous/Palaeogene (Maastrichtian/Palaeocene) boundary (Yassini, 1979; Ibrahim, 1993). These uppermost beds are also locally rich in bitumen and marine fish/reptile fragments (phosphatised) indicating stagnant bottom conditions in a shallower sea, but still below storm wave-base.

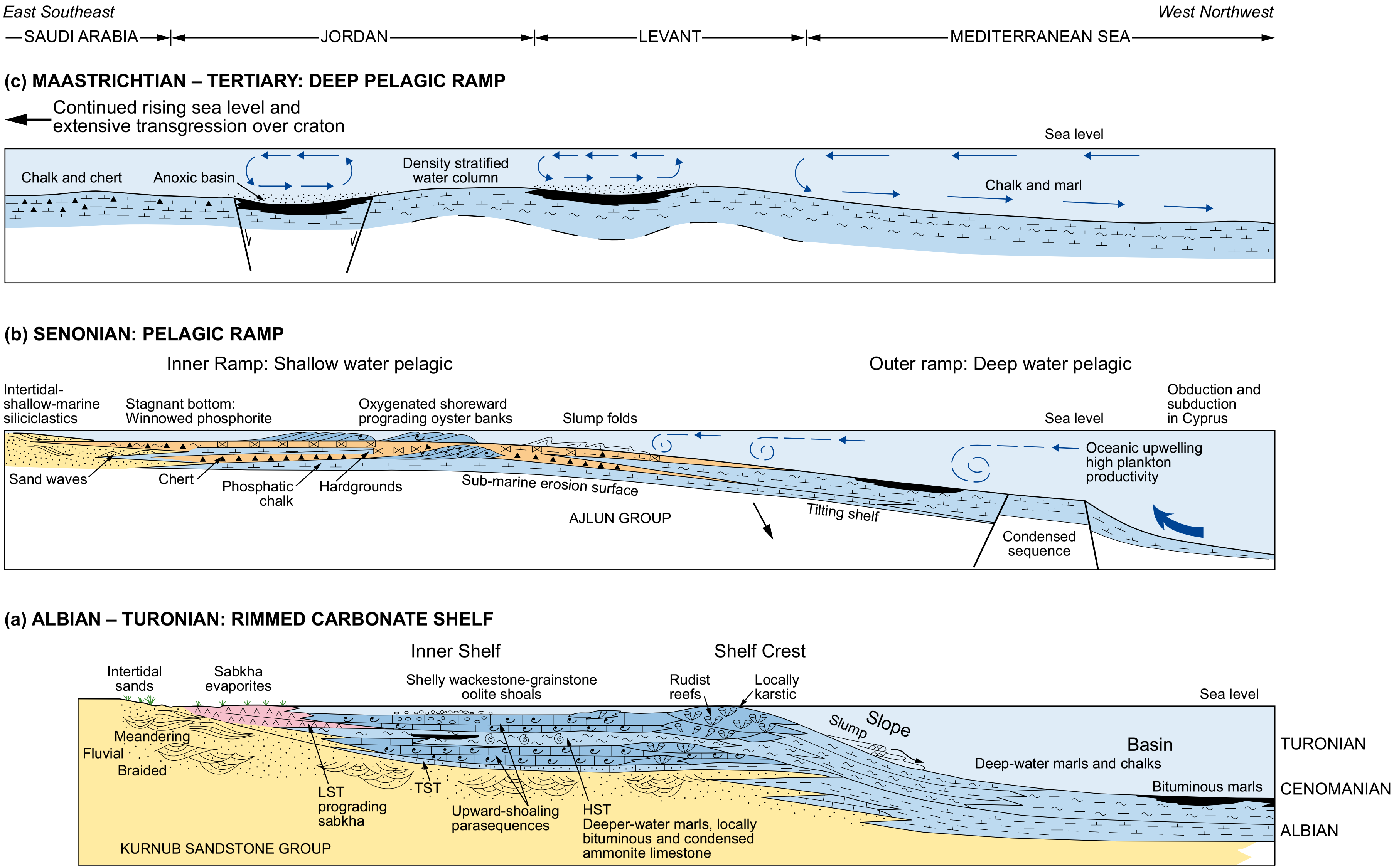

Figure 29: Schematic depositional settings, facies belts and evolution of the Cretaceous and Palaeogene depositional sequences viewed in WNW-trending cross-sections across the region: (a) Late Albian to Turonian rimmed carbonate shelf; (b) Coniacian to Maastrichtian shallow pelagic ramp; and (c) Maastrichtian to Palaeogene deep pelagic ramp. Symbols as in Figure 6.

Large-Scale Depositional Sequence (Belqa 4)

Pelagic Highstand Parasequence Set: The Early to Middle Eocene marks a phase of deeper, possibly density stratified, hypersaline water on the platform, with little evidence of shoreline facies in the eastern part of the Arabian Craton (Figure 29).

The highstand parasequnce set (Umm Rijam Chert-Limestone) consists of a monotonous succession of chalky limestone, chalk, chert, porcellanite and grey micro-crystalline limestone with abundant, diverse calcareous nanofossils, plantonic foraminifera and deep-water benthic foraminifera (Andrews, 1992). Macrofauna is conspicuously absent except for sparse phosphatic, skeletal fish fragments, and locally, limestone beds rich in gastropods and large nummulitids. The parasequence set represents maximum sea-level rise and onlap onto the Arabian Craton, during which the platform was largely covered by an epeiric sea characterised by uniform pelagic sedimentation. An exception to this pattern in the region is the local carbonate platform of the Galala Mountains, northern Egypt, which developed on a structural high resulting from syntectonic folding (Bandel and Kuss, 1987).

The absence of a shelly, benthic macrofauna, the predominance of planktonic and deep-water benthic foraminifera, calcareous nanoplankton, and uniform chalk/marl lithologies developed over a wide area, suggest a deep-water, pelagic environment. Bituminous horizons are also absent, indicating that the locally subsiding (?fault-bounded) anoxic basins characteristic of the Muwaqqar Chalk-Marl were infilled, and the seafloor was of uniform relief (low-gradient, homoclinal ramp). Fish fragments indicate a thriving nektonic fauna, but the paucity of benthic macrofossils suggests unfavourable bottom conditions; this could be attributed to very high, or very low, salinity, or deep water.

A depositional hiatus and condensed sequence at the top of the cycle are again indicated by glauconitic, phosphatic marls and chalks with *Thalassinoides* burrows, at the top of the parasequence set (SB 8).

Large-Scale Depositional Sequence (Belqa 5)

Regressive Parasequence Set: Littoral, marine sandstone and nummulitic limestones, above Sequence Boundary 8, indicate shallowing in Mid to Late Eocene time (Wadi Shallala Chalk). Tectonic activity associated with the compressional and transpressional deformation of the Syrian Arc and closure of the southern Neo-Tethys Ocean in Late Eocene to Oligocene times (Koch, in Bender, 1974; Cohen et al., 1990) resulted in rapid marine regression on the Arabian Platform.

The regressive facies are not well preserved in central Jordan due to Late Eocene erosion. However, the trend is recorded in the gradational upward passage from pelagic chalk/chert to nummulitic packstones and cross-bedded grainstones with quartz sand, indicating deposition in shallow-water, agitated lagoons. The shallow-marine facies

Figure 30: Burrow-mottled bituminous chalky marl core (38.0–42.0 m depth) Muwaqqar Chalk Marl (Maastrichtian), El Lajun area (photo by J. Powell).

are precursors to the widespread regression on the Arabian Platform in the Late Eocene to Miocene represented by the brackish Qirma Formation (Miocene) (Ibrahim, 1993). The final phase of the regression is, however, not recorded in the stratigraphic record in Jordan, since these beds were removed during Late Eocene erosion prior to the deposition of continental, syn-tectonic conglomerate and lacustrine facies (Dana Conglomerate) during the Oligocence (Barjous, 1992).

SEA-LEVEL CURVES: REGIONAL AND GLOBAL COMPARISONS

The excellent three-dimensional exposure of the Cretaceous and Early Palaeogene succession in Jordan and adjacent countries allows reconstruction of genetic depositional sequences and correlation of synchronous events across the 'passive' continental margin. Despite different lithostratigraphic schemes erected in surrounding countries (Egypt, Levant, West Bank and Saudi Arabia), the evolution of megasequences from a fluvial-dominated to rimmed carbonate-shelf and subsequent pelagic ramp can be readily correlated throughout the region (Sass and Bein, 1982; Flexer et al., 1986; Kuss, 1992; Bachmann and Kuss, 1998; Schulze et al., 2003, 2005; Wendler et al., 2009). Genetic depositional sequences in Jordan (Figure 26) can thus be considered in relation to global sea-level curves (Figure 31) for the Cretaceous (Haq et al., 1988; Sharland et al., 2001, 2004; Haq and Al-Qahtani, 2005) and regionally developed sea-level curves for Levant (Flexer et al., 1986), northeast Egypt and parts of

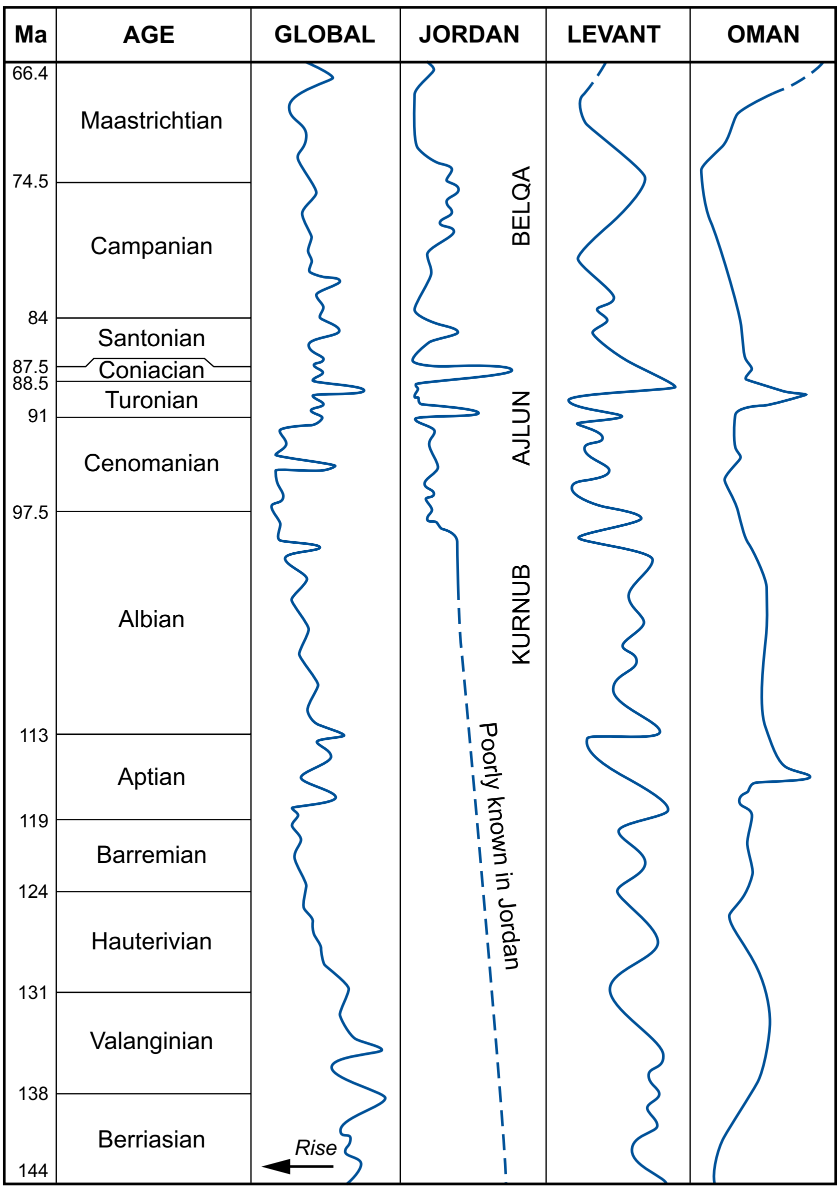

Figure 31: Comparison of relative sea-level curves for the southern Neo-Tethys (Jordan, Levant and Oman) compared to the global sea-level curve (Haq et al., 1988). Chronostratigraphic framework is from Scott et al. (1988).

south Jordan (Kuss, 1992; Bachmann and Kuss, 1998), and Arabia (Harris et al., 1984; Scott et al., 1988; Watts and Blome, 1990; Sharland et al., 2001). This allows local- to regional-scale tectonic, and autocyclic controls over relative sea level and sedimentation styles (Scott et al., 1988; Miall, 1991; Schlager, 1992) to be assessed independently from the effects of first- and second-order global, eustatic sea-level fluctuations, which have been considered, by some, to be the main control on the geometry of passive margin sequences (Haq et al., 1988; Sarg, 1988).

Global sea-level curves (Haq et al., 1988; Sharland et al., 2001, 2004; Haq and Al-Qahtani, 2005) show an overall rise of sea level during the Cretaceous, with onlap of Neo-Tethyan shorelines onto cratonic areas such as the Arabian Craton of the southern Tethyan realm. However, the relative sea-level curves deduced from this study in Jordan (Figure 27) shows many features at variance to the global trend (Figure 31). There are also marked local differences with some of the trends deduced from Saudi Arabia and Oman (Harris et al., 1984; Scott et al., 1988; Watts and Blome, 1990; van Buchem et al., 1996), although, with a few minor exceptions, there is good agreement at the megasequence level with trends deduced from coeval successions in Levant (Flexer et al., 1986) and northeast Egypt (Kuss, 1992) and with maximum flooding surfaces (MFS) and genetic sequences in general across the Arabian Plate, as established by Sharland et al. (2001).

Discrepancies between the predictive global sea-level curve for the Cretaceous (Haq et al., 1988) and the observed genetic depositional sequences recording marine onlap/offlap in Jordan and surrounding areas, suggests that factors other than eustasy controlled the development and geometry of the sequences. Rapid marine onlap and establishment of a carbonate-shelf (Ajlun 1) in Late Albian to Early Cenomanian time, over the region, may have been due to an increased, but punctuated rate of subsidence of the northern margin of the Arabian Craton. Autocyclic controls on the platform are inferred for the fourth-/fifth-order upward-shoaling parasequences, but the three large-scale depositional sequences (Ajlun 1 to 3) are probably a reflection of different rates of regional-scale subsidence on the platform and show good correspondence to the MFS markers K110 to K140 (Sharland et al., 2001). However, the Early Cenomanian Sequence Boundary 2, at the top of the Naur Formation can only be recognised in Jordan and Levant. Furthermore, the lowstand parasequence set (Early Turonian), above Sequence Boundary 3, which records peritidal conditions and subaerial exposure on the inner part of the platform (central Jordan; Figures 29 and 31) does not correspond to the global curve, and may represent a regional sea-level fall across the inner platform resulting from uplift of the hinterland that was accompanied by increased siliciclastic sediment flux. Also, the marked lowering of global sea level in Mid-Turonian times noted by Haq et al. (1988) is not apparent in the Turonian succession in Jordan (i.e. Wadi As Sir Limestone) unless there is an error in the age dating and this event is represented by the Early Turonian peritidal parasequence set noted above. Absence of evidence for a Mid-Turonian lowstand in the Levant might be the result of continued steady subsidence of the Arabian Platform margin, so that optimum carbonate-producing conditions were maintained on the rimmed shelf.

The erosional/depositional hiatus (Mid to Late Coniacian) represented by the sequence boundary between the Ajlun platform and the Belqa ramp sequences, is not apparent in the global sea-level curve which records steady state or rising sea level over this interval. The sudden change from platform to ramp has been attributed to regional, oceanic tectonism and concomitant changes in ocean productivity and circulation patterns, and is not reflected in global sea-level curves. This important regional sequence boundary (SB 4) does not fully conform to a sub-aerial Type 2 unconformity (*sensu* Sarg, 1988) but, nonetheless, marks a critical change in the geometry of, and sedimentation on, the Arabian Plate margin, which resulted in drowning of the platform (cf. Schlager, 1992).

Although the Late Coniacian to Maastrichtian global trend is one of rising global sea level and marine onlap, the regressive facies on the inner ramp (Belqa Sequence 2) during the Campanian appears to coincide, in part, with a lowstand in Early Campanian, but not with the rising sea level predicted for the Late Campanian. Furthermore, marine onlap represented by the Maastrichtian pelagic transgressive sequence (Muwaqqar Chalk-Marl) was deposited during falling global sea level (Haq et al., 1988). These discrepancies suggest that regional tectonism manifested in compressional flexuring and subsidence (Cloetingh, 1988) of the Arabian Craton, and regional transtensional or extensional rift-basins were the dominant factors controlling relative water depths and sedimentation in this region. Similar discrepancies in sea-level curves have been noted both worldwide (Scott et al., 1988) and regionally (Flexer et al., 1986; Kuss, 1992). Although there does appear to be worldwide correspondence of a mid-Aptian rise and a Mid-Cenomanian rise between the Texas Gulf Coast and the Arabian Gulf (Scott et al., 1988; Sharland et al., 2001), only the latter is tentatively recognised in central Jordan, as the transgressive and highstand sequence (Ajlun 2) above the Naur Formation (Figure 29).

CONCLUSIONS

(1) The Cretaceous to Palaeogene sequences in Jordan record an overall trend of progressive coastal onlap, punctuated by brief regressive, lowstand sequences, during a globally warm 'greenhouse' climatic regime.

(2) Megasequence 1 (Kurnub Sandstone) was deposited in alluvial environments, which show an upward trend from a braided, low-sinuosity alluvial plain with ferralitic palaeosols to a meandering, high-sinuosity alluvial plain with thin coals and gleysols. This change in depositional environments in the hinterland is attributed to increasing floodplain accommodation and alluviation resulting from marine onlap over the geomorphologically mature coastal plain, associated with high sea-level stands (second-/third-order) and regional MFS K80, K90 and K100.

(3) The Late Albian – Cenomanian transgression records a rapid rise in relative sea level (regional MFS K110), and initiation of a rimmed carbonate shelf in Jordan represented by Megasequence 2 (Ajlun Group). Sedimentation on the shelf is characterised by three large-scale sequences (Ajlun sequences 1 to 3), which record broadly upward-shoaling cycles (third-order). These are internally structured by smaller scale, upward-shoaling parasequences (fourth- and fifth-order cycles) representing autocyclic controls such as compaction and subsidence, or allocyclic obliquity- and precession-driven Milankovitch cycles. Rudistid patch reefs developed at the shelf crest. Late transgressive and highstand sequences are manifested in deeper-water calcareous mudstone and thin limestones. Bituminous mudstones and macroconch ammonite-bearing limestone represent phases of maximum flooding across the shelf (regional MFS K120, K130, K140) and are attributed to global sea-level rise during the Cenomanian and Turonian. Full oceanic circulation on the inner shelf is indicated by the ammomite-bearing limestone in Early Turonian times. It is overlain by a lowstand parasequence set, which marks the base of the third depositional sequence (Ajlun Sequence 3) which, in turn, is bounded (top) by a Type 2 sequence boundary. Peritidal sabkha evaporites and coeval fluvial siliciclastics (landwards) probably reflect uplift of the inner platform and hinterland resulting in increased siliciclastic flux along the coastline during this Early Turonian lowstand. Overlying shelf carbonates (Ajlun Sequence 3) represent a transgressive/highstand sequence. Lithofacies are similar to Ajlun Sequence 1 and are characterised by upward-shoaling ('keep-up') parasequences comprising wackestones and micrites with burrowed tops, and rudistid clusters.

(4) A marked change in depositional environment from rimmed carbonate shelf to hemi-pelagic/pelagic ramp occurred in Early Coniacian time, and is marked by a regional Type 2 sequence boundary (SB 4). Oceanic subduction/obduction seems to have triggered subsidence, basinward-tilting and local extension/transtension (Azraq Basin) of the platform margin which, in turn, resulted in drowning of the shelf, and the establishment of predominantly pelagic and hemi-pelagic sedimentation from Coniacian to Early Palaeogene time.

(5) Megasequence 3 (Belqa Group) records an overall progressive, marine onlap during the Late Cretaceous to Early Palaeogene, punctuated by brief, regressive lowstands. Six large-scale sequences are bounded by burrowed (glauconite/phosphate-rich) condensed horizons during periods of depositional hiatus, overlain by marine flooding surfaces during phases of rapid onlap. Depth-related facies belts which developed during Coniacian – Maastrichtian time range from outer, through mid- to inner-ramp settings (Belqa Sequence 2), characterised by a chalk-chert-phosphorite association with coeval deposition of siliciclastics in the littoral zone. Chalk was deposited during onlap and highstands; regressive/condensed facies on the inner shelf

are typified by a higher proportion of phosphorite, the latter commonly associated with giant, shoreward-prograding (retrogradational) oyster banks. A subsequent phase of marine onlap during the Maastrichtian to Eocene (Belqa sequences 3 and 4) resulted in more uniform pelagic chalk-chert sedimentation. However, organic-rich marls were locally deposited in anoxic basins, which were bounded, locally, by extensional faults.

(6) Regression of the Neo-Tethys Ocean in Late Eocene time (Belqa Sequence 5) is characterised by shallow-water nummulitic shoals and heterolithic, siliciclastic/carbonate facies.

(7) Good correlation of the regional (North Africa/Arabia) sea-level curves supports the overriding influence of eustatic control on second- or third-order cycles and in the geometry and development of genetic depositional megasequences. The most important extrinsic controls were: subsidence rates of the passive margin, which allowed 'seeding' and vertical aggradation of the carbonate shelf; mid-ocean tectonics and associated tilting of the platform that resulted in drowning of the shelf. Subsequent changes in ocean circulation, sea-water chemistry and plankton productivity resulted in pelagic and hemi-pelagic sedimentation in conditions unfavourable to the re-establishment of a benthic carbonate shelf fauna. Lack of correlation of fourth- and fifth-order depositional sequences with some major global sea-level fluctuations suggests that regional tectonics controls (tilting and subsidence of the platform, transpression, transtension and isostatic/geomorphic adjustments of the hinterland) were profound enough in the Levant/Arabian Plate to overprint the influence of global sea-level fluctuations.

ACNOWLEDGEMENTS

This study is based upon the cooperation between the Natural Resources Authority (NRA) and the British Geological Survey (BGS) during the 1:50,000 scale National Geological Mapping Project. The BGS involvement was funded by the Overseas Development Administration (ODA), now the Department for International Development (DfID). The authors thank the Director-Generals of the NRA for their enthusiastic support of the project, and for permission to publish a number of revised figures from NRA Bulletins. In particular, we thank Main El-Hiyari, formerly Director of the NRA, Darwish Jaser, Director of the Geology Directorate and Bassam Sunna for their support. Thanks are also due to the staff of the Geology Directorate (NRA) for their contributions to this study, particularly M.O. Bargous, K. Khdeir, A. Masri, I. Rabba, M. Rashdan, B. Tarawneh and G. Abdelhamid. We thank I.J. Andrews and R.B.O'B. Knox for their reviews of an early draft of the paper. We are indebted to Moujahed Al-Husseini and two anonymous reviewers for their helpful comments, which greatly improved the manuscript. We are grateful to Heather Paul-Pattison for preparing the figures. The first author publishes with the approval of the Executive Director, British Geological Survey (NERC), and the second author with the permission of Tafilah University, Jordan.

REFERENCES

Abed, A.M. 1982a. Depositional environments of the Early Cretaceous Kurnub (Hathira) Sandstones, north Jordan. Sedimentary Geology, v. 31, p. 267-279.

Abed, A.M. 1982b. Microfacies and palaeoenvironment of the Wadi Sir Formation (Upper Cretaceous), north Jordan. Facies, v. 7, p. 229-236.

Abed, A.M. 1984. Emergence of Wadi Mujib (central Jordan) during lower Cenomanian time and its regional tectonic implications. In J.E. Dixon and A.H.E. Robertson (Eds.), The Geological Evolution of the Eastern Mediterranean. Oxford, Blackwell Scientific Publications, p. 213-216.

Abed, A.M and M. ElHiyari 1986. Depositional environment and palaeogeography of the Cretaceous gypsum horizon in west-central Jordan. Sedimentary Geology, v. 47, p. 109-123.

Abed, A.M. and G.M. Kraishan 1991. Evidence for shallow marine origin of a 'Monterey Formation type' chert-phosphorite-dolomite sequence, Amman Formation (late Cretaceous), central Jordan. Facies, v. 24, p. 25-38.

Abed, A.M. and R. Sadaqah 1998. Role of Upper Cretaceous oyster build ups in the deposition and accumulation of high-grade phosphorites in central Jordan. Journal of Sedimentary Research, v. 68B, p. 1009-1020.

Abed, A.M. and W. Schneider 1982. The Cenomanian nodular limestone member of Jordan; from subtidal to supratidal environments. Neus Jahrbuch fur Geologische und Paläontologie Monatschefte, v. 9, p. 513-522.

Abed, A.M., K.H. Arouri and C.J. Boreham 2005. Source rock potential of phosphorite-bituminous chalk-marl sequence in Jordan. Marine Petroleum Geology, v. 22, p. 413-425.

Abed, A.M., R. Sadaqah and M. Al-Jazi 2007. Sequence stratigraphy and evolution of Eshidiyya phosphorite platform, southern Jordan. Sedimentary Geology, v. 198, p. 209-219.

Abu Ajamieh, M. 1980. An assessment of the ElLajjun oilshale deposit. Unpublished report, NRA. Amman.

Aharoni, E. 1964. Lithoelectric correlation of the "Kurnub Group" (Lower Cretaceous) in the Northern Negev. Israel Journal of Earth Sciences, v. 13, p. 63-81.

Allen, J.R.L. 1965. A review of the origin and characteristics of recent alluvial sediments. Sedimentology, v. 5, p. 89-191.

Almogi-Labin, A., A. Bein and E. Sass 1993. Late Cretaceous upwelling system along the southern Tethys margin (Israel): Interrelationship between productivity, bottom water environments, and organic matter preservation. Paleoceanography, v. 8, p. 671-690.

Aly, M.F., A. Smaadi and H. Abu Hazzam 2008. Late Cenomanian-Early Turonian ammonites of Jordan. Revue de Paleobiologie, Geneve, v. 27 (1), p. 43-71.

Amireh, B.S. 1992. Sedimentology and mineral composition of the Kurnub Sandstone in Wadi Qseib, SW Jordan. Sedimentary Geology, v. 78, p. 267-283.

Amireh, B.S. 1997. Sedimentology and palaeogeography of the regressive-transgressive Kurnub Group (Early Cretaceous) of Jordan. Sedimentary Geology, v. 112, p. 69-88.

Andrews, I.J. 1992. Cretaceous and Paleogene lithostratigraphy in the subsurface of Jordan. Subsurface Geology Bulletin 5, Geology Directorate, Subsurface Geology Division, NRA, Jordan.

Arkin, Y. and M. Hamaoui 1967. The Judea Group (Upper Cretaceous) in central southern Israel. Bulletin Geological Survey, Israel, v. 42, 17 p.

Bachmann, M. and J. Kuss 1998. The Middle Cretaceous carbonate ramp of the northern Sinai; sequence stratigraphy and facies distribution. In V.P. Wright and T.P. Burchette (Eds.), Carbonate Ramps. Geological Society of London, Special Publication no. 149, p. 253-280.

Bachmann, M., J. Kuss and J. Lehmann 2010. Controls and evolution of facies patterns in the Upper Barremian-Albian Levant Platform in North Sinai and Isreal. In C. Homberg and M. Bachmann (Eds.), Evolution of the Levant Margin and Western Arabia Platform since the Mesozoic. Geological Society of London, Special Publication no. 341, p. 99-131.

Bandel, G. 1981. New stratigraphical and structural evidence for lateral dislocation in the Jordan Rift Valley connected with the description of the Jurassic rock column in Jordan. Neus Jarbuch fuer Geologie und Paläeontologie Abhandlungen B, v. 161(3), p. 271-308.

Bandel, K. and J. Kuss 1987. Depositional environments of the pre-rift sediments Galala heights (Gulf of Suez, Egypt). Berliner Geowissenschaftliche Abhandlungen, (A), 78, p. 1-48.

Barjous, M.O. 1992. The geology of the Shawbak Map Sheet, No. 3151 III. Bulletin 19, Geology Directorate, NRA, Amman, 79 p.

Bartov, J., Z. Garfunkel, Y. Eyal and G. Steinitz 1972. Late Cretaceous and Tertiary stratigraphy and palaeoecology of southern Israel. Israel Journal of Earth Sciences, v. 21, p. 69-97.

Bartov, Y. and G. Steinitz 1977. The Judea and Mt. Scopus groups in the Negev and Sinai with trend surface analysis of the thickness data. Israel Journal of Earth Sciences, v. 26, p. 119-148.

Bartov, Y. and G. Steinitz 1982. Senonian ostreid bioherms in the Negev, Israel; implications for paleography and environment of deposition. Israel Journal of Earth Sciences, v. 31, p. 17-23.

Basha, S.H. 1978. Foraminifera from the Ajlun Group of east Jordan. Journal of the Geological Society of Iraq, v. 11, p. 67-91.

Bauer, J., A.M. Marzouk, T. Steuber and J. Kuss 2001. Lithostratigraphy and biostratigraphy of the Cenomanian–Santonian strata of Sinai, Egypt. Cretaceous Research, v. 22, p. 497-526.

Bauer, J., J. Kuss and T. Steuber 2003. Sequence architecture and carbonate platform configuration (Late Cenomanian–Santonian), Sinai, Egypt. Sedimentology, v. 50, p. 387-414.

Bein, A. 1976. Rudistid fringing reefs of the Cretaceous shallow carbonate platform of Israel. American Association of Petroleum Geologists, Bulletin, v. 60, p. 258-272.

Bein, A. and Y. Weiler 1976. The Cretaceous Talme Yafe Formation: A contour current shaped sedimentary prism of calcareous detritus at the continental margin of the Arabian craton. Sedimentology, v. 23, p. 511-532.

Bender, F. 1968. Geologie von Jordanien, Beitrage zur Regionalen Geologie der Erde. Band 7, Borntraeger, Berlin, 230 p.

Bender, F. 1974. Geology of Jordan. Gebrueder Borntraeger, Berlin, 196 p.

Bender, F. and K. Mädler 1969. Die sandige Schichtenfolge der Kriede mit einer Angiospermen Flora in Sudjordanian. Beihefte zum Geologischen Jahrbuch, v. 81, p. 35-92.

Bentor, Y.K. et al. 1960. LexiqueStratigraphique International, III, (Asie), Fasc 10 c. 2, Israel, CNRS, Paris.

Besly, B.M. and C.R. Fielding 1989. Palaeosols in Westphalian coal-bearing and red-bed sequences, Central and Northern England. Palaeogeography, Palaeoclimatology and Palaeoecology, v. 70, p. 303-330.

Bromley, R.G. and A.A. Ekdale 1987. Mass transport in European Cretaceous chalk; fabric criteria for its recognition. Sedimentology, v. 34, p. 1079-1092.

Buchbinder, B., C. Benjamini and S. Lipson-Benitah 2000. Sequence development of Late Cenomanian–Turonian carbonate ramps, platforms and basins in Israel. Cretaceous Research, v. 21, p. 813-843.

Burchette, T.P. and V.P. Wright 1992. Carbonate ramp depositional systems. Sedimentary Geology, v. 79, p. 3-57.

Burdon, D.J. 1959. Handbook of the Geology of Jordan; to accompany and explain the three sheets of 1:250,000 Geological Map, East of the Rift, by A.M. Quennell. Government of the Hashemite Kingdom of Jordan, 82 p.
Camoin, G.F. 1991. Sedimentologic and paleotectonic evolution of carbonate platforms on a segmented continental margin: Example of the African Tethyan margin during Turonian and Early Senonian times. Palaeogeography, Palaeoclimatology, Palaeoecology, v. 87, p. 29-51.
Chaimov, T.A., M. Barazangi, D. Al Saad, T.A. Sawaf and A. Gebran 1992. Mesozoic and Cenozoic deformation inferred from seismic stratigraphy in the southwestern intracontinental Palmyride fold-thrust belt, Syria. Geological Society of America Bulletin, v. 104, p. 704-715.
Cloetingh, S. 1988. Intraplate stresses: A tectonic cause for third-order cycles in apparent sea-level. In C.K. Wigus, B.S. Hastings, C.G.St.C. Kendall, H.W. Posamentier, C.A. Ross and J.C. Van Wagoner (Eds.), Sea-level Changes: An Integrated Approach. Society of Economic Paleontologists and Mineralogists, Special Publication no. 42, p. 125-154.
Cohen, Z., V. Kapstan and A. Flexer 1990. The tectonic mosaic of the southern Levant: Implications for hydrocarbon prospects. Journal of Petroleum Geology, v. 13, p. 437-462.
Dilley, F.C. 1985. Cretaceous correlations in the Hamza Wells 15. NRA Palaeontological Report, 6.
Duchafour, P. 1982. Pedology. Allen and Unwin, London, 448 p.
Edwards, W.N. 1929. Lower Cretaceous plants from Syria and Transjordan. Annals and Magazine of Natural History, 10, p. 394-405.
El-Hiyari, M. 1985. The geology of Jabal AlMutarammil, Map Sheet No. 3252 III, Bulletin 1. Geology Directorate, NRA, Amman, 51 p.
Fink, J.H. and Z. Reches 1983. Diagenetic density inversions and the deformation of shallow marine chert beds in Israel. Sedimentology, v. 30, p. 261-271.
Flexer, A. 1968. Stratigraphy and facies development of Mount Scopus Group (Senonian-Palaeocene) in Israel and adjacent countries. Israel Journal of Earth Sciences, v. 17, p. 85-114.
Flexer, A. and A. Starinsky 1970. Correlation between phosphate content and the foraminiferal plankton/benthos ratios in chalks (Late Cretaceous, northern Israel): Paleoenvironmental significance? Sedimentology, v. 14, p. 245-258.
Flexer, A. and A. Honigstein 1984. The Senonian succession in Israel lithostratigraphy, biostratigraphy and sea level changes. Cretaceous Research, v. 5, p. 303-312.
Flexer, A., A. Rosenfeld, S. Lipson-Benitah and A. Honigstein 1986. Relative sea-level changes during the Cretaceous in Israel. American Association of Petroleum Geologists Bulletin, v. 70, p. 1685-1699.
Freund, R. 1961. Distribution of Lower Turonian ammonites in Israel and the neighbouring countries. Bulletin Research Council, Israel, 10, 189205.
Freund, R., Z. Garfunkel, I. Zak, M. Goldberg, T. Weissbrod and B. Derin 1970. The shear along the Dead Sea Rift. Philosophical Transactions of the Royal Society of London. A. 267, p. 107-130.
Freund, R. and M. Raab 1969. Lower Turonian ammonites from Israel. Special Paper, Palaeontology, v. 4, 83 p.
Gale, A.S. 1989. A Milankovitch scale for Cemomanian time. Terra Nova, v. 1, p. 400-425.
Gale, A.S. 2000. The Cretaceous World. In S. Culver and P.F. Rawson (Eds.), Biotic Response to Global Change; the last 145 Million Years. Cambridge University Press, Cambridge, p. 4-19.
Galloway, W.E. 1989. Genetic stratigraphic sequences in basin analysis I: Architecture and genesis of flooding surface bounded depositional units. American Association of Petroleum Geologists Bulletin, v. 73, p. 125-142.
Garfunkel, Z. 1978. The Negev Regional synthesis of sedimentary basins. In Sedimentology Guidebook, Precongress Excursion A: International Congress on Sedimentology, 10th, Jerusalem, p. 35-110.
Glenn, C.R. and M.A. Arthur 1990. Anatomy and origin of a Cretaceous phophorite-greensand giant, Egypt. Sedimentology, v. 37, p. 123-154.
Ginsberg, R.N. 1971. Landward movement of carbonate mud: New model for regressive cycles in carbonates. American Association of Petroleum Geologists Bulletin, v. 55, p. 340, Abstract.
Greenberg, M. 1968. Type section of the Lower Cretaceous Hathira Formation in Hamakhtesh Hagadol Northern Negev. Geological Survey of Israel, Stratigraphical Section, v. 5, 6 p.
Gradstein, F.M., J.G. Ogg, A. Smith and others 2004. A Geologic Time Scale 2004. Cambridge University, Cambridge.
Harris, P.M., S.H. Frost, G.A. Seiglie and N. Schneidermann 1984. Regional unconformities and depositional cycles, Cretaceous of the Arabian Peninsula. In J.S. Schlee (Ed.), Interregional unconformities and hydrocarbon accumulation. American Association of Petroleum Geologists Memoir, v. 36, p. 67-80.
Haq, B.U., J. Hardenbol and P.R. Vail 1988. Mesozoic and Cenozoic chronostratigraphy and eustatic cycles. In C.K. Wilgus, B.S. Hastings, G.St.C. Kendall, H.W. Possamentier, C.A. Ross, J.C. Van Wagoner (Eds.), Sea-level Changes: An Integrated Approach. Society of Economic Palaeontologists and Mineralogists, Special Publication no. 42, p. 71-108.
Haq, B.U. and A.M. Al-Qahtani 2005. Phanerozoic cycles of sea level change on the Arabian Platform. GeoArabia, v. 10, no. 2, p. 127-160.
Hardie, L.A. and E.A. Shinn 1986. Tidal flats. In Carbonate Depositional Environments, Modern and Ancient. Part 3. Colorado School of Mines Quarterly, v. 80, 74 p.

Hunt, D. and M.E. Tucker 1993. Sequence stratigraphy of carbonate shelves with an example from the mid-Cretaceous (Urgonian) of southeast France. Special Publication of the International Association of Sedimentologists, v. 18, p. 307-341.

Ibrahim, K.M. 1993. Al Azraq map sheet, 3353 I. 1:50 000 Geological Map Series. Natural Resources Authority, Amman.

Issawi, B. 1972. Review of Upper Cretaceous-Lower Tertiary stratigraphy in central and southern Egypt. American Association of Petroleum Geologists Bulletin, v. 58, p. 1448-1463.

Jarvis, I., A. Gale, H.C. Jenkyns and M.A. Pearce 2006. Secular variation in Late Cretaceous carbon isotopes: A new ^{13}C carbonate reference curve for the Cenomanian–Campanian (99.6-70.6 Ma). Geological Magazine, v. 143, p. 561-608.

Jenkyns, H.C. 1980. Cretaceous anoxic events from continents to oceans. Journal of the Geological Society of London, v. 137, p. 171-188.

Kent, D.V. and F.M. Gradstein 1985. A Cretaceous and Jurassic geochronology. Geological Society of America, Bulletin, v. 96, p. 1419-1427.

Khdeir, K. 1974. The effect of coquina colonies in the deposition of phosphate in central Jordan. Proceedings of the 2nd Arab Mineral Resources Conference, Jeddah, p. 345-359.

Kolodner, K., D. Avigad, T.R. Ireland and Z. Garfunkel 2009. Origin of the Lower Cretaceous ('Nubian') sandstones of north-east Africa and Arabia from detrital zircon U-Pb SHRIMP dating. Sedimentology, v. 56, p. 2010-2023.

Kolodny, Y. 1969. Petrology of siliceous rocks in the Mishash Formation (Negev, Israel). Journal of Sedimentary Petrology, v. 39, p. 165-175.

Kolodny, Y. 1980. Carbon isotopes and depositional environment of a high productivity sedimentary sequence the case of the Mishash-Ghareb formations, Israel. Israel Journal of Earth Sciences, v. 29, p. 147-156.

Kolodny, Y. and R. Garrison 1994. Sedimentation and diagenesis in palaeo-upwelling zones of epeiric seas and platformal settings: A comparison of the Cretaceous Mishash Formation of Israel and the Miocene Monterey Formation of California. In A. Iijama, A.M. Abed and R. Garrison (Eds.), Siliceous, Phosphatic and Glauconitic Sediments in the Tertiary and Mesozoic. Proceedings of the 29th International Geological Congress, Part C. VSP, The Netherlands, p.133-158.

Kuss, J. 1992. The Aptian-Palaeocene shelf carbonates of northeast Egypt and southern Jordan: Establishment and break-up of carbonate platforms along the southern Tethyan shores. Zeitschrift Deutsche Geologischen, v. 143, p. 107-132.

Kuss, J. and M. Bachmann 1996. Cretaceous palaeogeography of the Sinai Peninsula and neighbouring areas. Comptes Rendu, Academie des Sciences, Paris, t. 322, p. 915-933.

Kuss, H.J., M.A.A. Bassiouni, J. Bauer, M. Bachmann, A.M. Marzouk, C. Scheibner and F. Schulze 2003. Cretaceous–Paleogene sequence stratigraphy of the Levant Platform (Egypt, Sinai, Jordan). In E. Gili, M.E.H. Negra and P.W. Skelton (Eds.), North African Cretaceous Carbonate Platform Systems. Dordrecht, The Netherlands, Kluwer Academic Publishers, p. 171-187.

Lang, B. and Y. Mimran 1985. An Early Cretaceous volcanic sequence in central Israel and its significance to the absolute date of the base of the Cretaceous. Journal of Geology, v. 93, p. 179-184.

Le Nindre, Y.M., D. Vaslet, S. Maddah and M. Al-Husseini 2008. Stratigraphy of the Valanginian? to Early Paleocene succession in central Saudi Arabia outcrops: Implications for regional Arabian sequence stratigraphy. GeoArabia, v. 13, no. 2, p. 51-85.

Lewy, Z. 1975. The geological history of southern Israel and Sinai during the Coniacian. Israel Journal of Earth Sciences, v. 24, p. 19-43.

Lewy, Z. 1990. Transgressions, regressions and relative sea-level changes on the Cretaceous shelf of Israel and adjacent countries. A critical evaluation of Cretaceous global sea-level correlations. Paleoceanography, v. 5, p. 619-637.

Lifshitz, A., A. Honigstein, A. Livnat, R. Roded and A. Flexer 1985. The Sayyarim Formation, Nahal Ya'alon area, Southern Arava Valley: Lithostratigraphy, ostracod biostratigrahy and palaeoenvironmental implications. Israel Journal of Earth Sciences, v. 34, p. 193-204.

Lillich, W. 1964. Stratigraphical investigations on the Palaeozoic and Mesozoic sandstones on the east side of the Dead Sea. Unpublished Report, German Geological Mission, NRA, Jordan.

Magaritz, M. 1974. Lithification of chalky limestone: A case study in Senonian rocks from Israel. Journal of Sedimentary Petrology, v. 44, p. 947-954.

Masri, M. 1963. Report on the geology of the Amman-Zerqa area. Unpublished report, Central Water Authority, Amman, Jordan.

Miall, A.D. 1991. Stratigraphic sequences and their chronostratigraphic correlation. Journal of Sedimentary Petrology, v. 61, p. 497-505.

Mikbel, S. and W. Zacher 1986. Fold structures in northern Jordan. Neus Jahrbuch fur Geologische und Paläontologie Monatschefte, v. 4, p. 248-256.

Moh'd, B.K. 1985. Sedimentology and microfacies of the Wadi As Sir Formation in the Ajlun-Irbid area with a review of Turonian lithostratigraphy in the Middle East. Unpublished MSc Thesis, University of Jordan, Amman, 112 p.

Morsi, A.-M.M. and J.E. Wendler 2010. Biostratigraphy, palaeoecology and palaeogeography of the Middle Cenomanian-Early Turonian Levant Platform in Central Jordan based on ostracods. In C. Homberg and M. Bachmann (Eds.), Evolution of the Levant Margin and Western Arabia Platform since the Mesozoic. Geological Society of London, Special Publication no. 341, p. 99-131.

Moshkovitz, S., A. Ehrlich and D. Soudry 1983. Siliceous microfossils of the Upper Cretaceous Mishash Formation, Central Negev, Israel. Cretaceous Research, v. 4, p. 173-194.

NACSN 1983 - NORTH AMERICAN COMMISSION ON STRATIGRAPHICAL NOMENCLATURE, North American Stratigraphic Code. Bulletin of the American Association of Petroleum Geologists, v. 67, p. 841-875.

Parker, D.H. 1970. The Hydrogeology of the Mesozoic-Cainozoic Aquifers of the Western Highlands and Plateau of East Jordan (4 vols). UNDP/FAO 212. Unpublished technical report, no. 2, 424 p.

Posamentier, H.W., M.T. Jervey and P.R. Vail 1988. Eustatic controls on clastic deposition, II. Sequence and systems tract models. In C.K. Wigus, B.S. Hastings, C.G.St.C. Kendall, H.W. Posamentier, C.A. Ross and J.C. Van Wagoner (Eds.), Sea-level Changes: An Integrated Approach. Society of Economic Paleontologists and Mineralogists, Special Publication no. 42, p. 125-154.

Powell, J.H. 1988. The geology of Karak; Map Sheet No 3152 III, Bulletin 8, Geology Directorate, NRA, Amman.

Powell, J.H. 1989. Stratigraphy and sedimentation of the Phanerozoic rocks in central and southern Jordan. Bulletin 11, Geology Directorate, Natural Resources Authority (Ministry of Energy and Mineral Resources) Amman, HK of Jordan. Part B: Kurnub, Ajlun and Belqa Groups. 161 p., 12 figures, 17 tables.

Powell, J.H and B.K. Moh'd 1993. Structure and sedimentation of Permo-Triassic and Triassic rocks exposed in small-scale horsts and grabens of pre-Cretaceous age; Dead Sea margin, Jordan. Journal of African Earth Sciences (and the Middle East), v. 17, p. 131-143.

Powell, J.H, K. Ibrahim and M. Rashdan 1988. Jabal Khureij: A reinterpretation of sedimentation and tectonics (Upper Cretaceous and Tertiary) in the Dead Sea-Gulf of Aqaba Rift, Jordan. 3rd Jordanian Geologists' Conference, Abstracts. Amman.

Powell, J.H, B. Humphreys and B.K. Moh'd 1990. Hardground development at the base of the Dhiban Chalk Member (Wadi Umm Ghudran Formation), Senonian, of Central and Southern Jordan. 3rd Jordanian Geologists' Conference. Special Publication no. 3 of the Jordan Geologists' Association, p. 251-282.

Powers, R.W. 1968. Lexique stratigraphique international Asie, 3, Fasc, 10, 61, Saudi Arabia. CNRS Paris.

Pufahl, P.K., K.A. Grimm, A.M. Abed and M.Y. Sadaqah 2003. Upper Cretaceous (Campanian) phosphorites in Jordan: Implications for the formation of a southern Tethyan phosphorite giant. Sedimentary Geology, v. 161, p. 175-205.

Quennell, A.M. 1958. The structural and geomorphic evolution to the Dead Sea Rift. Quarterly Journal of the Geological Society of London, v. 114, p. 1-24.

Read, J.F. 1985. Carbonate platform facies models. American Association of Petroleum Geologists Bulletin, v. 69, p. 121.

Reiss, Z., A. Almogi-Labin, A. Honigstein, Z. Lewy, S. Lipson-Benitah, S. Moshkovitz and Y. Zaks 1985. Late Cretaceous multiple stratigraphic framework of Israel. Israel Journal of Earth Sciences, v. 34, p. 147-166.

Rosenfeld, A. and M. Raab 1984. Lower Cretaceous ostracods from Israel and Sinai. Israel Journal of Earth Sciences, v. 33, p. 85-134.

Rosenfeld, A., F. Hirsch, A. Honigstein and M. Raab 1998. The palaeoenvironments of Early Cretaceous ostracods in Israel. In S. Crasquin-Soleau et al. (Eds.), What About Ostracoda! Bulletin de Centre Recherche et Exploration-Production de Elf-Aquitaine, Memoire 20, p. 179-195.

Ross, D. 1992. Sedimentology and depositional profile of a mid-Cretaceous shelf edge rudist reef complex, Nahal Ha'mearot, northwestern Israel. Sedimentary Geology, 79, 161-172.

Sarg, J.F. 1988. Carbonate sequence stratigraphy. In C.K. Wigus, B.S. Hastings, C.G.St.C. Kendall, H.W. Posamentier, C.A. Ross and J.C. Van Wagoner (Eds.), Sea-level Changes: An Integrated Approach. Society of Economic Paleontologists and Mineralogists, Special Publication no. 42, p. 155-181.

Sass, E. and A. Bein 1982. The Cretaceous carbonate platform in Israel. Cretaceous Research, v. 3, p. 135-144.

Schlager, W. 1981. The paradox of drowned reefs and carbonate platforms. Geological Society of America Bulletin, v. 95, p. 675-702.

Schlager, W. 1992. Sedimentology and sequence stratigraphy of reefs and carbonate platforms; a short course. American Association of Petroleum Geologists, Continuing Education Course Note Series no. 34, 71 p.

Schneider, W., A.M. Abed and E. Salameh 1984. Mineral content and diagenetic pattern - Useful tools for lithostratigraphic subdivision and correlation of Nubian series. Results of work in the Wadi Zarqa Main area, Jordan. Geologisches Jahrbuch, B 53, p. 550-575.

Schneidermann, N. 1970. Genesis of some Cretaceous carbonates in Israel. Israel Journal of Earth Sciences, v. 19, p. 97-115.

Schulze, F., Z. Lewy, J. Kuss and A. Gharaibeh 2003. Cenomanian-Turonian carbonate platform deposits in west central Jordan. International Journal of Earth Sciences, v. 92, p. 641-660.

Schulze, F., J. Kuss and A. Marzouk 2005. Platform configuration, microfacies and cyclicities of the upper Albian to Turonian of west-central Jordan. Facies, v. 50, p. 505-527.

Schulze, F., A.M. Marzouk, M.A.A. Bassiouni and J. Kuss 2004. The late Albanian–Turonian carbonate platform succession of west-central Jordan: Stratigraphy and crises. Cretaceous Research, v. 25, p. 709-737.

Schumm, S.A. 1993. River response to base level change: Implications for sequence stratigraphy. Journal of Geology, v. 101, p. 279-294.
Scotese, C.R. 1991. Jurassic and Cretaceous plate tectonic reconstructions. Palaeogeography, Palaeoclimatology, Palaeoecology, v. 87, p. 493-501.
Scott, R.W., S.H. Frost and B.L. Shaffer 1988. Early Cretaceous Sea-level Curves, Gulf Coast and Southeastern Arabia. In C.K. Wigus, B.S. Hastings, C.G.St.C. Kendall, H.W. Posamentier, C.A. Ross and J.C. Van Wagoner (Eds.), Sea-level Changes: An Integrated Approach. Society of Economic Paleontologists and Mineralogists, Special Publication no. 42, p. 275-284.
Sharief, F.A., K. Magara and H.M. Abdulla 1989. Depositional system and reservoir potential of the Middle East Cretaceous Wasia Formation in Central-Eastern Arabia. Marine and Petroleum Geology, v. 6, p. 303-315.
Shahar, J. 1994. The Syrian arc system: An overview. Palaeogeography, Plaeoclimatology, Palaeoecology, v. 112, p. 125-142.
Sharland, P.R., R. Archer, D.M. Casey, R.B. Davies, S.H. Hall, A.P. Heward, A.D. Horbury and M.D. Simmons 2001. Arabian Plate Sequence Stratigraphy. GeoArabia Special Publication 2. Gulf Petrolink Bahrain. 371 p.
Sharland, P.R., D.M. Casey, R.B. Davies, M.D. Simmons and O.E. Sutcliffe 2004. Arabian plate sequence stratigraphy – revisions to SP2. GeoArabia, v. 9, no. 1, p. 199-213.
Shaw, S.H. 1948. The geology and mineral resources of Palestine. Bulletin of the Imperial Institute, London, v. 46, p. 87-103.
Sir M. MacDonald and partners 1965. East Bank water resources. Hydrogeological Survey of the MadabaMaan area. 3 volumes. Central Water Authority, Amman, Jordan.
Soudry, D. and Y. Champetier 1983. Microbial processes in the Negev phosphorites. Sedimentology, v. 30, p. 411-423.
Soudry, D., Y. Nathan and R. Roded 1985. The Ashosh-Haroz Facies and their significance for the Mishash Palaeogeography and phosphorite accumulation in the northern and central Negev, Southern Israel. Israel Journal of Earth Sciences, v. 34, p. 211-220.
Speers, G.C. 1969. El Lajun oil-shale deposit, Jordan. Unpublished report, NRA and BP Research Centre, NRA, Amman.
Spicer, R.A. and R.M. Corfield 1992. A review of terrestrial and marine climates in the Cretaceous with implications for modelling the 'Greenhouse Earth'. Geological Magazine, v. 129, p. 169-180.
Spiro, B. and Z. Aizenshtat 1977. Bacterial sulphate reduction and calcite precipitation in hypersaline deposition of bituminous shales. Nature, v. 269, p. 235-257.
Spiro, B., D.H. Welte, J. Rullkotter and R.G. Schaefer 1983. Asphalts, oils, and bituminous rocks from the Dead Sea area: A geochemical correlation study. American Association of Petroleum Geologists Bulletin, v. 67, p. 1163-1175.
Stampfli, G.M. and G. Borel 2002. A plate tectonic model for the Paleozoic and Mesozoic constrained by dynamic plate boundaries and restored synthetic oceanic isochrones. Earth and Planetary Science Letters, v. 196, p. 17-33.
Steinitz, G. 1977. Evaporitechert associations in Senonian bedded cherts, Israel. Israel Journal of Earth Sciences, v. 26, p. 55-63.
Steinitz, G. 1981. Enigmatic chert structures in the Senonian cherts of Israel. Geological Survey of Israel Bulletin, v. 75, p. 146.
Sunn'a, B. (Ed.) 1974. Phosphate exploration and beneficiation studies. Vol. 1. Exploration and Geology. UNDP/NRA 70/521. Unpublished report, NRA, Jordan.
Vail, P.R., R.M. Mitchum and S. Thompson III 1977. Seismic stratigraphy and global changes in sea level from coastal onlap. In C.W. Payton (Ed.), Seismic Stratigraphy - Applications to hydrocarbon exploration. American Association of Petroleum Geologists, Memoir 26, p. 83-97.
Vail, P.R., F. Auemard, S.A. Bowman, P.N. Eisner and C. Perez-Cruz 1991. The stratigraphic signatures of tectonics, eustasy and sedimentology – An overview. In G. Einsele, W. Ricken and A. Seilacher (Eds.), Cycles and Events in Stratigraphy. Springer, Berlin, p. 617-659.
van Buchem, F.S.P., P. Razin, P.W. Homewood, J.M. Philip, G.P. Eberli, J.-P. Platel, J. Roger, R. Eschard, G.M.J. Desaubliaux, T. Boisseau, J.P. Leduc, R. Labourdette and S. Cantaloube 1996. High resolution sequence stratigraphy of the Natih Formation (Cenomanian/Turonian) in Northern Oman: Distribution of source and reservoir rocks. GeoArabia, v. 1, no. 1, p. 65-91.
van Buchem, F.S.P., P. Razin, P.W. Homewood, W.H. Oterdoom and J. Philip 2002. Stratigraphic organization of carbonate ramps and organic-rich intrashelf basins: Natih Formation (middle Cretaceous) of northern Oman. American Association of Petroleum Geologists, v. 86, p. 21-53.
van Houten, F.B., D.P. Bhattacharyya and S.E.I. Mansour 1984 Cretaceous Nubia Formation and correlative deposits, eastern Egypt: Major regressivetransgressive complex. Geological Society of America Bulletin, v. 95, p. 397-405.
Van Wagoner, J.C., H.W. Posamentier, R.M. Mitchum Jr., P.R. Vail, J.F. Sarg, T.S. Loutit and J. Hardenbol 1988. An overview of the fundamentals of sequence stratigraphy and key definitions. In C.K. Wigus, B.S. Hastings, C.G.St.C. Kendall, H.W. Posamentier, C.A. Ross and J.C. Van Wagoner (Eds.), Sea-level Changes: An Integrated Approach. Society of Economic Paleontologists and Mineralogists, Special Publication no. 42, p. 39-47.

Watts, K.F. and C.D. Blome 1990. Evolution of the Arabian carbonate platform margin slope and its response to orogenic closing of a Cretaceous oceanic basin, Oman. In M.E. Tucker, J.L. Wilson, P.D. Carvello, J.R. Sarg and J.F. Read (Eds.), Carbonate Platforms: Facies, Sequences and Evolution. Special Publication of the International Association of Sedimentologists, no. 9, p. 291-323.

Warren, J.K. and C.G.St.C. Kendall 1985. Comparison of sequences formed in marine sabkha (subaerial) and salina (subaqueous) settings modern and ancient. American Association of Petroleum Geologists Bulletin, v. 69, p. 1013-1023.

Weiler, Y. and E. Sass 1972. Karstic sandstone bodies in the Turonian limestones of Judea, Israel. Sedimentary Geology, v. 7, p. 137-152.

Weissbrod, T. and J. Nachmias 1986. Stratigraphic significance of heavy minerals in the Late Precambrian-Mesozoic clastic sequence ("Nubian Sandstone") in the NearEast. Sedimentary Geology, v. 47, p. 263-291.

Wetzel, R. and D.M. Morton 1959. Contribution à la Géologie de la Transjordanie. In M.L. Dubertret (Ed.), Notes et Mémoirs de la Moyen Orient, VII, p. 95-191.

Wendler, J., I. Wendler and H.J. Kuss 2009. Early Turonian shallow marine red beds on the Levant carbonate platform (Jordan), Southern Tethys. SEPM Special Publication no. 91, p. 179–187.

Wendler, J., J. Lehmann and J. Kuss 2010. Orbital time scale, intra-platform basin correlation, carbon isotope stratigraphy and sea-level history of the Cenomanian–Turonian Eastern Levant platform, Jordan. In C. Homberg and M. Bachmann (Eds.), Evolution of the Levant Margin and Western Arabia Platform since the Mesozoic. Geological Society of London, Special Publication no. 341, p. 171-186.

Wright, V.P. and S.B. Marriott 1993. The sequence stratigraphy of fluvial depositional systems: The role of floodplain sediment storage. Sedimentary Geology, v. 86, p. 203-210.

Wolfart, R. 1959. Geology and hydrogeology of the Irbid district (Hashemite Kingdom of Jordan). Bundesanstalt fur Bodenforschung. Hannover.

Yassini, I. 1979. Maastrichtian–Lower Eocene biostratigraphy and the planktic foraminiferal biozonation in Jordan. Revista Espãna de Micropalaeontologica, v. 11, p. 557.

ABOUT THE AUTHORS

John H. Powell *is Chief Geologist with the British Geologic Survey (BGS). He gained his BSc and PhD at the University of Newcastle upon Tyne, UK. John has over 30 years professional experience in sedimentology, applied geology and geological mapping in the UK and internationally. He has worked with the Natural Resources Authority, Jordan, on mapping, sedimentology and basin analysis of the Phanerozoic succession, especially the Lower Palaeozoic and Cretaceous – Eocene sequences. John was BGS Regional Geologist for the Middle East and Africa from 1998 to 2000, and has worked in Syria, Morocco, Mauritania and Mozambique. He serves on the Geological Society of London Accreditation Committee and GSL Stratigraphy Commission. John is an external examiner at the King Abdulaziz University, Jeddah, and is an Editor of the Proceedings of the Geologists' Association.*

jhp@bgs.ac.uk

Basem K. Moh'd *(stands for Mohammed), Geologist and Geomaterials Engineer, obtained an MSc in Carbonate Sedimentology from the University of Jordan and a PhD in Geomaterials Engineering (1996) from the University of London, UK. In addition to geological mapping, his more than 30 years of experience includes mining geology, mud logging, oil-shale exploration, technical editing, translation, construction materials, post-doctoral research (in Canada) and teaching (mining, geological and civil engineering since November 2001), at Tafila College (now Tafila Technical University), Jordan. Basem's research interests include geology and engineering of carbonates (construction and industrial materials, oil reservoirs, water aquifers), pore space, characterization and effects on physical and engineering properties, and the sedimentary geology of Jordan.*

mohdbk@yahoo.com

Manuscript received September 29, 2009
Revised February 23, 2011
Accepted March 16, 2011